Doctoral Dissertation

Fabrication of Poly(γ-glutamic acid)-Based Monoliths *via* Thermally Induced Phase Separation and Their Applications

(熱誘起相分離を利用したポリ−γ−グルタミン酸モノリスの作製と応用)

Sung-Bin Park

January 2014

Department of Applied Chemistry
Graduate School of Engineering
Osaka University

Contents

General Introduction

Biopolymers

Naturally occurring polymers have attracted considerable interest in recent years. This interest arose as a result of an increased awareness of the environment and a desire to produce environmentally safe materials. Limited resources of crude oil, global warming, environmental consciousness and new standards are also some of the factors that have led to this growing interest. Biopolymers offer a possible alternative to synthetic polymers. These biopolymers are not only come from natural sources but also biodegradable.[1] Biopolymers are a part of the ecosystem and fully renewable, do not contribute to an accumulation of carbon dioxide in the atmosphere after their life cycle. Biopolymers are a diverse and versatile class of materials that have potential applications in virtually all sectors of the economy because of their biocompatibility, biodegradability, and both environmental and human compatibility.[2] For example, they can be used as adhesives, absorbents, lubricants, soil conditioners, cosmetics, drug delivery vehicles, textiles, and high-strength structural materials. Indeed, currently many biopolymers are widely developed and used as packaging, cosmetics, food additives, clothing fabrics, water treatment, industrial plastics, absorbents, biosensors, and medical materials. Some biopolymers can directly replace synthetically derived materials in traditional application, whereas other process unique properties that could open up a range of new commercial opportunities.[3]

Biopolymers can be classified as natural biopolymer, microbial biosynthetic biopolymer, and synthetic biopolymer. Natural biopolymers are obtained by plants or animals for example cellulose, gelatin, collagen, and chitosan. polyhydroxyalkanoates (PHA), polyhydroxybutyrate (PHB), bacterial cellulose, and poly(γ-glutamic acid) (PGA) can be produced by microbial biological system. Synthetic biopolymers such as

poly(lactic acid) (PLA) and poly(butylene succinate) (PBS) are chemically synthesized from biological starting materials such as sugars, starch, natural fats, and oils.[4-7] The classified biopolymers are listed in Table 1.

Table 1. Classification of the biopolymers

Natural biopolymer	Polysaccharides
	Dextran
	Starches
	Cellulose and its derivatives
	Fibers
	Gelatin
	Collagen
	Chitin and chitosan
	Gums
Microbial biosynthetic biopolymer	Poly(γ-glutamic acid)
	Poly(3-hydroxybutyrate)
	Poly(3-hydroxybutyrate-co-hydroxyvalerate)
	Bacterial cellulose
	Polyhydroxyalkanoate
Synthetic biopolymer	Poly(lactic acid)
	Poly(glycolic acid)
	Biopolyethylene
	Poly(butylenes succinate)
	Poly(vinyl alcohol)
	Poly(vinyl acetate)

General properties of PGA and its applications

Recently, microbial biosynthetic biopolymers have received much attention because of their excellent biocompatibility and biodegradability. These polymers obtained from the natural cycles are harmless to humans and the environment.

PGA is a biopolymer that is produced by microbial fermentation.[8] In other words, PGA can be produced from sustainable resources therefore the development of PGA is both economically and environmentally valuable. PGA was first discovered by Ivanovics and co-workers as a capsule of *Bacillus anthracis* which was released into the medium upon autoclaving or upon aging and autolysis of the cells.[9] Since Bovarnick[10] showed that PGA freely secreted into the growth medium of *Bacillus subtilis* as a product of fermentation, several *Bacillus* species have been shown to produce PGA outside of the cells.[11-16]

PGA is an unusual anionic polypeptide in which D- and/or L-glutamate is polymerized *via* γ-amide linkages (Figure 1). It can be characterized by its molecular weight and the ratio of D- and L-glutamate monomers.[17] Three stereochemically different types of PGA have been reported:[18,19] the homopolymer composed of D-glutamate (D-PGA), a homopolymer of L-glutamate (L-PGA), and a copolymer in which the D- and L- glutamate units are lined up at random (DL-PGA). Various *Bacillus* species were suggested for the microbial production of PGA. Some strains of *Bacillus subtilis*, including the starters of *natto* a traditional Japanese fermented food made from soybeans,[20] and of *chungkookjang*, a traditional Korean fermented seasoning made from soybeans,[21] produce DL-PGA as a main component of the extracellular mucilage. Nowadays, the production of PGA already has been established on the industrial scale because it can be produced easily and extracellularly in high yield by culturing of microorganism in a fermentor. Especially, Sung *et al*. first discovered the preparation of high molecular weight DL-PGAs from *Bacillus subtilis* (*chungkookjang*), the molecular

weight of PGA in culture broth reaches over 10,000 kDa, which is the highest molecular weight reported so far.[22,23] In this thesis, the ultra high molecular weight of PGA produced from *Bacillus subtilis* (*chungkookjang*) was used as materials to development of new functional material for its various applications.

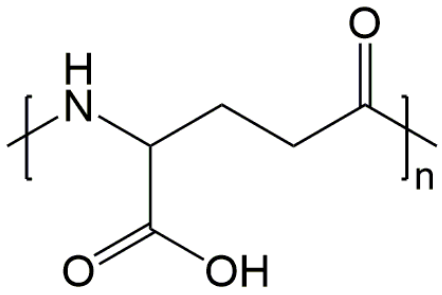

Figure 1. Structure of Poly(γ-glutamic acid).

Multi functionalities such as hydrophilicity, anionic property, biodegradability, nontoxicity, biocompatibility, and edibility[24-26] have made it a promising biopolymer for use as a health food, stabilizer in the food industry, moisturizer in cosmetics, chelating agent in waste-water treatment, hydrogel (especially super absorbent polymer, SAP) for environmental, biodegradable packing material, drug deliverer, gene vector, curative biological adhesive, dispersant, and enzyme-immobilizing material. The applications of PGA are summarized in Table 2. Indeed, PGA is already used for some commercial applications in health foods, cosmetics and wastewater purification.[1,23]

Table 2. Potential applications of PGA and its derivatives.

Wastewater treatment	Metal chelates or absorbents
	Bioflocculants
Medical	Drug carrier or sustained release materials
	Curable biological adhesive and hemostatic or medical bonding kit
	Suture thread
Cosmetic	Moisturizer
Membrane	Absorbents
	Enantioselective agents
Food industry	Thickener
	Cryoprotectant
	Bitterness relieving agents
	Aging inhibitor or texture enhancer
	Animal feed additives
Others	Water absorbents
	Dispersants

PGA based functional materials

Up to present, many PGA based functional materials has been developed for further up-value of the raw PGA powder.

The chemical crosslinking, γ-ray irradiation, freeze drying methods were generally used for preparation of PGA hydrogels. The specific water content was strongly dependent on pH and salt concentration in the swelling medium. Under acidic conditions or on addition of electrolytes, the specific water contents and degrees of swelling of the PGA hydrogels were markedly decreased. These PGA hydrogels with high water sorption or stimuli-response capacity has been interested in recent years because of their various potential applications such as drug controlled release, enzyme immobilization, or moisture absorbent.[27,28]

Treatment of contaminated soil and water, removal of environmentally harmful heavy metals were great interested in the field of environmental.[29] McLean *et al*. studied the metal-binding affinity of the anionic PGA of *Bacillus licheniformis* and found that it binds a variety of metals including Ni^{2+}, Cu^{2+}, Mn^{2+}, Al^{3+} and Cr^{3+}.[30,31] Undoubtedly, these strong metals adsorption properties of PGA can be further extended to the removal of toxic metals and also to the recovery of valuable metals from solutions.[8]

A novel proteins or drugs delivery system with self-assembled polymeric nanoparticles using PGA has been developed.[32-34] The different types of nanoparticles were designed to target refolding of inclusion body protein or using as drug-delivery vehicle. Generally, chitosan, gelatin, and cholesterol were used for the development of PGA nanoparticles. PGA nanoparticles can be degraded by γ-glutamyl transpeptidase, which is widely distributed in the whole body.[35] Nanoparticles composed of amphiphilic PGA and hydrophobic amino acids can immobilize proteins, peptides, and chemicals onto the surfaces and/or encapsulate these substances into the particles.[36-38]

The zeta-potential and particle size can be controlled by changing the composition and concentration of the reaction mixture.

PGA based composite nanofibers can be formed by the electrospinning technique. For instance, Yoshida *et al*. reported the preparation of water stable disulfide crosslinked electrospun PGA nonwovens with reduction responsiveness for tissue engineering applications.[39] Ko *et al*. prepared anti-adhesion membranes from PGA blended with poly(lactic-co-glycolic acid) (PLGA) with different mass ratios by electrospinning.[40] The incorporation of a nonsteroidal anti-inflammatory drug within PGA/PLGA nanofibers was demonstrated to be effective in preventing tissue adhesion and in inducing wound healing. In another study, Lee *et al*. reported the preparation of water-insoluble electrospun PGA butyl ester ultrafine fibers by the addition of poly(ethylene glycol) (PEG) and Triton X-100 into the electrospinning solution.[41] These literature data clearly suggest that PGA is an important polymer material that can be electrospun to form nanofibers for biomedical applications.

Ester derivatives of PGA have been investigated for their capability to form biodegradable fibers and films that can replace currently used non-biodegradable polymers. It was found that the esterified PGA served as an excellent thermoplastic and that poly(γ-glutamic acid α-benzyl ester) could be processed into fibers or membranes with excellent strength, transparency and elasticity by the standard methods used in polymer processing.

In this stream, development of the new featured PGA based functional materials requires for improvement of PGA application studies.

Porous polymeric monoliths

Monoliths are single-piece bulk materials having a three-dimensionally developed, continuous porosity inside.[42,43] During the last decade, this new category of materials have been developed rapidly and widely used in various fields.[44] Such a monolithic structure is featured by several key aspects such as high surface area, high stability, high permeability, and fast mass transfer performance.[45-48] Generally, monoliths can be categorized into polymer based monolith and silica based monolith. Among these two kinds of monoliths, polymer based monoliths which emerged in the early 1990s have attracted significant attention because of their biocompatibility, pH stability, high chemical stability, easy chemical modifications, and past mass transfer performance. Polymer based monoliths have been applied in various fields such as chromatography, biomolecule immobilization, and support catalysis because of their useful properties.[49-51]

These monoliths are prepared using a simple molding process carried out within the confines of a closed mold. Up to present, there have been already many methods reported to produce porous polymer monoliths by using various biopolymers, which include thermally induced phase separation, particulate leaching, porogen leaching, fiber bonding, solvent casting, particle sintering, three-dimensionally printing, gas foaming, and emulsion freeze drying.[52-60]

The thermally induced phase separation technique is based on thermodynamic demixing of a homogeneous polymer solvent solution into a polymer rich phase and a polymer poor phase, usually by either exposure of the solution to another immiscible solvent or cooling the solution below a bimodal solubility curve. One of the advantages of this technique is that various porous structures can be easily obtained by adjusting various thermodynamic and kinetic parameters.

The salt leaching technique is suitable for controlling pore sizes by changing

the size of salt particulates. Porogen leaching method has been the well known method, and involves the casting of a polymer/porogen composite followed by aqueous washing out of the incorporated porogens. Various porogens such as salts, carbohydrates, and polymers can be used to produce porous materials.

The emulsion freeze drying method is another approach for the production of porous scaffolds, but this method often results in a closed cellular structure in the matrix. The expansion technique using a high pressured CO_2 gas also resulted in a closed pore structure, and a combination technique of gas induced foaming and particulate leaching was recently proposed to improve the pore structure. The three-dimensionally printing technique using the principle of ink-jet printing appears useful, while its application is still in infancy.[61, 62] Variety fabrication methods of polymer-monoliths are illustrated in Figure 2.

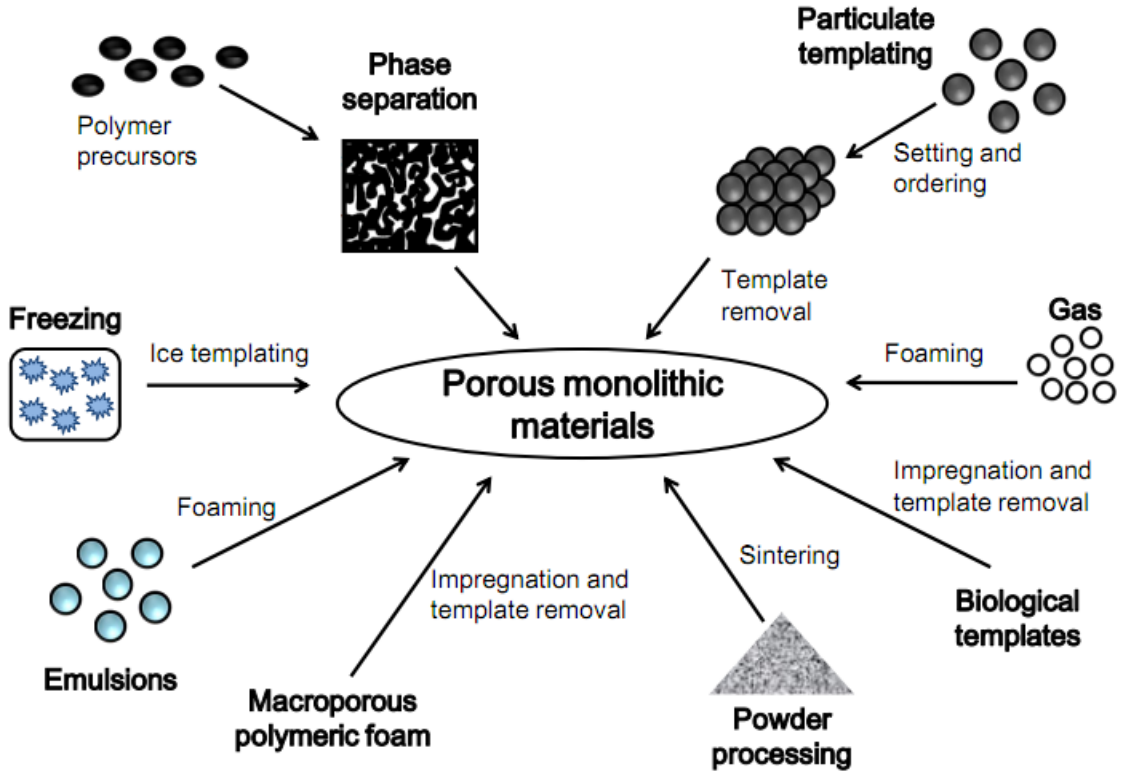

Figure 2. Fabrication methods of porous polymeric monoliths (adapted and reproduced with permission of Springer).

The monolith can be further up-valued by engineering the porosity and its chemical nature. The porous properties of the monolith can be controlled over a broad range.

Recently, the author's laboratory has developed fabrication of polymer-based monoliths by using variety polymers *via* thermally induced phase separation (TIPS) method. This approach is straightforward and offers a great opportunity for the fabrication of various monolithic structures depending on the choice of polymer and the phase separation conditions. Moreover, the shape of the monoliths can also be modified by altering the shape of the vessel. The polymethylmethacrylate (PMMA) monolith is firstly described monolith by TIPS method in author's laboratory.[63,64] The fabrication process for PMMA monolith is as follows. PMMA resin is dissolved in a mixture of solvent (ethanol) and non-solvent (water) by heating at 60 ^{o}C, followed by cooling to 20 ^{o}C, leading to formation of the porous polymer monolith. During the cooling step, the phase separation of the polymer solution took place to from the PMMA monolith with high surface area and uniform porosity without using any template. Up to now, there are many kinds of polymer-based monoliths already fabricated through phase separation method in the author's laboratory and the applications of the monoliths are under way in the author's laboratory. Their properties and possible applications are listed in Table 3.

Table 3. Properties and possible applications of polymer-based monoliths fabricated through phase separation method.

Polymer	Properties	Possible applications
Acrylic resin	Chemical modification	Separation matrix
	Solvent resistance	Catalyst matrix
Poly(vinyl alcohol)	Hydrophilic	Biomaterial
	Solvent resistance	Separation matrix
Poly(lactic acid)	Biodegradability	Agriculture material
	Biocompatibility	Biomaterial
Poly(acrylonitrile)	Heat resistance	Precursor for battery material
	Solvent resistance	Separation matrix
Cellulose	Hydrophilic	Biomaterial
	Solvent resistance	Catalyst matrix
Silk	Hydrophilic	Biomaterial
	Biocompatibility	Cosmetic
Polyurethane	Flexibility	Acoustic material
	Absorbability	Cosmetic
Polyolefin	Heat resistance	Battery separator
	Solvent resistance	Matrix for fuel gas

With the background described above, this doctoral thesis focusing on the development of new functional polymeric monoliths based on the PGA *via* TIPS method and the preliminary studies on their applications.

This thesis includes four chapters as follows:

In Chapter 1, PGA monoliths with three-dimensional continuous interconnected porous structure in a single piece are fabricated *via* a thermally induced phase separation technique using a mixture of dimethyl sulfoxide, water, and ethanol (Figure 3). The morphology of the obtained monolith was observed by scanning electron microscopy and the surface area of the monolith was evaluated by the Brunauer Emmett Teller method. The effects of fabrication parameters such as the concentration and molecular mass of PGA and the solvent composition have been systematically investigated. The PGA monolith was cross-linked with hexamethylene diisocyanate to produce the water-insoluble monolith. The addition of sodium chloride to the phase separation solvent affected the properties of the porous structure of monolith. The swelling ratio of the cross-linked monolith toward aqueous solutions depended on the buffer pH as well as the monolith fabrication condition. Furthermore, the unique deformability of the wet cross-linked monolith was found. copper(II) ions were efficiently adsorbed on the cross-linked PGA monolith, and the obtained copper(II)-immobilized monolith showed strong antibacterial activity for *Escherichia coli*. By combination of the characteristic properties of PGA (*e.g.*, biocompatibility and biodegradability) and the unique features of monoliths (*e.g.*, through-pore structure, large surface area, and high porosity with small pore size), the PGA monolith possesses large potentials for various industrial applications in the biomedical, environmental, analytical, and separation fields.

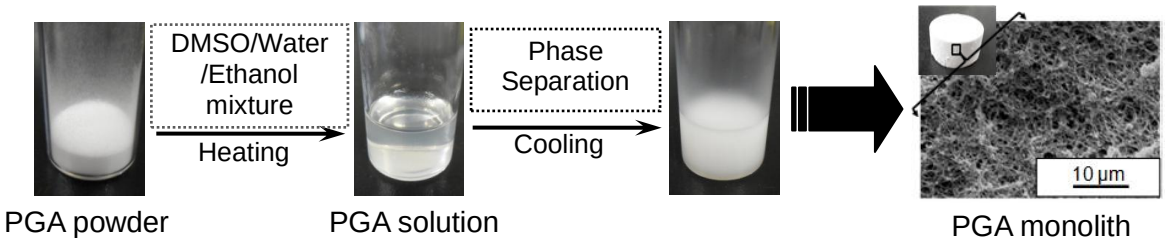

Figure 3. PGA monolith fabricated *via* a thermally induced phase separation technique.

In Chapter 2, describes a unique PGA monolith that included both submillimeter-sized large and submicron-sized small pores by a combination of particulate templates leaching and phase separation technique (Figure 4). The monolith was then subjected to internal crosslinking reaction with hexamethylene diisocyanate, followed by washing off the salt particles with water. This simple procedure was found to successfully furnish a unique solid material in which submillimeter-sized cavities are uniformly distributed over a monolithic three-dimensionally microporous network created by the phase separation. This characteristic structure was confirmed by cross-sectional analysis using scanning electron microscopy. A large surface area was suggested by the Brunauer Emmett Teller method. Moreover, remarkable pH-responsivity was demonstrated in therms of fully reversible expansion/shrinkage and capture/release of copper(II) ions. On this basis, the present monolith has promising prospects for a wide range of applications, especially in biomedicine, biotechnology and environmental fields.

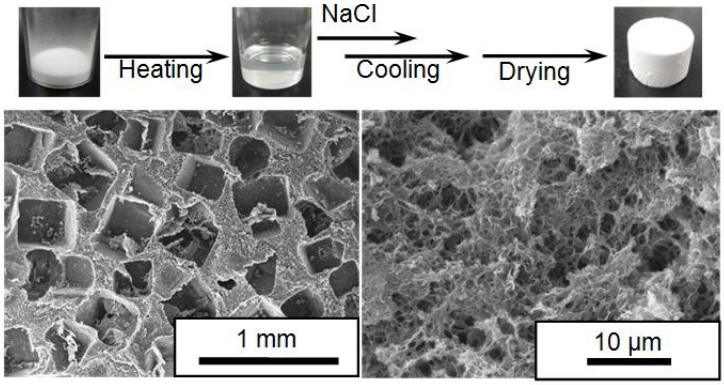

Figure 4. PGA monolith prepared by a combination of particulate templates leaching and thermally induced phase separation technique.

Chapter 3 deals with preparation of PGA and hydroxyapatite hybrid monolith (PGA/HAp monolith) and its application in bone tissue engineering (Figure 5). The PGA monolith was prepared by combination of salt leaching and thermally induced phase separation technique. The HAp forming ability of PGA monolith was assessed by soaking in simulated body fluid. The effect of pretreatment with $CaCl_2$ on HAp formation was also examined. The $CaCl_2$ pretreated PGA monoliths showed higher HAp forming ability than that $CaCl_2$ untreated PGA monolith. The murine osteoblastic cells (MC3T3-E1) efficiently attached and proliferated on the both the PGA and PGA/HAp monolith. MTT assay showed that the obtained PGA monoliths had no apparent toxicity. Moreover, bone morphogenetic proteins-2 (BMP-2) was absorbed onto the monoliths *via* electrostatic interaction and slowly released into the culture medium. The cells cultured on the BMP-2 loaded PGA/HAp monolith showed increased ALP activity compare to the PGA monolith. Therefore, present PGA/HAp monolith has advantages in bone tissue engineering applications.

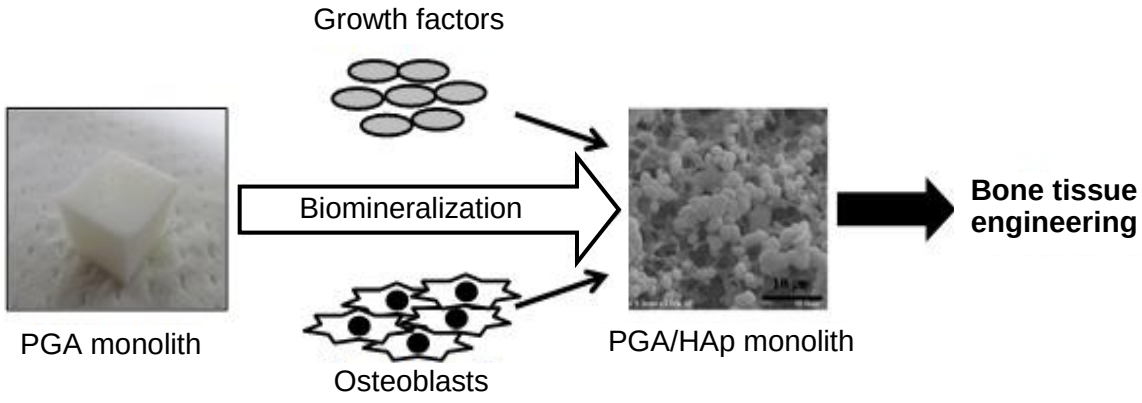

Figure 5. PGA/HAp monolith prepared by biomineralization for bone tissue engineering.

Chapter 4 deals with the PGA monolith crosslinked with a low-toxic oxazoline component polymer (Figure 6). The morphology of the obtained monolith was observed by scanning electron microscopy and the surface area of the monolith was evaluated by the Brunauer Emmett Teller method. A pH-controlled degradability and thermal stability of the crosslinked PGA monolith were demonstrated. A cytotoxicity test and calcium loading/release were also performed aiming at its application in tissue engineering. PGA monolith shows pH-controlled degradability and high thermal stability. Moreover, Ca(II)Cl_2 was loaded to the monoliths and slowly released into the media from the monoliths. On this basis, the PGA monolith crosslinked with an oxazoline-functionalized polymer has large potential as a cell scaffolding material.

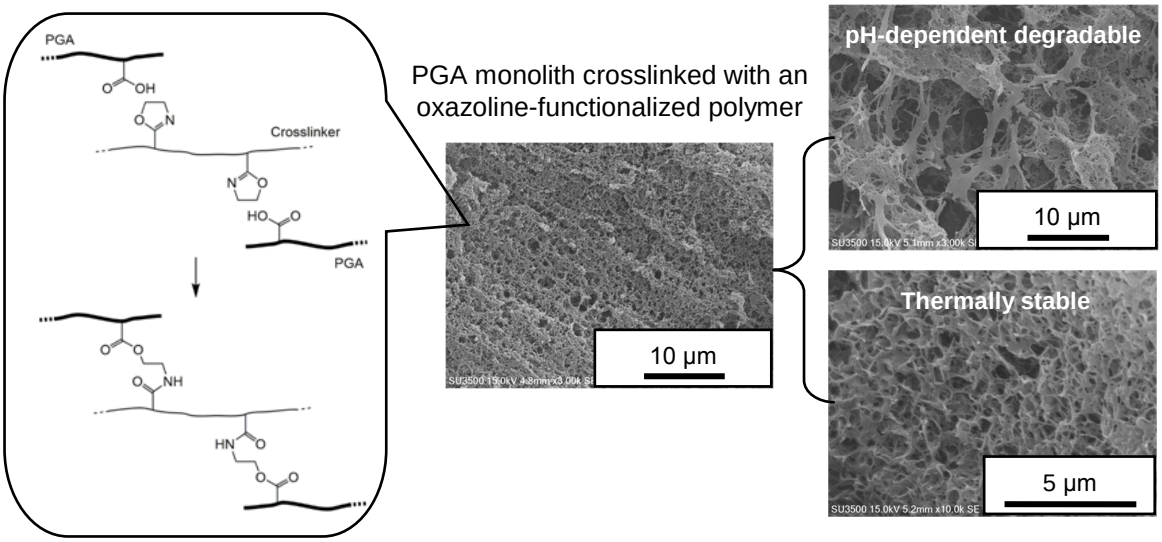

Figure 6. Porous PGA monolith crosslinked with an oxazoline-functionalized polymer.

References

[1] M. H. Sung, C. Park, C. J. Kim, H. Poo, K. Soda, M. Ashiuchi, *Chem. Rec.* **2005**, *5*, 352.

[2] K. Van de Velde, P. Kiekens, *Polym. Test.* **2002**, *21*, 433.

[3] R. C. Herdman, G. G. Allan, N. Bikales et al, Biopolymers: Making Materials Nature's way, OTA-BP-E-102, NTIS order #PB94-107638, **1993**.

[4] J. W. Rhim, P. K. Ng, *Crit. Rev. Food. Sci. Nutr*. **2007**, *47*, 411.

[5] M. Z. Elsabee, E. S. Abdou, *Mater. Sci. Eng. C* **2013**, *33*, 1819.

[6] K. O. Doh, Y. Yeo, *Ther. Deliv*. **2012**, *3*, 1447.

[7] R. Raftery, F. J. O'Brien, S. A. Cryan, *Molecules*. **2013**, *18*, 5611.

[8] I. L. Shih, Y. T. Van, *Bioresour. Technol*. **2001**, *79*, 207.

[9] G. Ivanovics, V. Bruckner, *Z. Immunitaetsforsch* **1937**, *90*, 304.

[10] M. Bovarnick, *J. Biol. Chem*. **1942**, *145*, 415.

[11] C. Cheng, Y. Asada, T. Aaida, *Agric. Biol. Chem*. **1989**, *53*, 2369.

[12] A. Goto, M. Kunioka, *Biosci. Biotechnol. Biochem*. **1992**, *56*, 1031.

[13] T. Hara, A. Aumayr, Y. Fujio, S. Ueda, *S. Appl. Environ. Microbiol*. **1982**, *44*, 1456.

[14] T. Hara, Y. Fujio, S. Ueda, *J. Aool. Biochem*. **1982**, *4*, 112.

[15] H. Kubota, Y. Nambu, T. J. Endo, *J. Polym. Sci. Part A Polym. Chem*. **1993**, *31*, 2877.

[16] H. Kubota, T. Matsunobu, K. Uotani, H. Takebe, A. Satoh, T. Tanaka, M Tanghuchi, *Biosci. Biotechnol. Biochem*. **1993**, *57*, 1212.

[17] M. Ashiuchi, H. Misono, *Appl. Microbiol. Biotechnol*. **2002**, *59*, 9.

[18] M. Ashiuchi, H. Nakamura, T. Yamamoto, T. Kamei, K. Soda, C. Park, M. H. Sung, T. Yagi, H. J. Misono, *J. Mol. Catal. B* **2003**, *23*, 249.

[19] T. Tanaka, K. Fujita, S. Takenishi, M. Taniguchi, *J. Ferment. Bioeng*. **1997**, *84*,

361.

[20] H. Kubota, T. Matsunobu, K. Uotani, H. Takebe, A. Satoh, T. Tanaka, M. Taniguchi, *Biosic. Biotechnol. Biochem*. **1993**, *57*, 1212.

[21] M. Ashiuchi, T. Kamei, D. H. Baek, S. Y. Shin, M. H. Sung, K. Soda, T. Yagi, H. Misono, *Appl. Microbiol. Biotechnol*. **2001**, *57*, 764.

[22] M. H. Sung, C. Park, S. P. Hong, K. S. Kim, M Ashiuchi, S. Kenji, J. J. Song, H. Poo, E. G. Rha, S. G. Lee, Poly-gamma-glutamate having ultra high molecular weight and method for using the same, KR/10-0399091, 09, 09, **2003**.

[23] H. Poo, C. Park, M. S. Kwak, D. Y. Choi, S. P. Hong, I. H. Lee, Y. T. Lim, Y. K. Choi. S. R. Bae, H. Uyama, C. J. Kim, M. H. Sung, *Chem. Biodivers*. **2010**, *7*, 1555.

[24] M. Ashiuchi, T. Kamei, H. Misono, *J. Mol. Catal. B Enzym*. **2003**, *23*, 101.

[25] M. Ashiuchi, C. Nawa, T. Kamei, J. J. Song, S. P. Hong, M. H. Sung, K. Soda, H. Misono, *Eur. J. Biochem*. **2001**, *268*, 5321.

[26] T. Candela, A. Fouet, *Mol. Microbiol*. **2006**, *60*, 1091.

[27] S. A. Dubrovskii, M. V. Afanaseva, M. A. Lagutina, K. S. Kazanskii, *Polym. Bull.* **1990**, *24*, 107.

[28] T. G. Park, A. S. Hoffman, *J. Appl. Polym. Sci*. **1992**, *46*, 659.

[29] L. E. Macaskie, G. Basnakova, *Environ. Sci. Technol*. **1998**, *32*, 184.

[30] R. C. McLean, D. C. Wolf, F. G. Ferris, T. J. Beveridge, *Appl. Environ. Microbiol.* **1990**, *56*, 3671.

[31] R. C. McLean, D. Beauchemin, T. J. Beveridge, *Appl. Environ. Microbiol*. **1992**, *58*, 405.

[32] Y. H. Lin, C. K. Chung, C. T. Chen, H. F. Liang, S. C. Chen, H. W. Sung, *Biomacromolecules* **2005**, *6*, 1104.

[33] H. W. Sung, H. F. Liang, H. Tu, **2006**, US Pat. 20060073210.

[34] M. H. Sung, C. Park, C. J. Kim et al, **2006**, Patent Cooperation Treaty Application Number WO2006001567.

[35] T. Uto, X. Wang, K. Sato, M. Haraguchi, T. Akagi, M. Akashi, M. Baba, *J. Immunol*. **2007**, *178*, 2979.

[36] T. Akagi, T. Kaneko, T. Kida, M. Akashi, *J. Control. Release*, **2005**, *108*, 226.

[37] S. Okamoto, H. Yoshii, M. Matsuura, A. Kojima, T. Ishikawa, T. Akagi, M. Akashi, M. Takahashi, K. Yamanishi, Y. Mori, *Clin. Vaccine. Immunol*. **2012**, *19*, 17.

[38] X. Wang, T. Uto, T. Akagi, M. Akashi, M. Baba, *J. Virol*. **2007**, *81*, 10009.

[39] H. Yoshida, K. Klinkhammer, M. Matsusaki, M. Moller, D. Klee, M. Akashi, *Macromol. Biosci*. **2009**, *9*, 568.

[40] Y. K. Ko, S. H. Kim, H. J. Ha, S. J. Yoon, J. M. Rhee, M. S. Kim, H. B. Lee, G. Khang, *Key Eng. Mater*. **2007**, *342*, 173.

[41] E. H. Lee, H. Uyama, O. H. Kwon, M. H. Sung, *Polym. Bull*. **2009**, *63*, 735.

[42] M. R. Buchmeiser, *Polymer* **2007**, *48*, 2187.

[43] O. G. Potter, E. F. Hilder, *J. Sep. Sci*. **2008**, *31*, 1881.

[44] F. Svec, J. M. J. Frechet, *Anal. Chem*. **1992**, *64*, 820.

[45] J. Courtois, E. Bystrom, K. Irgum, *Polymer* **2006**, *47*, 2603.

[46] F. J. Svec, *Chromatogr A* **2010**, *1217*, 902.

[47] F. Svec, C. G. Huber, *Anal. Chem*. **2006**, *78*, 2100.

[48] S. Wei, Y. L. Zhang, H. Ding, J. Liu, J. Sun, Y. He, et al. *Colloids Surf. A* **2011**, *380*, 29.

[49] A. M. Siouffi, *J. Chromatogr. A* **2003**, *1000*, 801.

[50] O. Nunez, K. Nakanishi, N. Tanaka, *J. Chromatogr. A* **2008**, *1191*, 231.

[51] A. Ghanem, T. Ikegami, *J. Sep. Sci*. **2011**, *34*, 1945.

[52] H. Lo, M. S. Ponticiello, K. W. Leong, *Tissue Eng*. **1995**, *1*, 15.

[53] H. Lo, S. Kadiyala, E. Guggino, K. W. Leong, *J. Biomed. Mater. Res*. **1996**, *30*, 475.

[54] C. Schugens, V. Maguet, C. Grandfils, R. Jerome, P. Teyssie, *J. Biomed. Mater. Res*. **1996**, *30*, 449.

[55] L. Freed, J. C. Marquis, A. Nohria, J. Emmanual, A. G. Mikos, *J. Biomed. Mater. Res*. **1993**, *27*, 11.

[56] L. Freed, G. Vunjak-Novokovic, R. J. Biron, D. B. Eagles, D. C. Lesnoy, S. K. Barlow, R. Langer, *Biotechnology* **1994**, *12*, 289.

[57] A. G. Mikos, G. Sarakinos, S. M. Leite, J. P. Vacanti, R. Langer, *Biomaterials* **1993**, *14*, 323.

[58] D. J. Mooney, D. F. Baldwin, N. P. Suh, J. P. Vacanti, R. Langer, *Biomaterials* **1996**, *17*, 1417.

[59] L. D. Harris, B. S. Kim, D. J. Mooney, *J. Biomed. Mater. Res*. **1998**, *42*, 396.

[60] K. Whang, C. H. Thomas, K. E. Healy, G. Nuber, *Polymer* **1995**, *36*, 837.

[61] A. Park, B. Wu, L. G. Griffith, *J. Biomater. Sci. Polym. Ed*. **1998**, *9*, 89.

[62] Z. Zou, Y. Guo, Y. Li, J. Lv, H. Liu, J. Xu, Y. Li, *Macromol. Rapid Commun*. **2009**, *30*, 1940.

[63] K. Okada, M. Nandi, J. Maruyama, T. Oka, T. Tsujimoto, K. Kondoh, H. Uyama, *Chem. Commun*. **2011**, *47*, 7422.

[64] M. Nandi, K. Okada, H. Uyama, *Funct. Mater. Lette*. **2011**, *4*, 407.

Chapter 1

Fabrication of Poly(γ-glutamic acid) Monolith by Thermally Induced Phase Separation and Its Application

1.1 Introduction

Poly(γ-glutamic acid) (PGA) is a natural polymer prepared by polymerization of glutamate *via* γ-peptide linkages by microorganisms such as *Bacillus subtilis*. PGA has various unique properties and functions;[1-3] it is non-toxic, hydrophilic, anionic, edible, biocompatible and biodegradable. Based on these features, many industrial applications of PGA have been studied, mainly in the fields of health foods, cosmetics, drug delivery systems, and wastewater treatment.[4,5]

Monoliths are functional porous materials with an open-cellular three-dimensional continuous interconnected pore structure in a single piece.[6,7] They can be used for various applications due to their high permeability, fast mass transfer performance, high stability and ease of chemical modification.[8-19] For example, the through-pore structure and large surface area are important factors for the application of monoliths as adsorbents, immobilization supports, and tissue engineering scaffolds. The large surface area allows for adsorption and immobilization of a large amount of target and functional molecules, respectively, and the monolithic configuration enables column permeability and mass transfer to be maximized simultaneously in the adsorption and immobilization.[20,21]

This chapter deals with the fabrication of PGA monolith by thermally induced phase separation (TIPS) and its application for metal chelation. By selecting the appropriate combination of solvent and non-solvent for the phase separation, a PGA monolith of uniform shape in submicron skeleton size was formed. The crosslinking of the PGA monolith with hexamethylene diisocyanate (HDI) produced the water-insoluble monolith with high stability toward water and organic solvents. Furthermore, the crosslinked monolith effectively adsorbed copper(II) ions on the basis of the strong chelation of PGA for metals.[22] In relevant to this study, the electrospinning method conveniently provided ultrafine fibers of PGA in the submicron or micron size;[23,24] however, the thickness of the resulting mat was less than 100 μm, which prevents the above-mentioned applications in most cases. Thus, the present PGA monolith with its remarkable advantages will provide a new opportunity for applications of PGA, such as water treatment, recovery of rare metals, drug delivery, and tissue engineering.

1.2 Experimental

Materials

PGAs (acid form) with different molecular masses were products of BioLeaders Corp. (Korea). HDI was purchased from Wako Pure Chemical Industries, Ltd. (Japan). All reagents were of analytical grade and used as received without further purification.

Measurements

Scanning electron microscopic (SEM) images were recorded on a Hitach S-3000N instrument at 15 kV. A thin gold film was sputtered on the samples before the images were collected. Nitrogen adsorption/desorption isotherms were measured with a NOVA 4200e Surface Area & Pore Size Analyzer (Quantachrome Instruments) at 25 ^{o}C. The Brunauer Emmett Teller (BET) method was utilized to determine specific surface areas. Before the measurements, all samples were degassed at 25 ^{o}C for 12 h under vacuum. Fourier transform infrared (FT-IR) measurements by the attenuated total reflectance (ATR) method were performed by Thermo Scientific Nicolet iS5 with the iD5 ATR accessory. The Cu(II)Cl_2 concentration in aqueous solution was determined by a Hitachi U-2810 UV-visible spectrometer at 816 nm. The energy dispersive X-ray spectrometeric (EDX) measurement for elemental analysis of the monolith surface was conducted by a Hitachi Miniscope TM3000 with a Swift3000 equipment.

Porosity was measured by using a gravimetric method. Ethanol was used as the solvent for measurement of the volume of the non-porous PGA powder, based on which the density of PGA was determined (D_{powder}). The volume of the PGA monolith was calculated from diameter and height of the cylinder shape of the monolith, and the density of the monolith (D_{monolith}) was estimated from the weight and volume of the monolith. The porosity of the monolith was calculated by using the following equation:

$$\text{Porosity (\%)} = (1 - D_{\text{monolith}}/D_{\text{powder}}) \times 100 \quad (1)$$

Swelling ratio was determined from the weights of the dry and wet (swollen) monoliths (W_{d} and W_{w}, respectively). The monolith was immersed in a buffer of different pH values (4, 7, or 10) at 25 ^{o}C. In most cases, the weight value of the wet monolith was almost constant after 24 h. Thus, the weight of the wet monolith after 24 h

was used for the determination of the swelling ratio by using the following equation:

$$\text{Swelling ratio (\%)} = (W_w/W_d - 1) \times 100 \quad (2)$$

Water retention was determined from the weight change by centrifugation. At first, the PGA monolith swollen in water was weighted (W_w). Then, it was placed in a tube, which was subjected to centrifugation at 4,000 rpm for 30 sec. The sample was carefully ejected from the tube and weighted (W_r). The water retention was calculated by using the following equation:

$$\text{Water retention (\%)} = W_r/W_w \times 100 \quad (3)$$

Fabrication procedure of PGA monolith

A typical fabrication protocol is as follows (Figure 1-1). PGA powder (450 mg) was dissolved completely in a mixture of dimethyl sulfoxide (DMSO), ethanol and water (3 mL) by heating at 80 °C. Then, the solution was cooled to 25 °C. During the cooling stage, the phase separation took place to form a monolith. The resulting monolith was washed repeatedly with acetone to remove the trapped solvents and subsequently dried under vacuum.

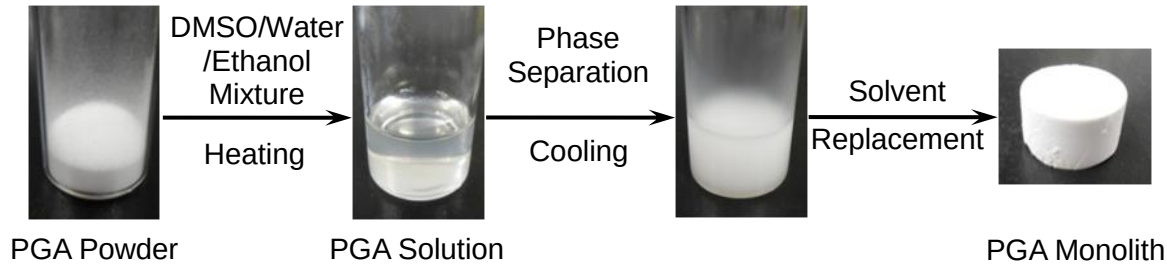

Figure 1-1. Fabrication procedure for PGA monolith *via* the TIPS method.

Crosslinking of PGA monolith by HDI

The PGA monolith (450 mg, 3.49 mmol of monomer unit) was mixed with HDI (1 mL, 5.89 mmol) in acetone (10 mL) and left for 6 h. 300 μL of water was then added dropwise to the mixture. The crosslinking was carried out at 50 ^{o}C with gentle stirring for 24 h. The resulting monolith was washed with acetone repeatedly and dried under vacuum.

Copper(II) ion adsorption

The crosslinked monoliths (100 mg for a single piece) were immersed in $CuCl_2$ solution (0.1 M, 10 mL). The mixture was gently shaken at 25 ^{o}C. The concentration of $Cu(II)Cl_2$ in the supernatant was measured with a UV-visible spectrometer at 816 nm.

In vitro antibacterial assay

The monolith and copper(II)-immobilized monolith samples were sterilized with 80% ethanol and rinsed with sterile water to remove the ethanol. *Escherichia coli (E. coli)* strain JM109 was subcultured in Luria-Bertani (LB) medium at 37 ^{o}C for 12 h with reciprocal shaking of 600 rpm. The harvested cells were suspended into three culture tubes containing 10 mL of sterile 0.85% NaCl solution in the presence or absence of the monolith samples. After 0, 5 and 10 h incubation at 37 ^{o}C and 600 rpm, aliquots of the cell suspension were withdrawn and spread on LB agar plates. The number of colonies that appeared on the plates after overnight cultivation at 37 ^{o}C were counted visually, and the antibacterial effects of the monolith samples were evaluated based on the colony formation.

1.3 Results and Discussion

Fabrication of PGA monolith

A mixture of DMSO, water and ethanol was used as the solvent for TIPS in the fabrication of the PGA monolith. In general, the selection of a combination of solvent and non-solvent is a crucial factor to fabricate monoliths. DMSO is known to solubilize PGA in the acid form, and the other two solvents, water and ethanol, were selected as non-solvents for PGA owing to the good miscibility of DMSO. The PGA monolith was not formed by the solo use of water or ethanol as non-solvent.

The effects of the molecular mass and concentration of PGA as well as the solvent composition on the morphology of the monolith have been systematically examined. At first, the monolith was prepared by using PGA with molecular mass of 5,000 kDa in a mixture of DMSO/water/ethanol = 9/1/20. When the PGA concentration was 15%, the uniform shape of the monolith was formed (Figure 1-2). The SEM observation showed the three-dimensional continuous interconnected porous structure of the monolith. The average pore and skeleton sizes of the monolith was 0.1-0.3 μm and 0.2-1.0 μm, respectively, indicating the formation of the monolith in the submicron scale.

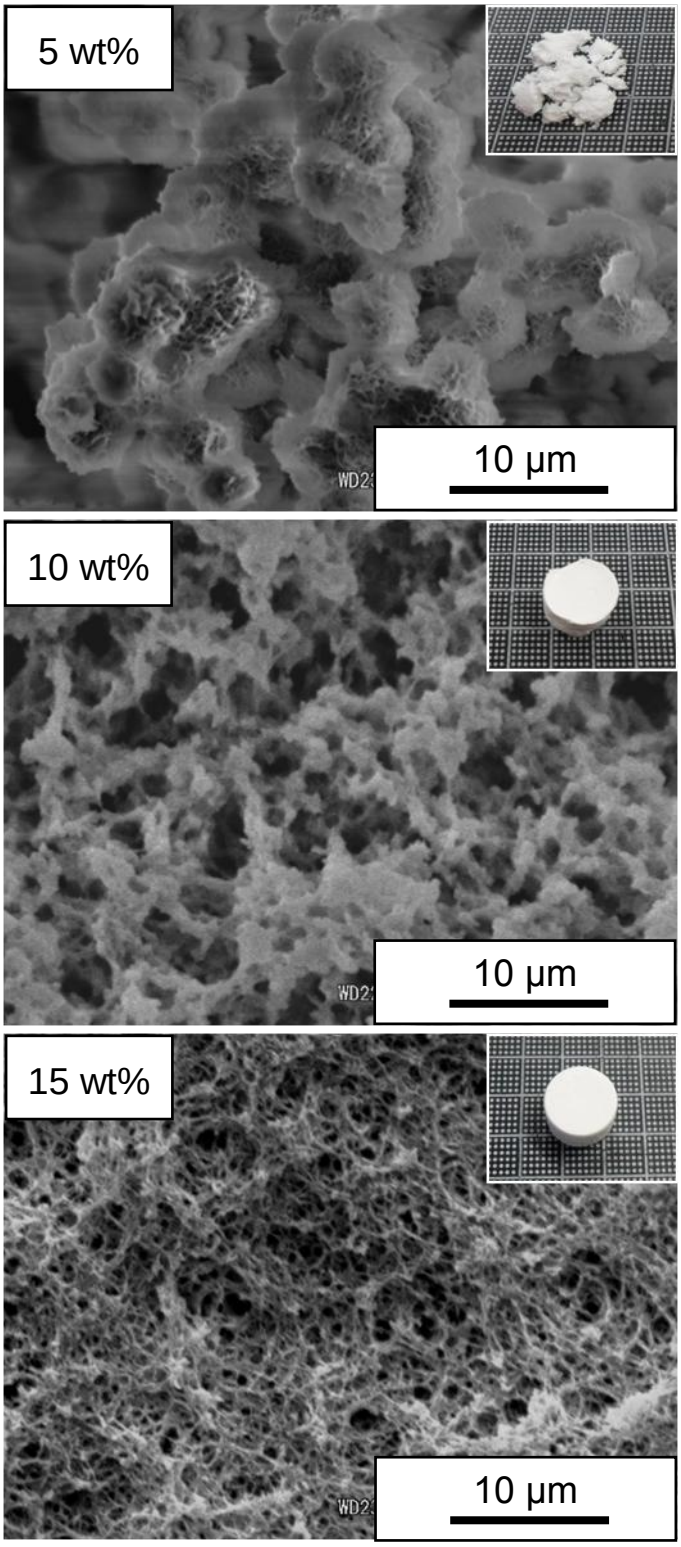

Figure 1-2. SEM images of the PGA monoliths with different concentration of PGA (molecular mass of PGA: 5,000 kDa).

Figure 1-3 shows the adsorption/desorption isotherms of the PGA monolith (molecular mass of PGA: 5,000 kDa, concentration of PGA: 15 wt%, mixture of DMSO/water/ethanol = 9/1/20). The obtained traces were assigned to a type II adsorption with H3 type hysteresis loop in the P/P_0 range from 0.8 to 1.0, characteristic of unrestricted monolayer-multilayer adsorption of macroporous absorbents.[25-27] The specific surface area was determined to be 75 m^2/g, considering monolayer adsorption by using the BET method. This result indicates the relatively large surface area of the PGA monolith.

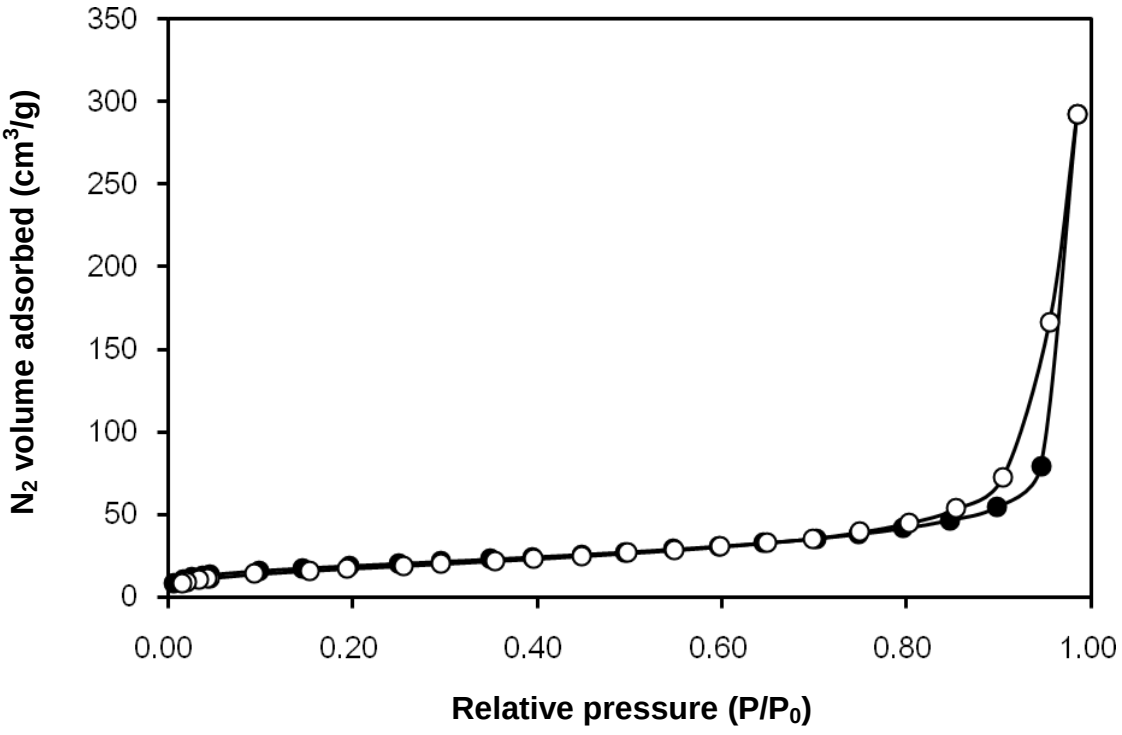

Figure 1-3. Nitrogen adsorption/desorption isotherms of PGA monolith (molecular mass of PGA: 5,000 kDa; concentration of PGA: 15 wt%; mixture of DMSO/water/ethanol = 9/1/20). Adsorption points are marked by filled circles and desorption points by empty circles.

The concentration of PGA strongly affected the formation of the monolith. In the concentration of 10%, the monolith was obtained; however, the edge of the monolith was broken, suggesting the low strength of the monolith. Such a monolith prone to be easily broken by physical impact is not suitable for applications. The monolith shape was not maintained during the work-up procedure in the concentration of 5%. These data indicate that the concentration of 15% is suitable for the fabrication of the PGA monolith with uniform structure. The BET surface area increased slightly as a function of the concentration; the surface area values of the product obtained in the concentration of 5 and 10% were 56 and 70 m^2/g, respectively.

The effect of the molecular mass of PGA has been examined in the fixing of the PGA concentration at 15% (Figure 1-4). The monolith was not formed from the low molecular mass PGA (50 kDa). When the molecular mass of PGA was 500 kDa, the monolith was obtained with uniform structure; however the edge of the monolith was partly broken. These results show that a high molecular mass (5,000 kDa) is required for the fabrication of the PGA monolith with high strength. The BET surface area of the monolith from PGA with molecular mass of 500 kDa was 74 m^2/g, suggesting the little effect of the molecular mass on the surface area.

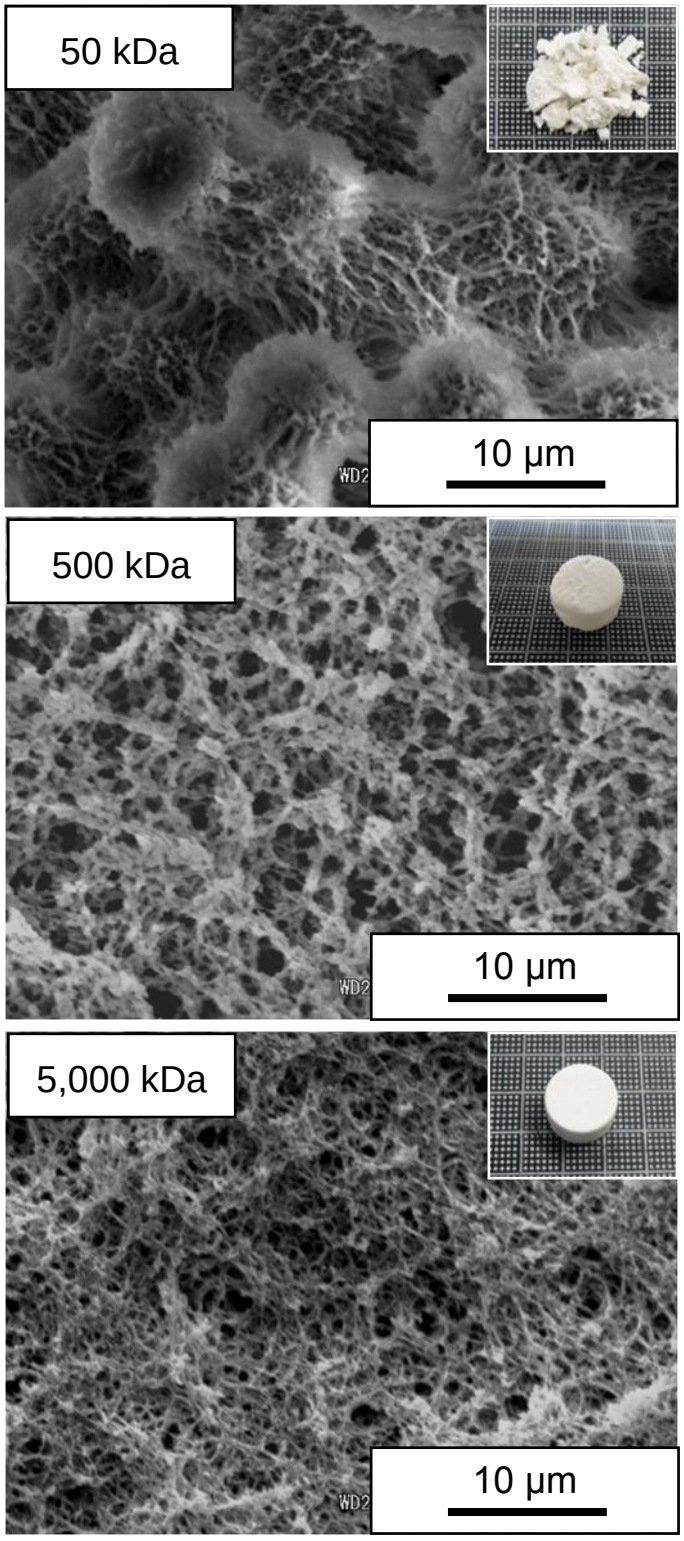

Figure 1-4. SEM images of PGA monoliths with different molecular mass (concentration of PGA: 15 wt%).

The structure of the monolith also depended on the solvent composition. In fixing the ratio of water under the conditions of the PGA concentration of 15% and the molecular mass of 5,000 kDa, the mixed ratio of DMSO and ethanol varied. In all the cases examined (DMSO/water/ethanol = 9/1/20, 11/1/18, 13/1/16 and 15/1/14 (v/v)), the monolith with the uniform shape was obtained (Figure 1-5).

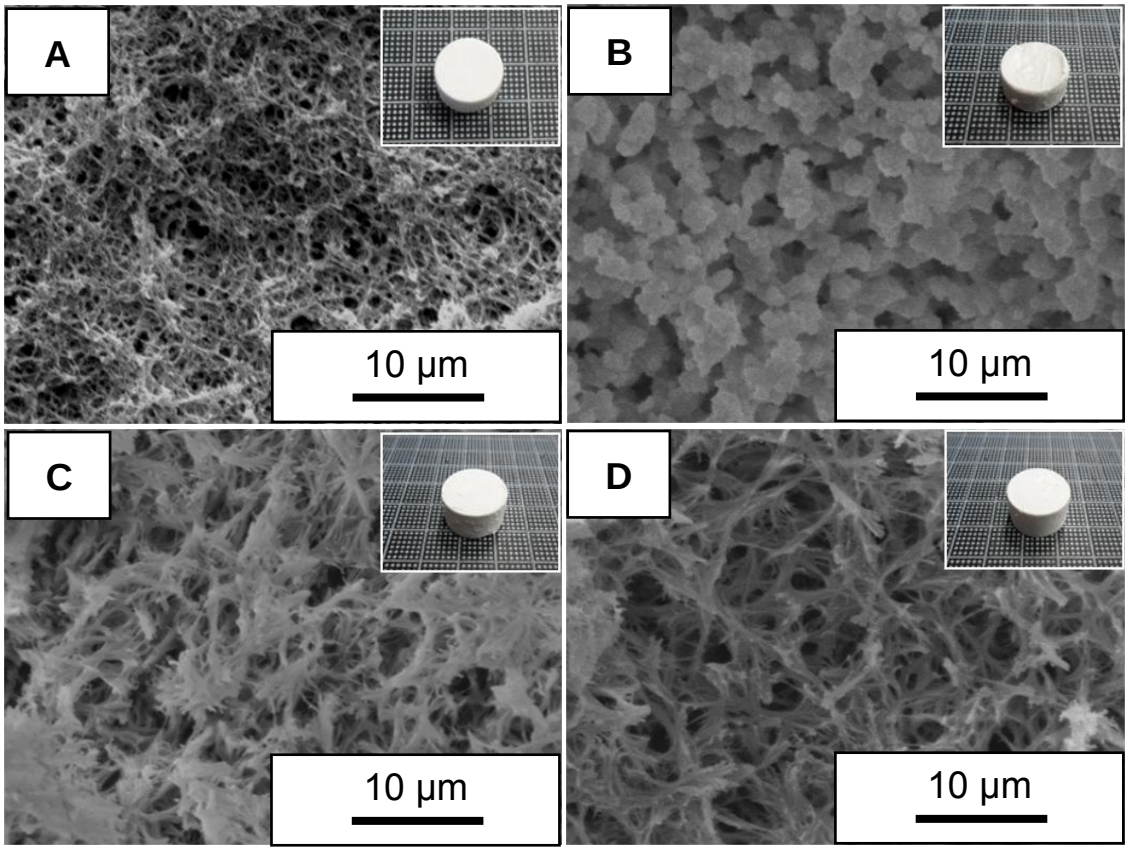

Figure 1-5. SEM images of PGA monoliths with different solvent compositions. DMSO/water/ethanol = 9/1/20 (A), DMSO/water/ethanol = 11/1/18 (B), DMSO/ water/ethanol = 13/1/16 (C), DMSO/water/ethanol = 15/1/14 (D) (molecular mass of PGA: 5,000 kDa; concentration of PGA: 15 wt%).

The ratio of DMSO in the mixed solvent strongly affected the average pore size (Figure 1-6). The pore size was the lowest when the DMSO ratio was 30%, and the size hardly changed in the range of the DMSO ratio from 37% to 50%. This could be explained as follows. When the ratio of solvent (DMSO) for PGA was smaller, the movement of PGA molecules was limited and the phase separation took place faster due to the lower solubility of PGA toward the mixed solvent, resulting in the reduction of the pore size. As for the specific surface area of the monolith, the opposite tendency was observed; the surface area was the largest in the smallest ratio of DMSO.

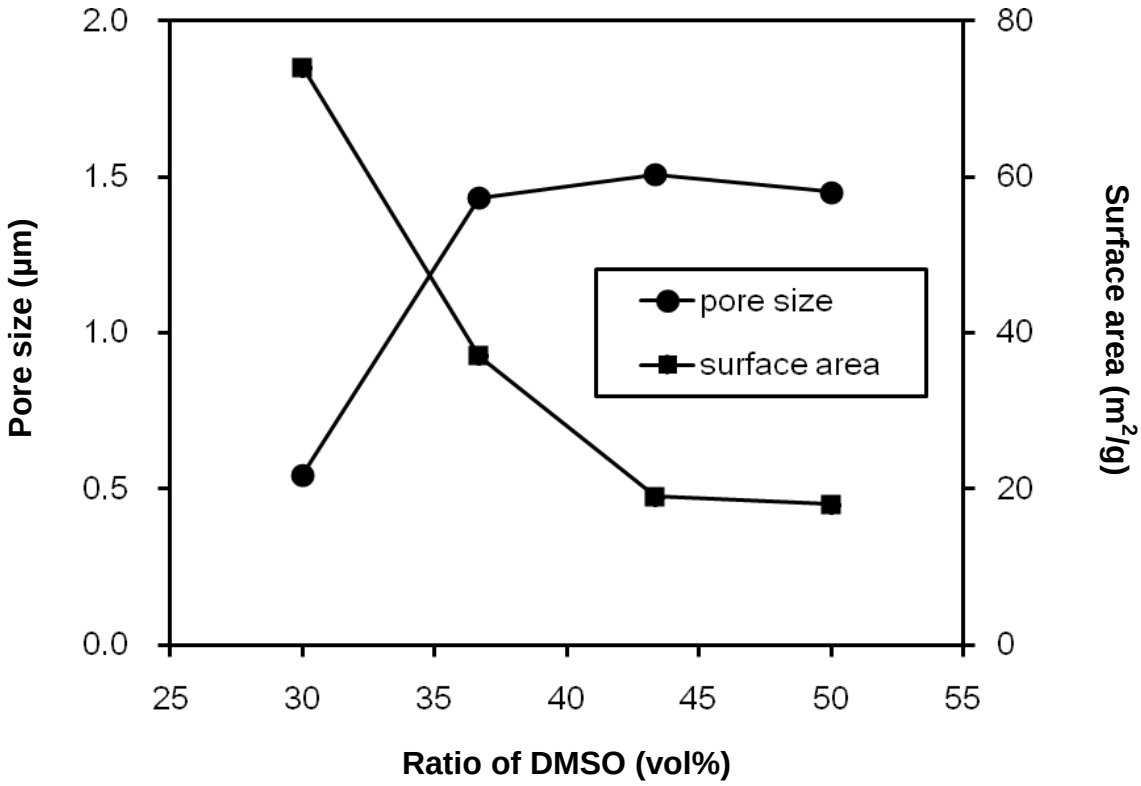

Figure 1-6. Effect of solvent composition on pore size and surface area of the PGA monolith (molecular mass of PGA: 5,000 kDa; concentration of PGA: 15 wt%).

Crosslinking of PGA monolith

The sodium form of PGA shows high solubility toward water; thus, the PGA monolith was quickly soluble in neutral and basic aqueous media owing to the large surface area of the monolith. The fast solubilization may be preferable in some applications; however, water resistance monolith is often required for usage in various fields. Therefore, the crosslinking of the PGA monolith has been examined.

So far, various crosslinking methods of PGA have been reported. PGA in an aqueous solution was easily crosslinked by γ-irradiation to produce a PGA hydrogel with high degree of swelling.[28] For the chemical crosslinking of PGA, several agents such as polyfunctional epoxy, amine, and alcohol compounds were used;[29-32] however, the reaction was often used in an aqueous medium, which cannot be applied for the crosslinking of the PGA monolith owing to the fast solubilization of the monolith toward aqueous media.

In this study, HDI was used as crosslinking agent. HDI is insoluble in water and the crosslinking with HDI is often performed in a non-aqueous medium. The crosslinking of PGA with HDI was already reported.[33] In general, a reaction of isocyanate and carboxylic acid proceeds under relatively mild conditions without any catalysts and additives. Here, the monolith fabricated by using PGA with the molecular mass and concentration of 5,000 kDa and 15%, respectively, in a mixture of DMSO/water/ethanol = 9/1/20 was used for the crosslinking with HDI.

At first, the PGA monolith was crosslinked in acetone. When the resulting material was immersed in water, the monolith did not maintain its original shape. This may be because the crosslinking in acetone did not proceed uniformly. Acetone is a non-solvent for PGA; thus, the crosslinking in acetone might take place only at the surface of the skeleton of the PGA monolith.

To improve the affinity of the PGA skeleton toward the crosslinking solvent, a small amount of water was added to the reaction mixture, which produced the monolith with high resistance toward water as well as organic solvents such as DMSO, *N*,*N*-dimethylformamide, methanol, chloroform, and hexane; the monolith shape hardly changed by the immersion into these organic solvents, and the weight change after the immersion was almost zero. Figure 1-7 shows the FT-IR spectra of the PGA monolith before and after the crosslinking with HDI. The relative intensity of a peak at 1730 cm^{-1} ascribed to the C=O stretching of the carboxylic acid significantly became smaller after the reaction, indicating that the carboxylic acid groups of PGA had reacted with HDI to form the crosslinked monolith. A reaction of isocyanates with water is well known; thus HDI might be competitively reacted with PGA and water. The high solvent resistance and FT-IR analysis of the crosslinked monolith suggest that the preferential reaction of PGA with HDI took place under the present conditions.

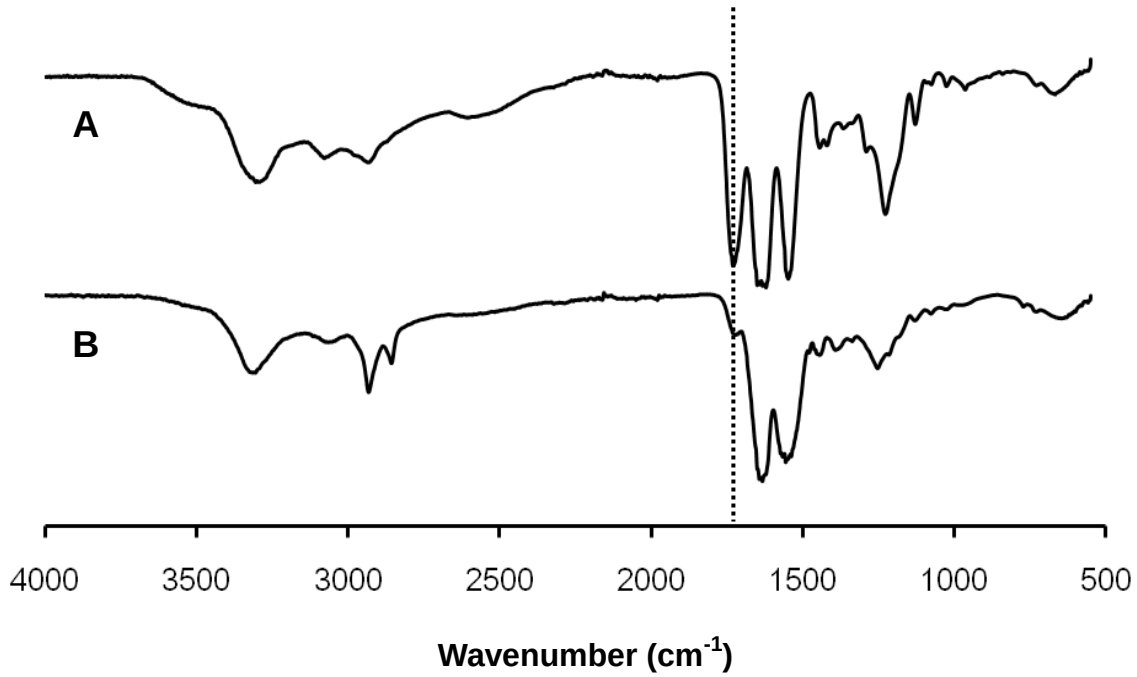

Figure 1-7. FT-IR spectra of the PGA monolith (A) and crosslinked PGA monolith (B).

The morphology of the monolith after the crosslinking was confirmed by SEM. The morphology was almost the same before and after the crosslinking; the similar porous structure was observed in the SEM photograph of the crosslinked PGA monolith. The BET surface area of the crosslinked monolith was 78 m^2/g. This value was very close to that before the crosslinking. These data strongly suggest that the morphology was scarcely changed by the crosslinking.

Monolith fabrication using sodium chloride solution

In aqueous solutions containing a salt, the PGA conformation and properties are known to change in comparison with those in water.[4,5,22] A sodium chloride aqueous solution was used instead of water for the monolith fabrication of PGA with molecular mass of 5,000 kDa. The concentration of sodium chloride was 0.3% for the total solution of DMSO/sodium chloride solution/ethanol = 9/1/20. The monolith was similarly obtained by using the sodium chloride solution, which was crosslinked with HDI in the aqueous acetone solution.

After the crosslinking, sodium chloride was removed with water repeatedly, followed by the solvent replacement with acetone in the monolith and drying *in vacuo* to give the purified monolith. The morphology of the crosslinked monolith was similar to that without sodium chloride (Figures 1-8A and B). The specific surface area of the monolith obtained by using the sodium chloride solution was smaller than that without sodium chloride, whereas the porosity was almost the constant even in the presence of sodium chloride (Table 1-1).

SEM observation of the monolith swollen in water was performed by using the samples obtained by lyophilization (Figures 1-8C and D). The pore size of the lyophilized monolith obtained by using the sodium chloride was larger than that without sodium chloride; the pore sizes of the monolith prepared in the absence and presence of

sodium chloride was 1.0-5.0 μm and 5.0-10 μm, respectively.

Table 1-1. Properties of crosslinked PGA monolith fabricated without and with sodium chloride

Sodium chloride[a)]	Surface area[b)] (m^2/g)	Porosity (%)	Swelling ratio[c)] (%) Buffer[d)] pH			Water Retention (%)
			4	7	10	
Absence	78	90	540	550	520	85
Presence	47	90	630	760	1,000	88

[a)]Concentration of sodium chloride: 0.3%; [b)]Determined by BET method; [c)]Data after 24 h; [d)]pH standard solution (pH 4: phthalate buffer; pH 7: phosphate buffer; pH 10: carbonate buffer).

The swelling ratio of the PGA monolith was measured in buffers of different pH (4, 7, and 10). The monolith was rapidly swollen and the equilibrium of the swelling was reached after 24 h. The swelling ratio of the monolith obtained in the presence of sodium chloride was larger than that without sodium chloride, probably due to the morphological difference of the swollen monolith as shown in Figure 1-8. The swelling ratio of the monolith prepared in the absence of sodium salt hardly changed despite the difference of pH of the buffer. On the other hand, the swelling ratio increased as a function of the buffer pH by using the sodium chloride solution for the fabrication of the monolith. This may be because the acid form of PGA was converted to the sodium form

during the monolith fabrication in the presence of sodium chloride, resulting in a different inside structure of the monolith. This pH-sensitive swelling behavior can be applied for the matrix of controlled drug delivery and biosensor.[34]

The water retention was slightly increased by the addition of sodium chloride in the fabrication of the monolith. This also suggests the morphological difference of the swollen monolith owing to the presence of sodium chloride in the monolith fabrication.

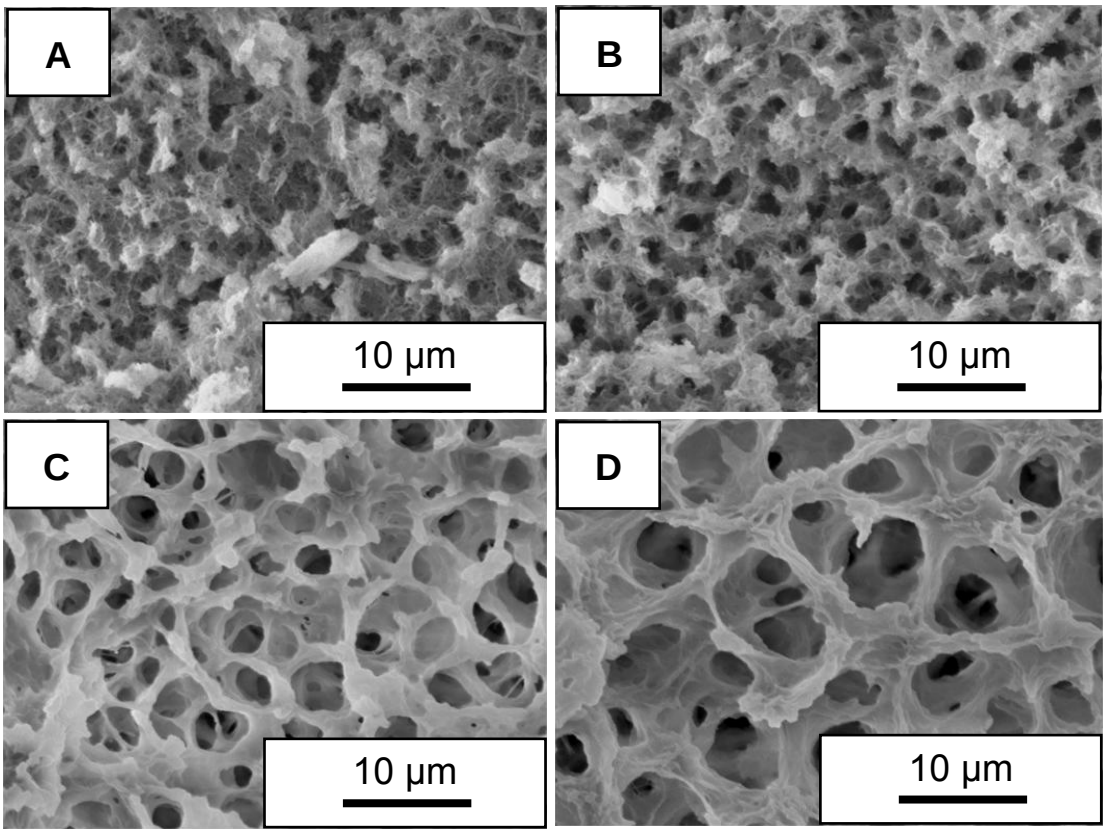

Figure 1-8. SEM images of PGA monoliths.

crosslinked PGA monolith fabricated without sodium chloride (A) and with sodium chloride (B), and lyophilized PGA monolith fabricated without sodium chloride (C) and with sodium chloride (D) (molecular mass of PGA: 5,000 kDa; concentration of PGA: 15 wt%).

Interestingly, the wet PGA monolith showed deformability (Figure 1-9). By the finger compression, water was easily released from the wet monolith and the resulting monolith rapidly returned to the original shape by absorption of water. The monolith could be repeatedly deformed by the compression and water absorption. Unlike in the case of materials with closed pore, monoliths generally do not show good flexibility in water. Therefore, this unique behavior will expand the application of the PGA monolith in various fields.

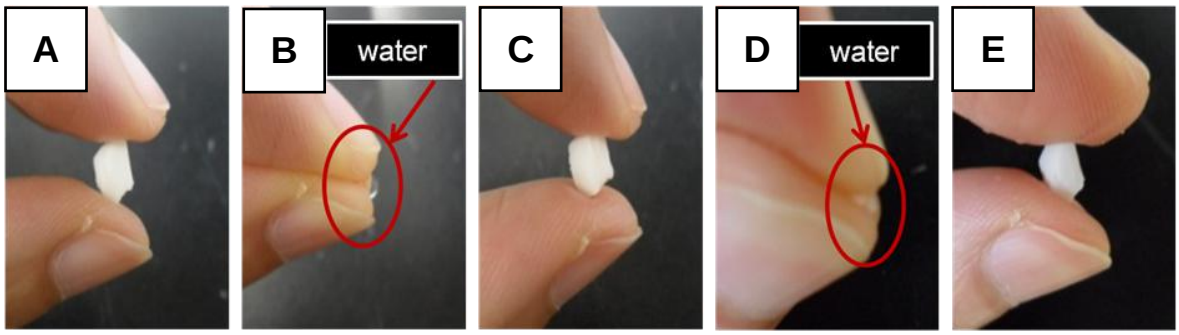

Figure 1-9. Deformation of a wet crosslinked PGA monolith.

water-absorbed monolith (A), water release upon finger compression (B), return to original shape by water absorption (C), second compression (D), and second return to original shape (E).

Copper(II) adsorption by crosslinked PGA monolith

Removal of toxic metals and recycling of noble metals are important technologies in various industrial fields.[35,36] For example, heavy metals in the environment are a matter of great concern and threaten public health; thus, high-performance adsorbents for environmental remediation are strongly desired, in which fast treatment of a large amount of waste and efficient removal ability are simultaneously required.

As one of the possible applications of the crosslinked PGA monolith, the adsorption of copper(II) on the monolith has been examined by a batch method. The crosslinked monoliths fabricated in the absence and presence of sodium chloride were used. Previously, we reported that PGA has strong chelation ability toward Ca^{2+}, Mg^{2+}, Fe^{2+}, *etc.*, owing to the unique polyanionic structure of PGA.[22] The amide and carboxylate groups of PGA in the crosslinked monolith would possess high affinity toward heavy and noble metals. Figure 1-10 shows the time-course of the $Cu(II)Cl_2$ adsorption capacity of the monolith, which was determined by the change of the $Cu(II)Cl_2$ concentration in the supernatant. In the initial period, the $Cu(II)Cl_2$ was rapidly adsorbed on the monolith. Later, the adsorbed amount gradually increased until 24 h and, afterwards, it was almost constant. The adsorption capacity of the monolith fabricated in the presence of sodium chloride was somewhat larger than that without sodium chloride, and the final adsorption capacity reached 1.0 mmol per g of the monolith. This fast adsorption may be ascribed to the characteristic structure of the monolith.[13]

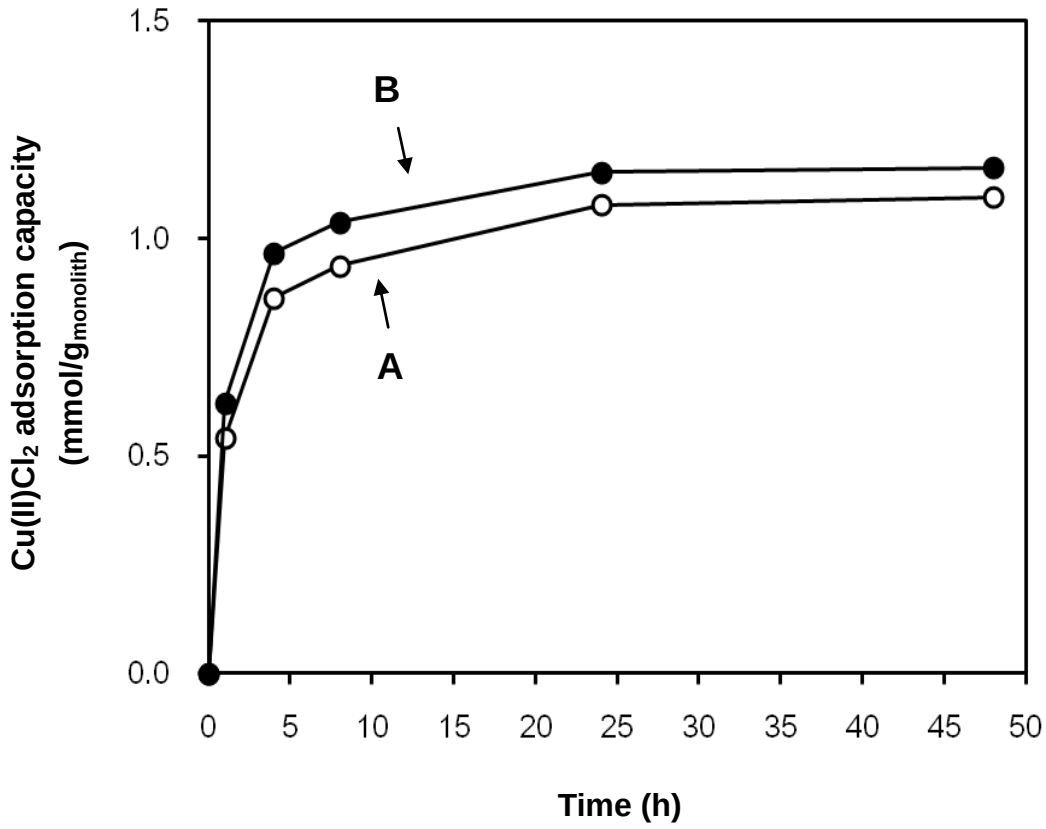

Figure 1-10. $Cu(II)Cl_2$ adsorption capacity of crosslinked PGA monoliths.
Fabricated without sodium chloride (A) and with sodium chloride (B) (molecular mass of PGA: 5,000 kDa; concentration of PGA: 15 wt%).

The surface and inside of the monolith after the immersion in the $CuCl_2$ solution were uniformly blue-colored, and the morphology of the copper(II)-immobilized monolith was almost the same as that before the adsorption (Figure 1-11). The chelation of $Cu(II)Cl_2$ on the crosslinked PGA monolith was confirmed by FT-IR spectroscopy; peaks ascribed to the C=O stretching were slightly changed (Figure 1-12).

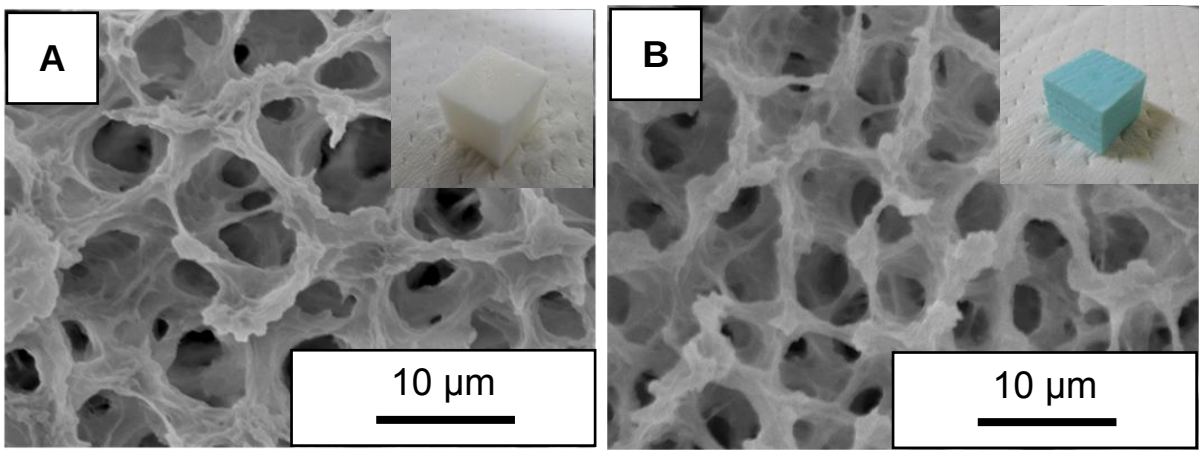

Figure 1-11. SEM images of the crosslinked PGA monolith before (A) and after (B) adsorption of $Cu(II)Cl_2$.

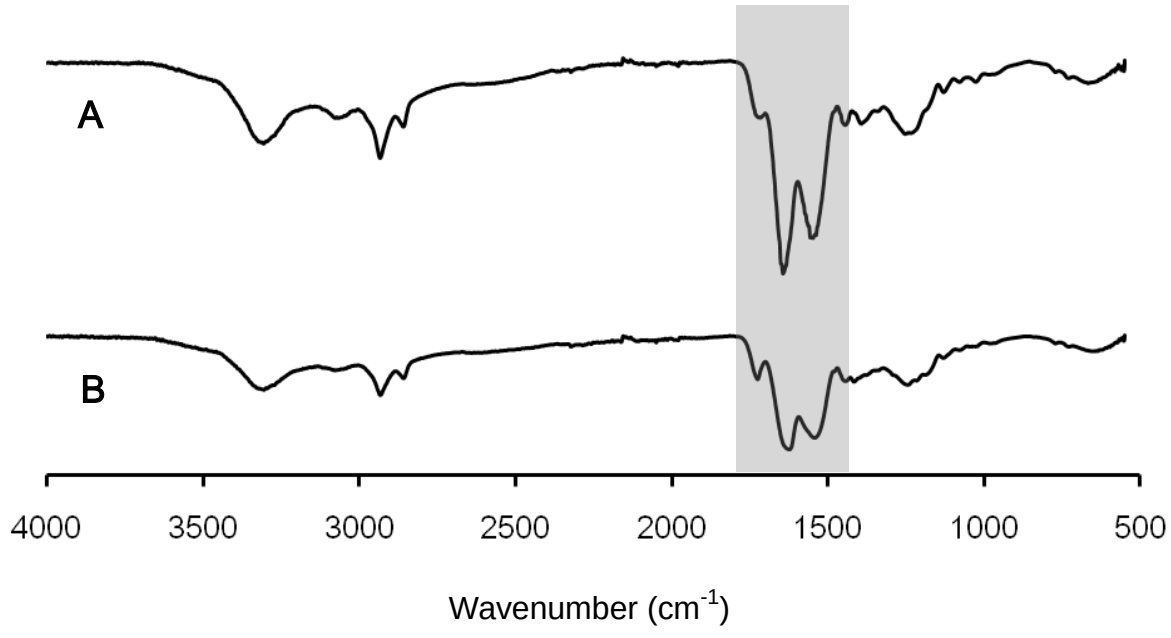

Figure 1-12. FT-IR spectra of the crosslinked PGA monolith before (A) and after (B) adsorption of $Cu(II)Cl_2$.

The existance of copper in the monolith was found by the EDX analysis; in the EDX spectrum, peaks of the copper element at 0.9, 8.1 and 8.9 keV were detected, demonstrating the immobilization of copper(II) on the crosslinked monolith. Figure 1-13 shows EDX images of the crosslinked PGA monolith before and after the adsorption of $Cu(II)Cl_2$, which clearly shows that $Cu(II)Cl_2$ was homogeneously immobilized on the surface of the resulting monolith. The increase of the copper amount on the monolith was confirmed by the EDX elemental analysis; the copper ratios before and after the immobilization of copper were 0.63 and 6.94 wt%, respectively.

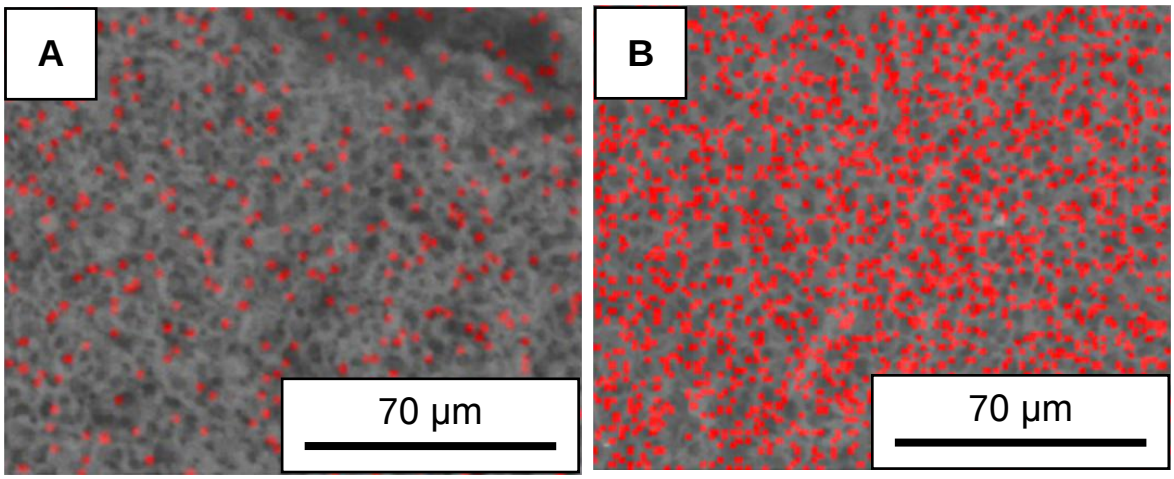

Figure 1-13. EDX images of crosslinked PGA monolith before (A) and after (B) adsorption of $Cu(II)Cl_2$ (red spot; copper element).

Antibacterial activity

Copper(II) ion exhibits high antibacterial activity *in vitro*, and various kinds of complexes of copper(II) ion and organic compounds having remarkable antimicrobial activity were synthesized.[37] The antibacterial activity of the copper(II)-immobilized crosslinked PGA monolith was examined by the incubation of *E. coli* in the presence of the monolith (Figure 1-14). The initial seeding number of *E. coli* was 4.84×10^7 CFU/mL (black bars in Figure 1-14A). The number of colony formation was almost the same in the absence and presence of the crosslinked PGA monolith after 10 h, which suggests no bacteria-killing action. On the other hand, the number of colony formation decreased greatly to 4.10×10^2 CFU/mL after 5 h, and all the cells were dead after 10 h in the presence of the copper(II)-immobilized crosslinked PGA monolith, indicating its strong antibacterial activity.

Figure 1-14B shows pictures of the LB agar plates, on which *E. coli* cells incubated for 10 h in the NaCl solution with or without the monolith samples were spread. Almost all the cells were viable in the presence of the crosslinked PGA monolith, confirming that the crosslinked PGA monolith has no antibacterial effect against *E. coli* cells. However, no viable cells were observed in the presence of the copper(II)-immobilized monolith. These data clearly suggest that the copper(II)-immobilized crosslinked PGA monolith has large potential as an antibacterial biodegradable material in the environmental and biomedical fields.

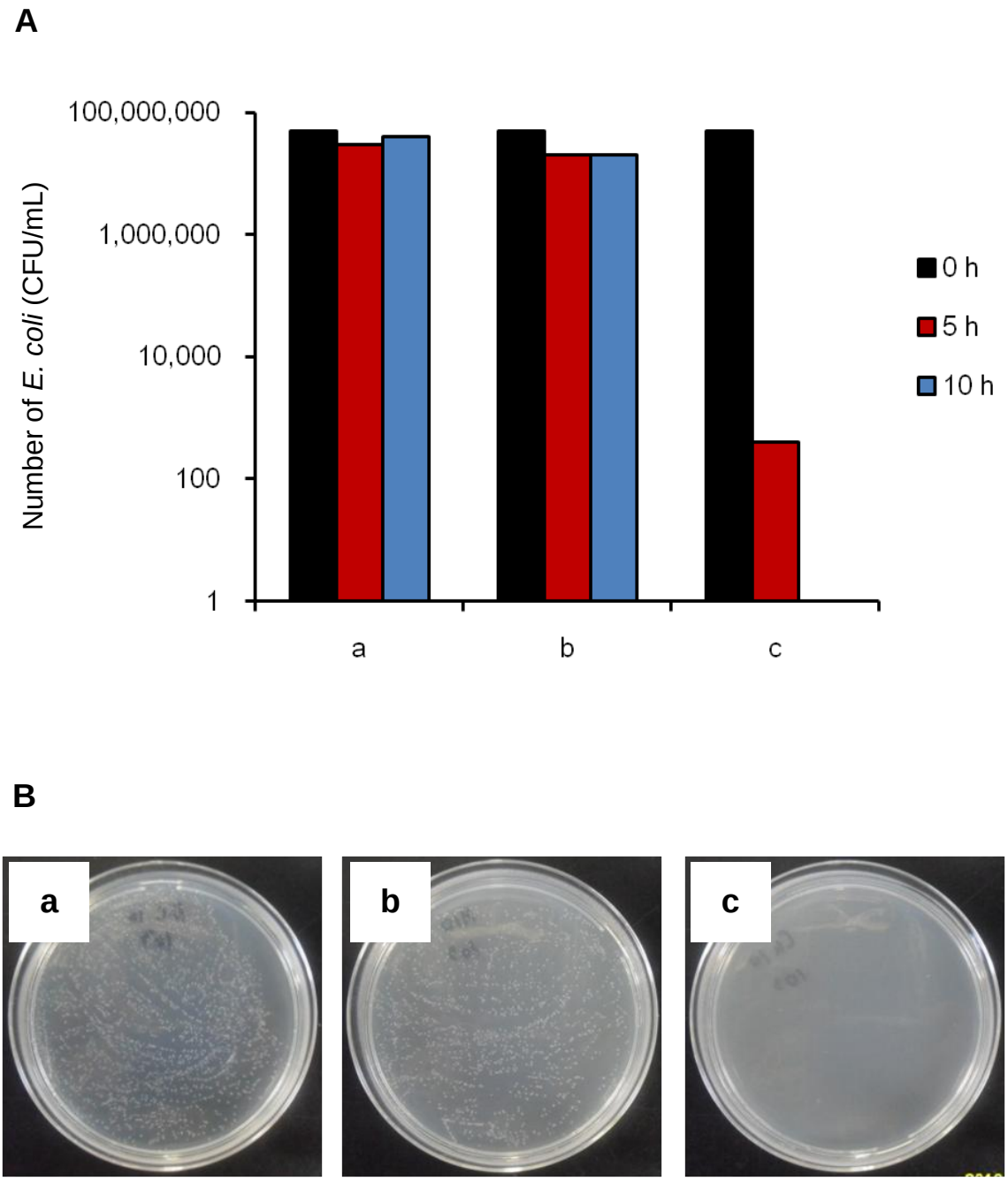

Figure 1-14. Number of *E. coli* colonies after different incubation times (0, 5 and 10 h) (A) and representative pictures of viable *E. coli* colonies on LB agar plates for 10 h (B) incubation without crosslinked PGA monolith (a), with crosslinked PGA monolith (b), and copper(II)-immobilized crosslinked PGA monolith (c).

1.4 Conclusion

Polymeric monoliths have large potentials for various applications in industrial fields. In this study, the fabrication of a new class of new functional polymeric monolith based on PGA was successfully achieved by the TIPS technique. A combination of DMSO, water, and ethanol enabled the production of the PGA monolith with a uniform shape. The monolith had a relatively large surface area in the pore and skeleton sizes of sub-micron range. The PGA monolith was converted to the water-insoluble monolith by crosslinking with HDI. The crosslinked monolith possessed high resistance toward water as well as organic solvents. The unique deformability of the wet crosslinked monolith was found. Furthermore, the crosslinked monolith effectively adsorbed $Cu(II)Cl_2$ from the aqueous solution, and the copper(II)-immobilized crosslinked PGA monolith showed strong antibacterial activity against the *E. coli* cells. The present crosslinked PGA monolith having a peptide bond and a carboxylic acid groups, is expected to be applied for biomedical and environmental functional materials.

References

[1] M. Ashiuchi, T. Kamei, H Misono, *J. Mol. Catal. B: Enzym.* **2003**, *23*, 101.

[2] M. Ashiuchi, C Nawa, T Kamei, J. J. Song, S. P. Hong, M. H. Sung, K. Soda, T. Yagi, H. Misono, *Eur. J. Biochem.* **2001**, *268*, 5321.

[3] T. Candela, A. Fouet, *Mol. Microbiol.* **2006**, *60*, 1091.

[4] H. Poo, C. Park, M. S. Kwak, D. Y. Choi, S. P. Hong, I. H. Lee, Y. T. Lim, Y. K. Choi, S. R. Bae, H. Uyama, C. J. Kim, M. H. Sung, *Chem. Biodivers.* **2010**, *7*, 1555.

[5] M. H. Sung, C. Park, C. J. Kim, H. Poo, K. Soda, M. Ashiuchi, *Chem. Rec.* **2005**, *5*, 352.

[6] M. R. Buchmeiser, *Polymer* **2007**, *48*, 2187.

[7] O. G. Potter, F. F. Hilder, *J. Sep. Sci.* **2008**, *31*, 1881.

[8] J. Courtois, E. Bystrom, K. Irgum, *Polymer* **2006**, *47*, 2603.

[9] F. Svec, *J. Chromatogr. A* **2010**, *1217*, 902.

[10] F. Svec, C. G. Huber, *Anal. Chem.* **2006**, *78*, 2100.

[11] S. Wei, Y. L. Zhang, H. Ding, J. Liu, J. Sun, Y. He, Z. Li, F. S. Xiao, *Colloids Surf. A* **2011**, *380*, 29.

[12] K. Okada, M. Nandi, J. Maruyama, T. Oka, T. Tsujimoto, K. Kondoh, H. Uyama, *Chem. Commun.* **2011**, *47*, 7422.

[13] H. Uyama, *Kobunshi Ronbunshu.* **2010**, *67*, 489.

[14] M. Nandi, K. Okada, A. Dutta, A. Bhaumik, J. Maruyama, D. Derks, H. Uyama, *Chem. Commun.* **2012**, *48*, 10283.

[15] M. Nandi, K. Okada, H. Uyama, *Funct. Mater. Lett.* **2011**, *4*, 407.

[16] Y. Xin, T. Fujimoto, H. Uyama, *Polymer* **2012**, *53*, 2847.

[17] Y. Xin, H. Uyama, *Chem. Lett.* **2012**, *41*, 1509.

[18] Y. Xin, H. Uyama, *Polym. Res. J.* **2013**, *7*, 149.

[19] X. Sun, T. Fujimoto, H. Uyama, *Polym. J.* **2013**, *45*, 1101.

[20] S. R. Bae, C. Park, J. C. Choi, H. Poo, C. J. Kim, M. H. Sung, *J. Microbiol. Biotechnol.* **2010**, *20*, 803.

[21] I. L. Shih, Y. T. Van, *Bioresour. Technol.* **2001**, *79*, 207.

[22] T. Tsujimoto, J. Kimura, Y. Takeuchi, H. Uyama, C. Park, M. H. Sung, *J. Microbiol. Biotechnol.* **2010**, *20*, 1436.

[23] E. H. Lee, H. Uyama, O. H. Kwon, M. H. Sung, *Polym. Bull.* **2009**, *63*, 735.

[24] T. Tajima, S. Ueno, N. Yabu, S. Sukigara, F. Ko, *J. Appl. Polym. Sci.* **2011**, *122*, 150.

[25] L. Cao, Y. Shi, J. Q. Geng, D. Yang, *Mater. Chem. Phys.* **2011**, 130, 1280.

[26] B. Holland, *J. Porous Mater.* **2003**, *10*, 17.

[27] M. Khalfaoui, S. Knani, M. A. Hachicha, A. B. Lamine, *J. Colloid Interface Sci.* **2003**, *263*, 350.

[28] M. Kunioka, *Macromol. Biosci.* **2004**, *4*, 324.

[29] B. Cao, J. Yin, S. Yan, L. Cui, X. Chen, Y. Xie, *Macromol. Biosci.* **2011**, *11*, 427.

[30] E. H. Lee, Y. Kamigaito, T. Tsujimoto, H. Uyama, M. H. Sung, *J. Microbiol. Biotechnol.* **2010**, *20*, 1424.

[31] A. Sugino, T. Miyazaki, C. Ohtsuki, *J. Mater. Sci. Mater. Med.* **2008**, *19*, 2269.

[32] S. Murakami, N. Aoki, *Biomacromol.* **2006**, *7*, 2122.

[33] G. Tillet, B. Boutevin, B. Ameduri, *Prog. Polym. Sci.* **2011**, *36*, 191.

[34] Y. Qiu, K. Park, *Adv. Drug Deliv. Rev.* **2001**, *53*, 321.

[35] J. R. Hayes, G. W. Nyce, J. D. Kuntz, J. H. Satcher, A. V. Hamza, *Nanotechnology* **2007**, *18*, 275602.

[36] F. Xu, N. Zhang, Y. Long, Y. Si, Y. Liu, X. Mi, X. Wang, F. Xing, X. You, J. Gao, *J. Hazard. Mater.* **2011**, *188*, 148.

[37] W. R. Du, Y. L. Xu, Z. R. Xu, C. L. Fan, *Nanotechnology* **2008**, *19*, 085707.

Chapter 2

Macroscopic Cavities within a Microporous 3-D Network: A Poly(γ-glutamic acid) Monolith Prepared by Combination of Particulate Templates and a Phase Separation Technique

2.1 Introduction

Poly(γ-glutamic acid) (PGA) comprises a carboxylic acid/carboxylate in each repeat unit. This allows PGA to act as a pH-responsive material and at same time as a powerful polyvalent ligand to capture various metals efficiently.[1-7] On the basis of these characteristics, PGA was already used for some commercial applications.[8-13]

In Chapter 1, PGA monoliths were successfully fabricated by the thermally induced phase separation (TIPS) method. Thereby, interconnected small pores were introduced into the monoliths.[14-18] The monolith can be further upvalued by engineering the porosity and its chemical nature.[19-22] If the useful properties of PGA are successfully integrated into a monolith whose porosity is properly engineered, the resultant monolith will find innovative applications hitherto unexplored.

This chapter describes a unique PGA monolith in which submillimeter-sized cavities are uniformly distributed over a microporous 3-D network. Firstly, a monolith was prepared by the TIPS method from a solution of PGA in which particulate salt templates were dispersed. This as-prepared monolith was then subjected to internal crosslinking so that the monolithic structure covalently stabilized to resist water. This

allowed the salt templates to be washed off with water leaving macroscopic cavities inside the monolith. The resultant monolith was expanded and shrunk in aqueous solvents in response to pH changes. It also could capture and release metal ions in a controlled manner. These responsive behaviors were found to be fully reversible and reproducible. Thus, PGA monolith that include both large and small pores holds great promise for its technical use, *e.g.*, in gathering/recycling of rare metals, for controlled release of drugs and as a scaffold for cell growth in tissue engineering.

2.2 Experimental

Materials

PGA (acid form, $M_w = 5\times10^3$ kDa) was provided by BioLeaders Corp. (Korea). HDI was purchased from Wako Pure Chemical Industries, Ltd. (Japan). Sodium chloride (+80 mesh particle size; Sigma-Aldrich) was used as a particulate template. All reagents were of analytical grade and used as received without further purification.

Measurements

Scanning electron microscopic (SEM) images were recorded on a Hitachi S-3000N instrument at 15 kV. A thin gold film was sputtered on the samples before the images were collected. Nitrogen adsorption/desorption isotherms were measured with a NOVA 4200e Surface Area & Pore Size Analyzer (Quantachrome Instruments) at 25 ^{o}C. The Brunauer Emmett Teller (BET) method was utilized to determine specific surface areas. Before the measurements, all samples were degassed at 25 ^{o}C for 12 h under vacuum. Fourier transform infrared (FT-IR) measurements by the attenuated total

reflectance (ATR) method were performed by Thermo Scientific Nicolet iS5 with the iD5 ATR accessory. Differential scanning calorimetry (DSC) thermograms are taken using a Seiko DSC6220 instrument. The measurement is performed at the heating rate of 10 ^{o}C/min under nitrogen. Thermogravimetric analysis (TGA) is performed with an EXSTAR TG/DTA 7200 thermogravimetric analyzer from 40 to 500 ^{o}C at a heating rate of 10 ^{o}C/min, under a steady flow of nitrogen of 250 mL/min. The copper(II) concentration in aqueous solution was determined by a Hitachi U-2810 UV-visible spectrometer at 816 nm. The energy dispersive X-ray spectrometric (EDX) measurement for elemental analysis of the monolith surface was conducted by a Hitachi Miniscope TM3000 with a Swift3000 equipment.

Density of a monolith ($D_{monolith}$) was estimated from the weight and the volume of a monolith by the following equation (1). Note that the monolith was cylindrically shaped and the volume was calculated from its diameter and height.

$$D_{monolith} = \text{Weight of monolith} / \text{Volume of monolith} \quad (1)$$

Preparation of PGA monolith by TIPS with particulate salt templates

A typical procedure is as follows (Figure 2-1). PGA powder (450 mg) was completely dissolved in a mixture of dimethyl sulfoxide (DMSO), water, and ethanol (3 mL, DMSO/water/ethanol = 9/1/20) by heating at 80 ^{o}C. Sodium chloride particles (5.5 g) were then added to the solution and cooled to 25 ^{o}C. The resultant monolith was repeatedly washed with acetone to remove the solvents and subsequently dried under vacuum.

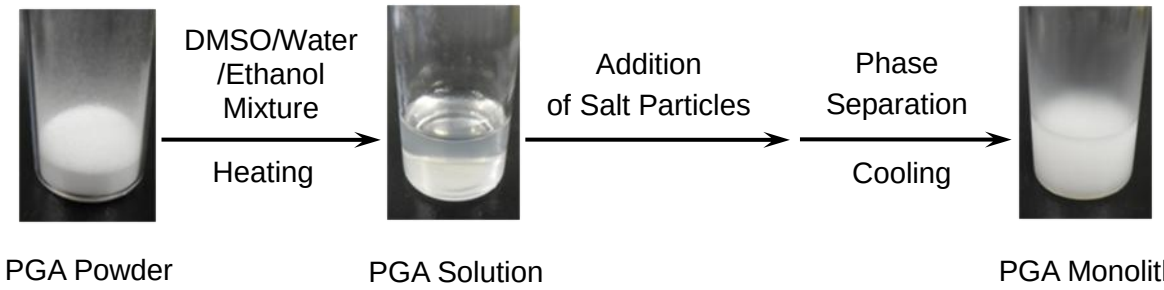

Figure 2-1. Procedure for preparation of PGA monolith *via* TIPS with particulate salt templates.

Crosslinking of PGA monolith

The as-prepared monolith (3.49 mmol monomer unit of PGA) was mixed with HDI (1 mL, 5.89 mmol) in acetone (10 mL) and left for 6 h. 300 μL of water was then added dropwise to the mixture.[23] The reaction was carried out at 50 ^{o}C with stirring gently for 24 h. The crosslinked PGA monolith was repeatedly washed with water to remove sodium chloride particles. Residual water was replaced with acetone and dried in *vacuo* to afford a salt-free crosslinked PGA monolith.

Swelling and shrinkage of PGA monolith

Swelling ratio was determined from the weights of dry and swollen monoliths (W_d and W_w, respectively) by the following equation (2). A monolith was immersed in a pH 2.0 acetate or a pH 7.0 phosphate buffer at 25 ^{o}C. The swelling process reached equilibrium within 24 h and the weight of the swollen monolith became constant thereafter. This weight was used as W_w in order to calculate the swelling ratio presented in Figure 2-9.

$$\text{Swelling ratio} = (W_w/W_d - 1) \quad (2)$$

To examine pH-responsivity, the monolith was first immersed in the buffer (pH 7.0) for 3 h, then transferred into the buffer (pH 2.0) and kept there for another 2 h. This cycle was repeated three times. Swelling ratio of the monolith was measured every hour and plotted in Figure 2-10.

Adsorption and desorption of cupric salt

Adsorption and desorption of copper(II) was examined by a batch method. A dry monolith (100 mg as a single piece) was first immersed in a 0.10 M $CuCl_2$ solution (10 mL) at pH 4.5 for 24 h. It was then transferred into a pH 1.0 buffer and gently shaken at 25 ^{o}C. The desorption process reached equilibrium in 20 h and the amount of copper(II) in the solution became constant. This amount represents the $Cu(II)Cl_2$ adsorption capacity presented in Figure 2-11.

To examine pH-responsivity, the monolith was first immersed in the pH 1.0 buffer for 5 h, then transferred into the 0.10 M $CuCl_2$ solution at pH 4.5 and kept there for another 5 h. This cycle was repeated three times with the solution temperature kept at 25 ^{o}C. The $Cu(II)Cl_2$ amount was determined after each adsorption (or desorption) step by UV-vis absorption spectroscopy and plotted in Figure 2-16.

2.3 Results and Discussion

Preparation and characterization of PGA monolith

A monolith was prepared by the TIPS method from a PGA solution containing crystalline particles of sodium chloride (Figure 2-1). SEM observation indicated that the particles were cubic and ranged 0.2-0.6 mm in size (Figure 2-2). The phase separation

conditions were similar to those reported previously.[23] The sodium chloride particles showed little solubility in the present solvent system so that the phase separation little affected.[24-28] This as-prepared PGA monolith was readily soluble in water. The monolith was therefore subjected to internal crosslinking by the reaction with HDI. The crosslinking successfully occurred as confirmed by suppression of the solubility and infrared absorption (IR) spectroscopic analysis (Figure 2-3).

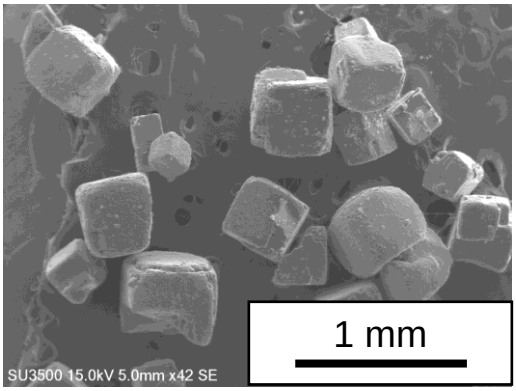

Figure 2-2. SEM image of sodium chloride particles used as templates.

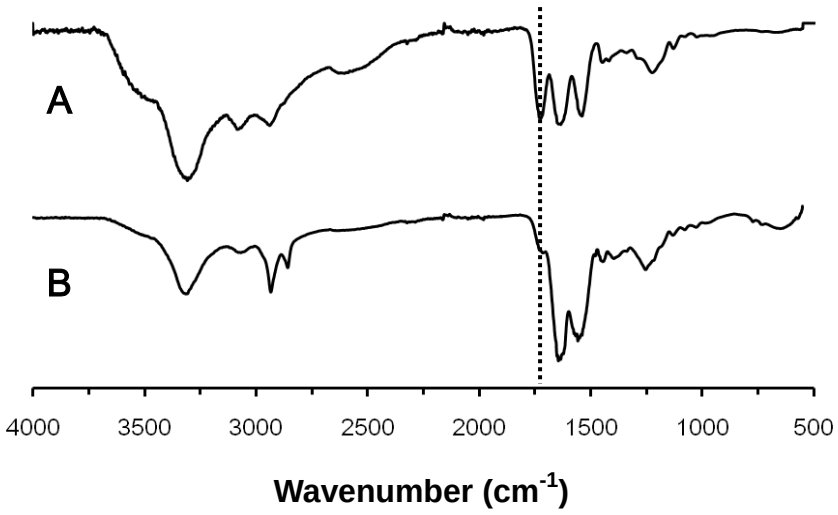

Figure 2-3. FT-IR spectra of PGA monolith before (A) and after crosslinking (B). (solid state samples).

The crosslinked material was repeatedly washed with water, whereby the salt particles incorporated in the monolith were washed off. The monolith stayed intact during the washing process. Complete removal of the salt particles was confirmed by the corresponding weight loss and cross-sectional analysis by SEM. The SEM images show the appearance of 0.2-0.3 mm-sized cavities at the positions where the salt particles resided (Figure 2-4A). The shape and size of the cavities were largely inherited from the salt particles as expected. These cavities were embedded in the monolithic matrix comprising small pores (0.2-0.8 μm) created by the phase separation. The successful leaching of the salt particles proved that the small pores were interconnected with each other to form a microporous network over the matrix. In other words, water had good access to the cavities through the microchannels and permeated the entire monolith.

Interestingly, the cavities were uniformly distributed inside the monolith. This suggests that the salt particles were homogeneously dispersed in the polymer solution from which the monolith formed. Note that such distribution could be achieved only when the content of the sodium chloride particles in the polymer solution was set to be 1.8 g/mL. With a lower sodium chloride content (1.5 g/mL), the particles settled in the polymer solution so that cavities localized in the lower part of the resultant monolith. When the monolith was prepared with a higher sodium chloride content (2.2 g/mL), the amount of the polymer solution was too small to fill the voids between particles entirely. This gave rise to the cavities that were considerably interconnected with each other, and thereby the resultant monolith turned out to be mechanically instable.

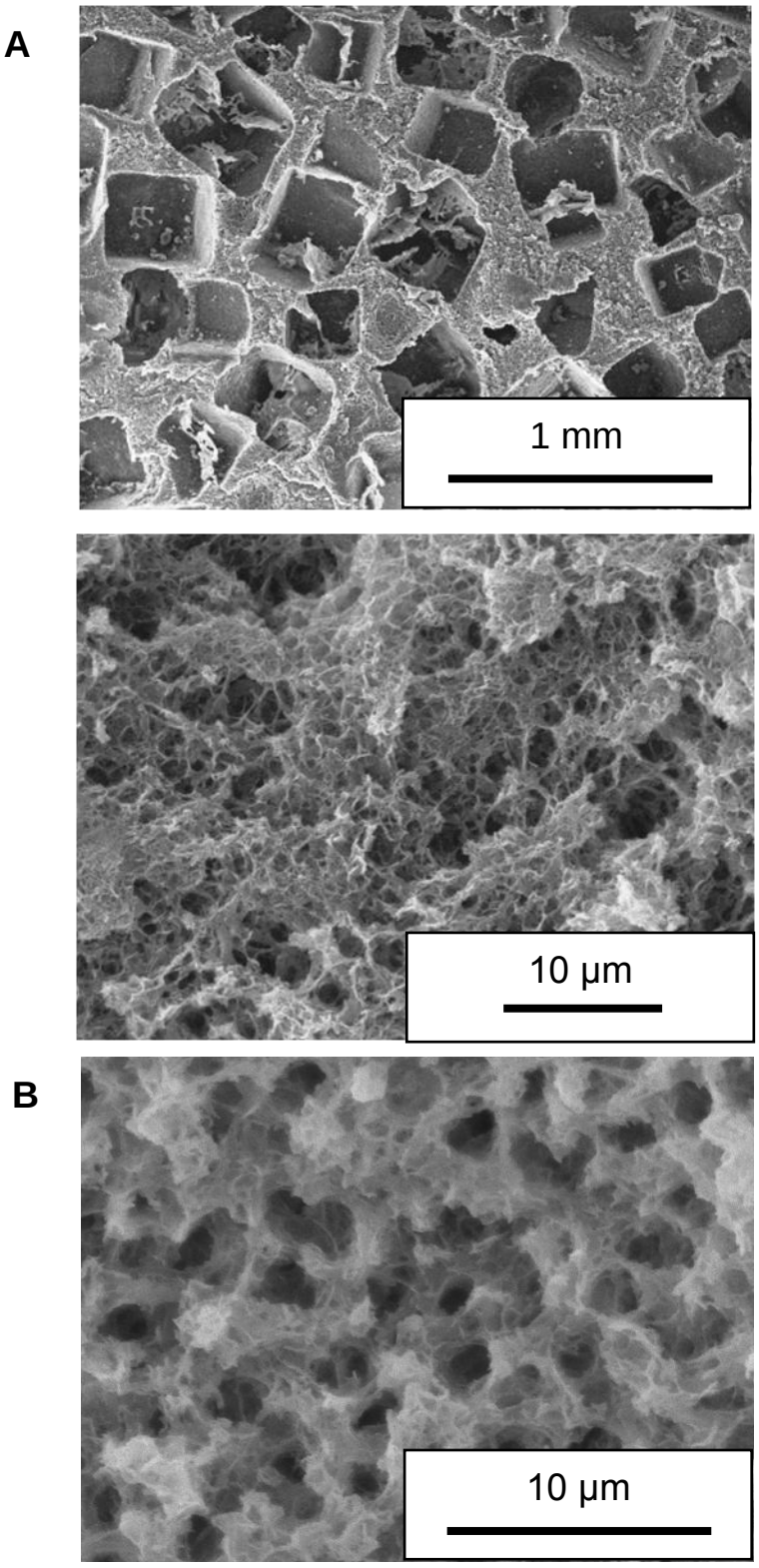

Figure 2-4. SEM images of present PGA monolith (A) (upper: low magnification, below: high magnification) and reference (B).

The specific surface area of the present monolith was estimated as 53 m^2/g by the BET method assuming monolayer adsorption (Figure 2-5). For comparison, a reference monolith was prepared according to a similar procedure but without the use of the salt templates. SEM cross-sectional analysis confirmed that the reference monolith lacked the large internal cavities, while the microporous network structure remained (Figure 2-4B). The specific surface area of the reference monolith was estimated as 47 m^2/g (Table 2-1). These results suggest that the surface area per unit mass was enlarged by installation of the cavities in the monolith. The volume of the present monolith was nearly twice larger (thus the density smaller) than the reference monolith with the same mass (Figure 2-6). The present monolith and the reference adsorbed 14.7 and 5.4 g of water per unit mass, respectively. Thus the water retention capacity of the present monolith was found more than twice larger than that of the reference.

Table 2-1. Basic features of PGA monoliths.

Method	**Surface Area[a)] [m^2/g]**	**Density [mg/cm^3]**	**Water Retention Capacity [g/g]**
Present monolith	53.3 ± 4.5	88.5 ± 17.5	14.7 ± 2.1
Reference	46.5 ± 3.3	165.5 ± 22.5	5.4 ± 0.1

[a)]Determined by BET method. Three samples were tested in each experiment.

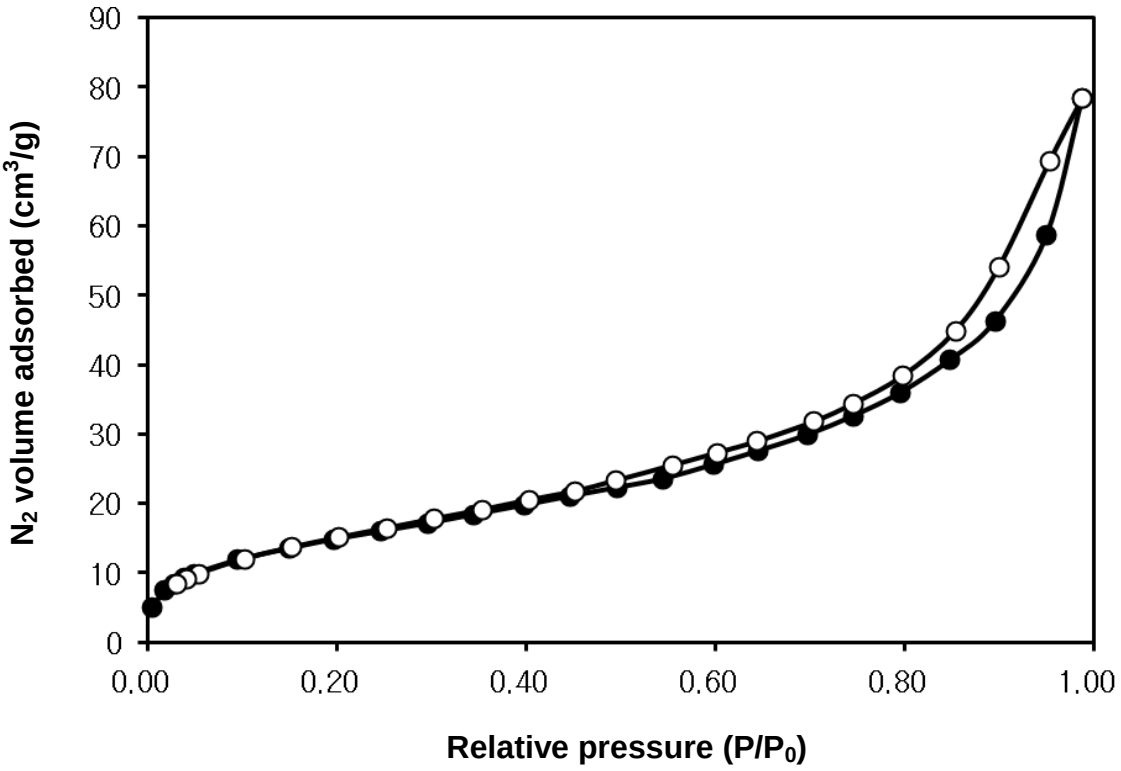

Figure 2-5. Nitrogen adsorption/desorption isotherms of PGA monolith presently prepared. Adsorption points are marked with filled circles and desorption with empty circles.

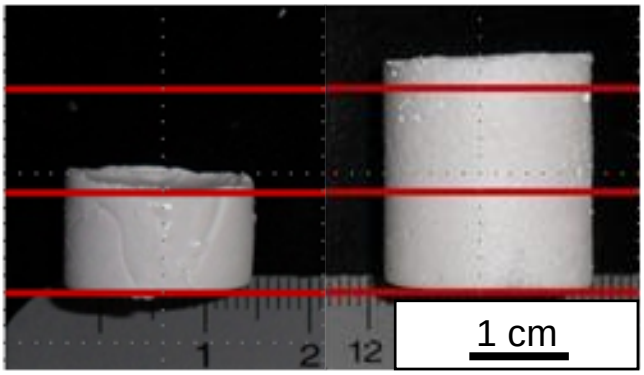

Figure 2-6. Photograph of the reference (left) and the present monolith (right).

The present monolith was also analyzed by DSC and TGA. The results were compared with those of the reference monolith and a raw powder of PGA (Figure 2-7). The TGA results revealed that all samples show an onset of the first significant weight loss around 200 ^{o}C, which is attributed to degradation of the PGA polymer chain. Weight losses before 200 ^{o}C were 1.5, 2.7 and 3.3% for the raw power, the reference and the present monolith, respectively. These may correlate with their surface areas in the same order. The DSC analysis proved that these weight losses were indeed caused by desorption of adsorbates. An endothermic process over a wide range of temperature was observed only in the first heating of each sample from 0 to 190 ^{o}C. The absence of any other endothermic process suggested no transition in structure before decomposition.[29] The maintenance of the monolithic structures after heated up to 190 ^{o}C was confirmed by SEM observation, pointing to their considerable thermal stability. In contrast with the raw powder, degradation profiles of the monoliths were featured by shoulders and shifted to higher temperatures. This is most likely attributed to their crosslinked structures. The degradation profile of the present monolith was somewhat different from that of the reference. It remains undemonstrated whether this difference was caused by a different degree of crosslinking or the presence of the large internal cavities.

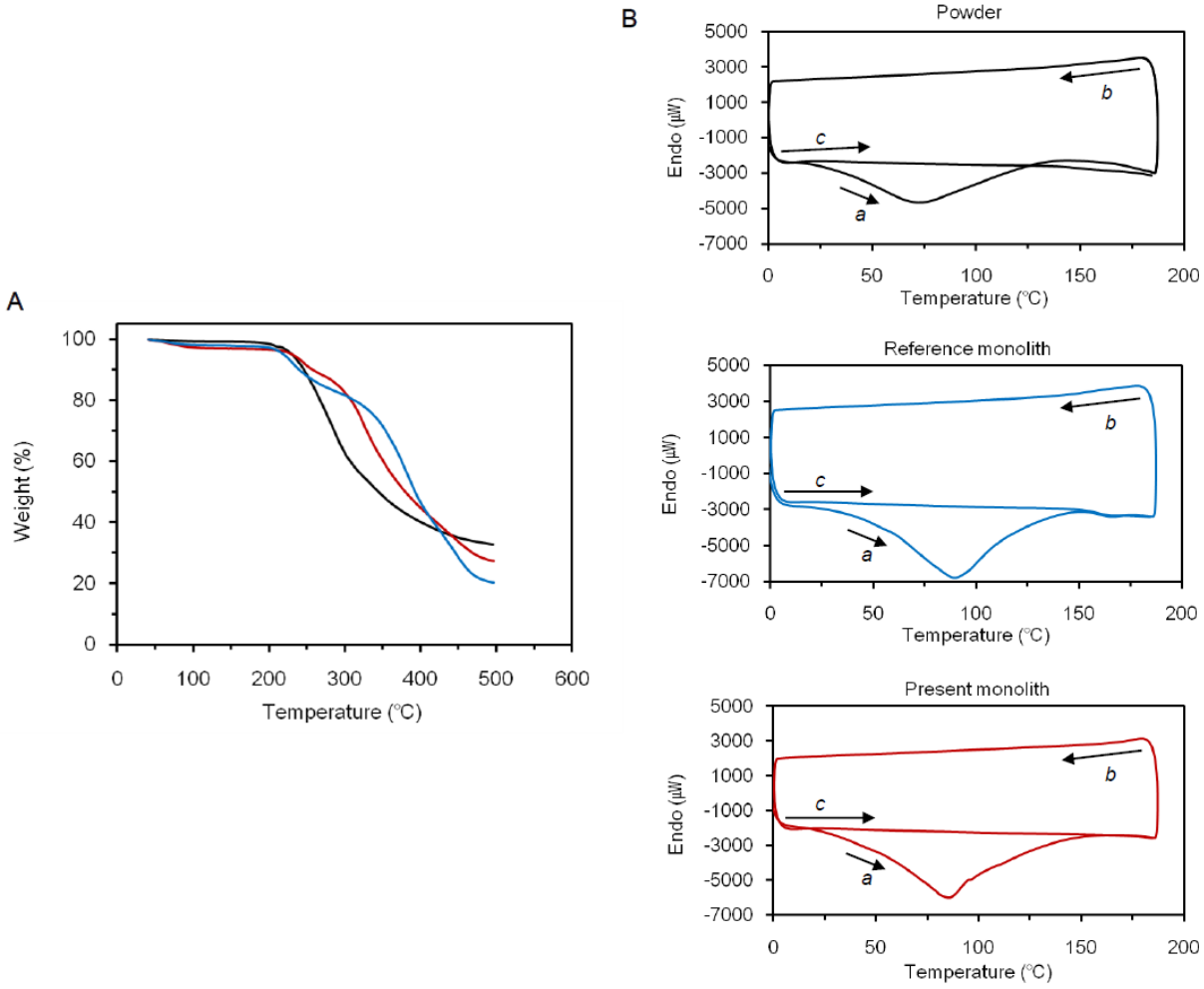

Figure 2-7. TGA (A) and DSC results (B). The curves obtained from a PGA raw powder, the reference monolith and the present monolith are indicated in black, blue and red, respectively. The arrows in DSC thermograms show the directions of temperature change. The symbols *a*, *b* and *c* represent the first heating process from 0 to 190 ^{o}C, the subsequent cooling from 190 to 0 ^{o}C and the second heating from 0 to 190 ^{o}C, respectively.

The present monolith showed reversible deformability (Figure 2-8). Water could be squeezed out from the monolith by simple compression by hand. The compressed monolith readily recovered its original shape and volume after putting it back in water. Such deformation could be repeated reproducibly. Although the reference monolith could also deform in a similar fashion,[23] less force was needed for compression of the present monolith.

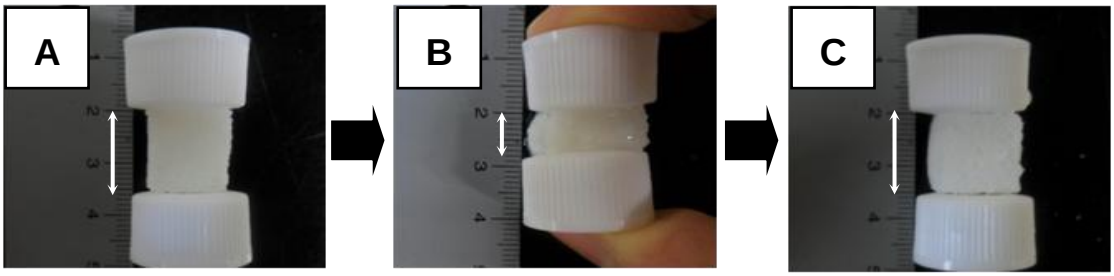

Figure 2-8. Deformation of swollen PGA monolith presently prepared. The photographs show the PGA monolith before (A) and after compression (B). The compressed monolith could recover the original shape and size by soaking in water again (C).

pH-responsive expansion and shrinkage

The swelling ratio was measured on the monolith immersed in a pH 2.0 or 7.0 buffer for 24 h (Figure 2-9). The monolith readily got swollen to reach equilibrium within 24 h. The swelling ratio from the neutral buffer was calculated as 24. This value was much larger than that from the acidic buffer (10). The higher swelling ratio may have a direct bearing on a higher content of carboxylate ion at pH 7.0 (pK_a of PGA : 4.8). The swelling ratio of the present monolith was nearly twice larger than that of the reference at both pH 2.0 and 7.0, corresponding to their volume difference per unit mass.

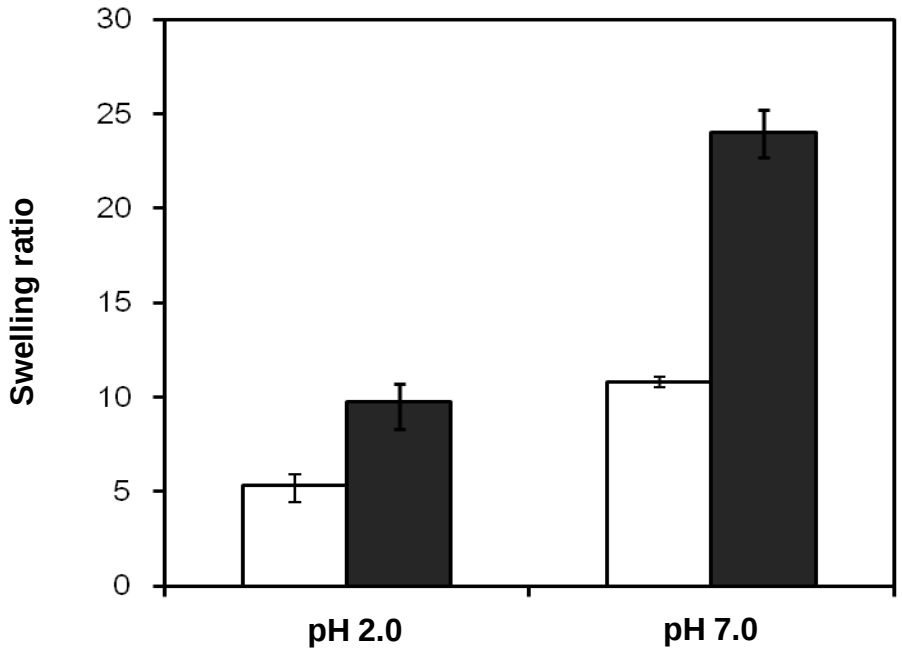

Figure 2-9. Swelling ratio of PGA monoliths in buffer solutions at pH 2.0 and pH 7.0 (filled bar: present monolith, empty bar: reference).

The present monolith expanded and shrank back and forth in response to pH changes between pH 7.0 and 2.0. This expansion-shrinkage cycle was repeated several times and confirmed to be fully reversible and reproducible (Figure 2-10). Both shape and volume of the monolith recovered after each cycle. While a similar pH-responsivity was observed on the reference monolith, the volume change of the present monolith was much more significant. Note that excellent swelling behaviors of PGA hydrogels were previously reported by others.[3,30] Those gels, however, deformed irreversibly and could not recover their original shape in most cases.

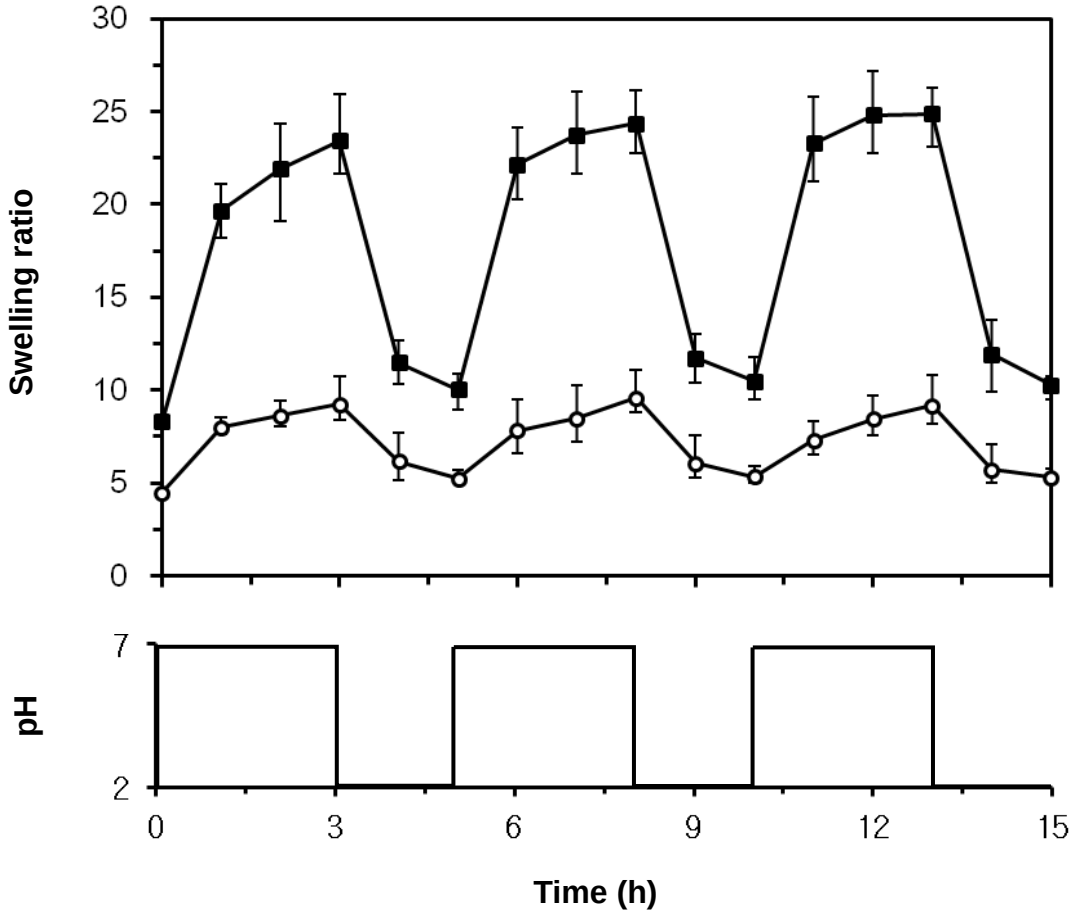

Figure 2-10. Repeated expansion-shrinkage of PGA monoliths in response to pH changes between pH 7.0 and pH 2.0 (filled square: present monolith, empty circle: reference).

pH-responsive capture and release of copper(II)

The chelating activity of the present monolith in a solution of $CuCl_2$ was examined under various pH conditions. When the solution pH was below 1.5, the monolith adsorbed little $Cu(II)Cl_2$. The loss of chelating activity may be ascribed to the absence of carboxylate ions on PGA under highly acidic conditions.[31,32] The amount of $Cu(II)Cl_2$ adsorbed on the monolith increased monotonously as pH increased from pH

2.0 to 4.5 (Figure 2-11). The amount could not be estimated at pH exceeding 5 because of precipitation of the cupric salt.

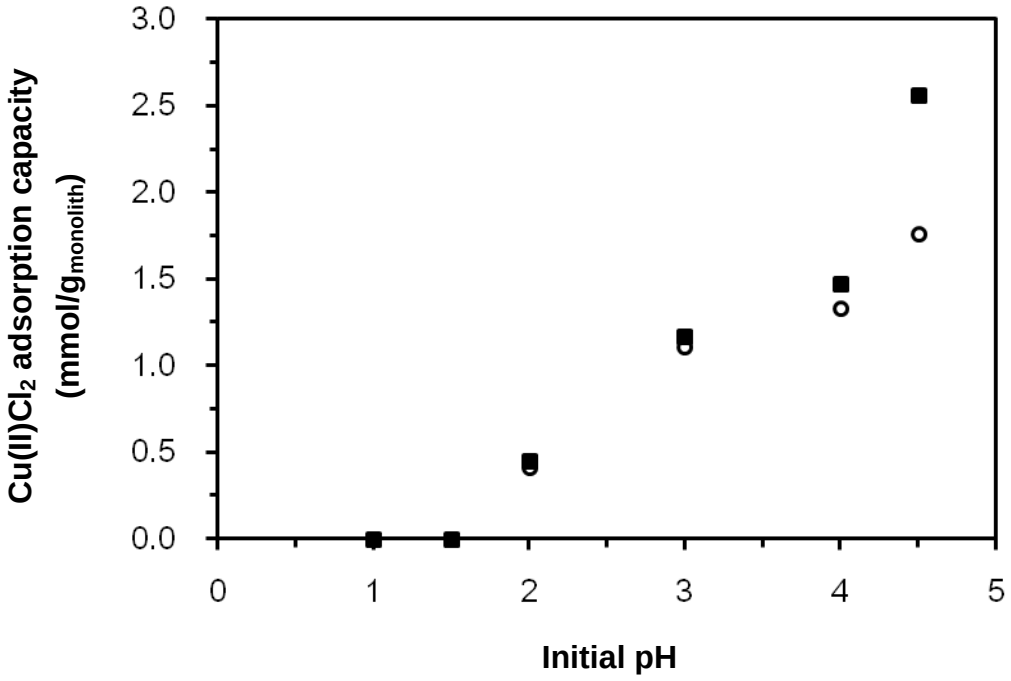

Figure 2-11. Effect of pH on adsorption of $Cu(II)Cl_2$ on PGA monoliths (filled square: present monolith, empty circle: reference). The $Cu(II)Cl_2$ amount in the solution was estimated by UV-vis absorption spectroscopy at 816 nm.

Figure 2-12 shows a time course of the $Cu(II)Cl_2$ adsorption at pH 4.5. It is noteworthy that the present monolith adsorbed $Cu(II)Cl_2$ rapidly at the initial stage in contrast to the reference (0.25 and 0.06 mmol/g·min, respectively). This suggests that the cavities helped the $CuCl_2$ solution permeate the monolith. The adsorption slowed with time and eventually equilibrated. The amount of $Cu(II)Cl_2$ adsorbed at the equilibrium state represents the $Cu(II)Cl_2$ capacity of the monolith, which was 2.6 and

1.8 mmol/g for the present monolith and the reference, respectively. The improved capacity may correlate with the increased surface area aforementioned.

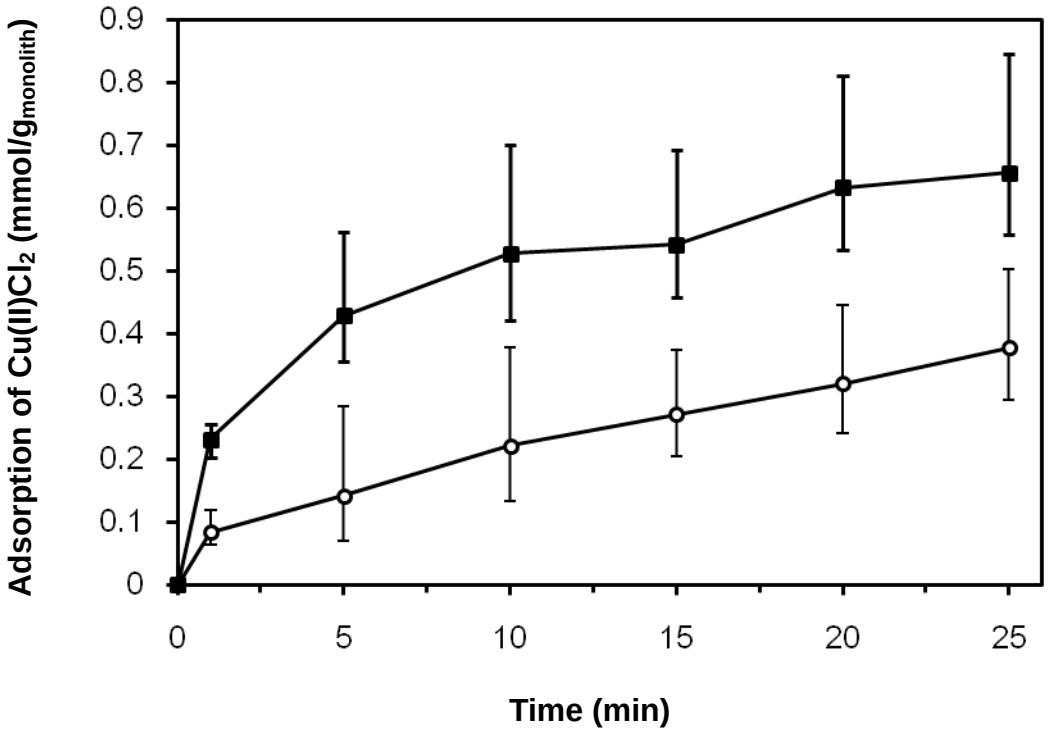

Figure 2-12. Time-course of $Cu(II)Cl_2$ adsorption on PGA monoliths at pH 4.5 (filled square: present monolith, empty circle: reference). The $Cu(II)Cl_2$ amount in the solution was estimated by UV-vis absorption spectroscopy at 816 nm.

Both surface and inside of the monolith turned homogeneously blue after the adsorption of copper(II) (Figure 2-13). SEM cross-sectional analysis confirmed that the porosity of the monolith unchanged. EDX analysis showed the appearance of characteristic signals at 0.9, 8.1 and 8.9 keV to prove the incorporation of copper(II) in the monolith. Homogeneous distribution of copper(II) inside the monolith was also confirmed (Figure 2-14).

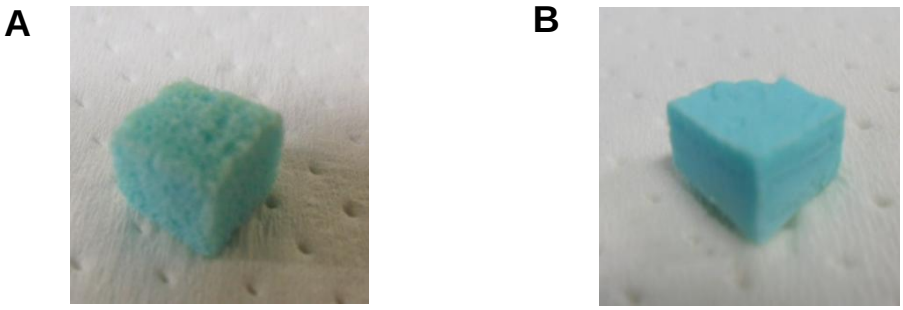

Figure 2-13. Photographs of the present PGA monolith (A) and the reference (B) after adsorption of copper elements.

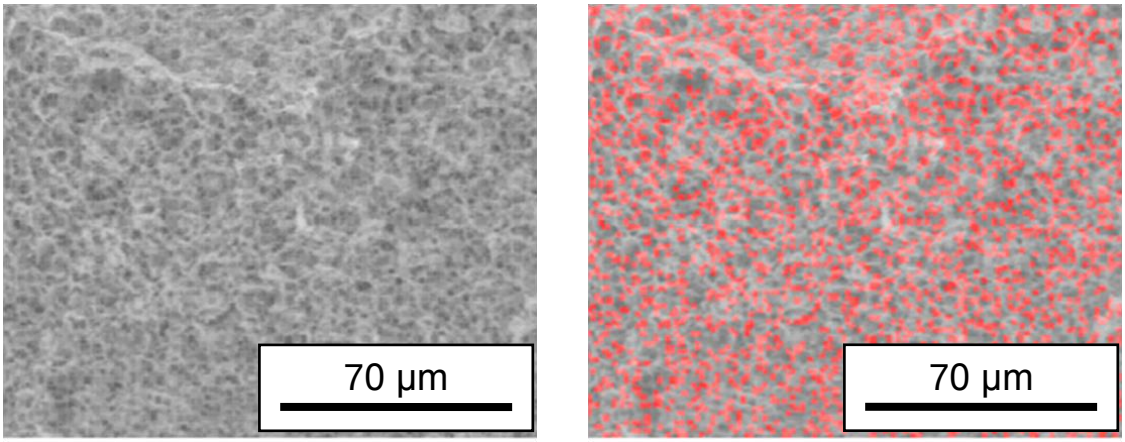

Figure 2-14. EDX image of the Cu(II)Cl_2-loaded PGA monolith presently prepared. The red spots in the right image represent where copper element resides locate in the monolith shown in the left image.

Next, the Cu(II)Cl_2-loaded monolith (ca. 100 mg) was transferred into a pH 1.0 buffer where the chelating activity of the present monolith was assumed to be suppressed. Indeed, copper(II) concentration of the solution increased gradually and recovered nearly quantitatively in 2 h (Figure 2-15). The blue-colored monolith turned white concomitantly. These results proved that the monolith can release the metal ion under the acidic conditions. Similar to adsorption, the initial rate of desorption was higher than that of the reference.

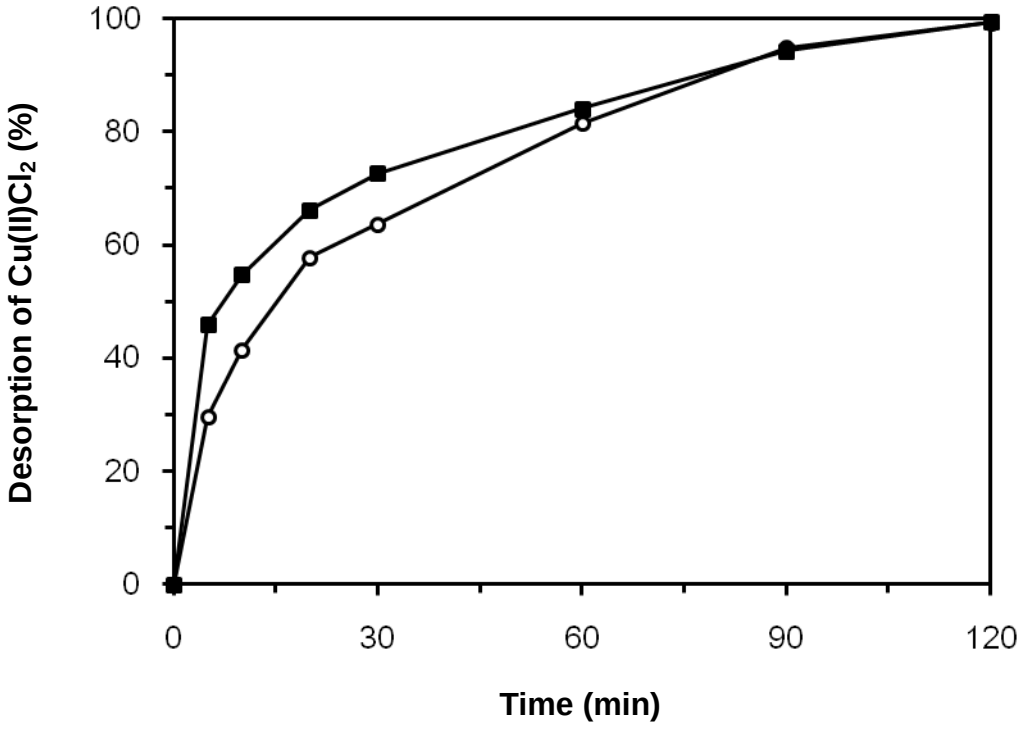

Figure 2-15. Time-course of copper(II) desorption from PGA monoliths at pH 1.0 (filled square: present monolith, empty circle: reference). The copper(II) amount in the solution was estimated by UV-vis absorption spectroscopy at 816 nm.

$Cu(II)Cl_2$ adsorption and desorption were repeated on the present monolith by switching pH between 4.5 and 1.0 back and forth. As shown in Figure 2-16, this process was found to be fully reversible and reproducible. In addition, similar results were obtained by using other metal ions such as $Ni(II)Cl_2$, $Co(II)Cl_2$ and $Fe(II)Cl_2$, indicating that this pH-switchable adsorption-desorption behavior of the present monolith is applicable to various metal ions (Figure 2-17).

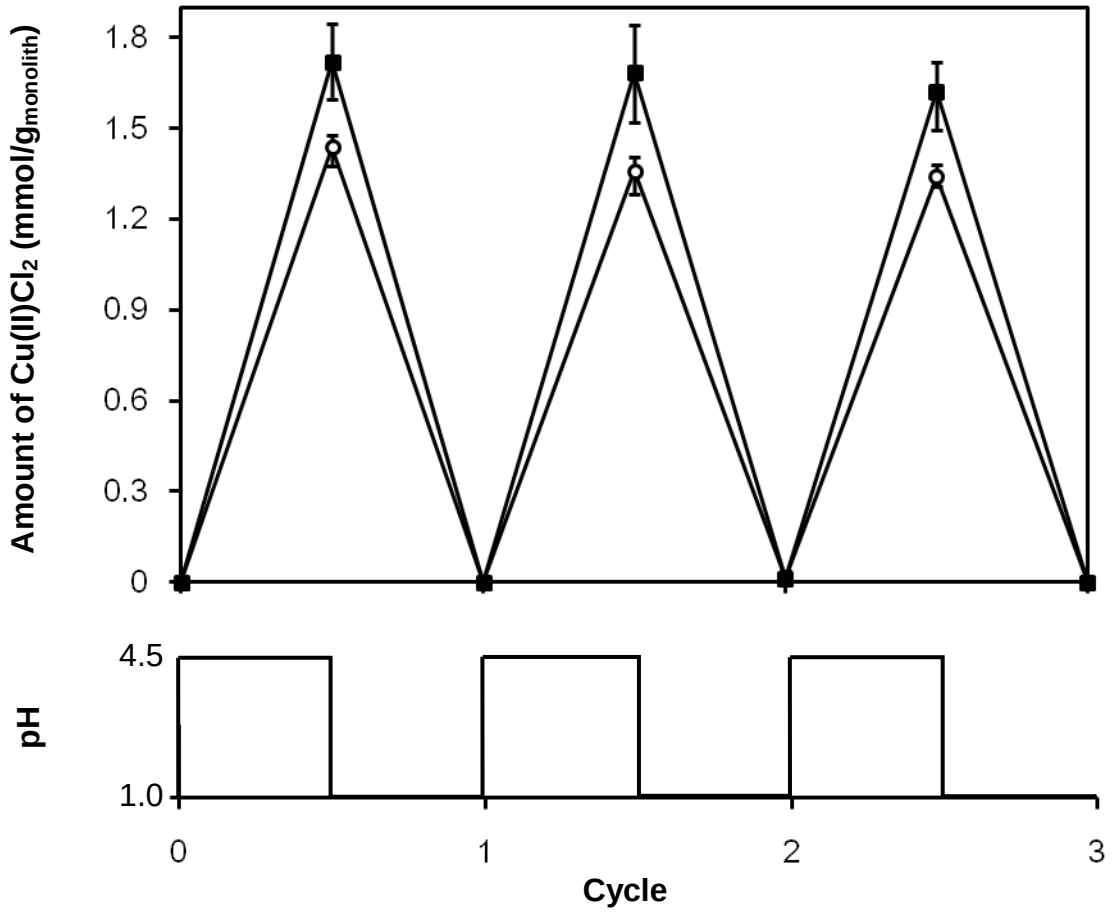

Figure 2-16. Repeated capture and release of $Cu(II)Cl_2$ by PGA monoliths in response to pH changes between 4.5 and 1.0 (filled square: present monolith, empty circle: reference). Three samples were tested in each experiment. The copper(II) amount in the solution was estimated by UV-vis absorption spectroscopy at 816 nm.

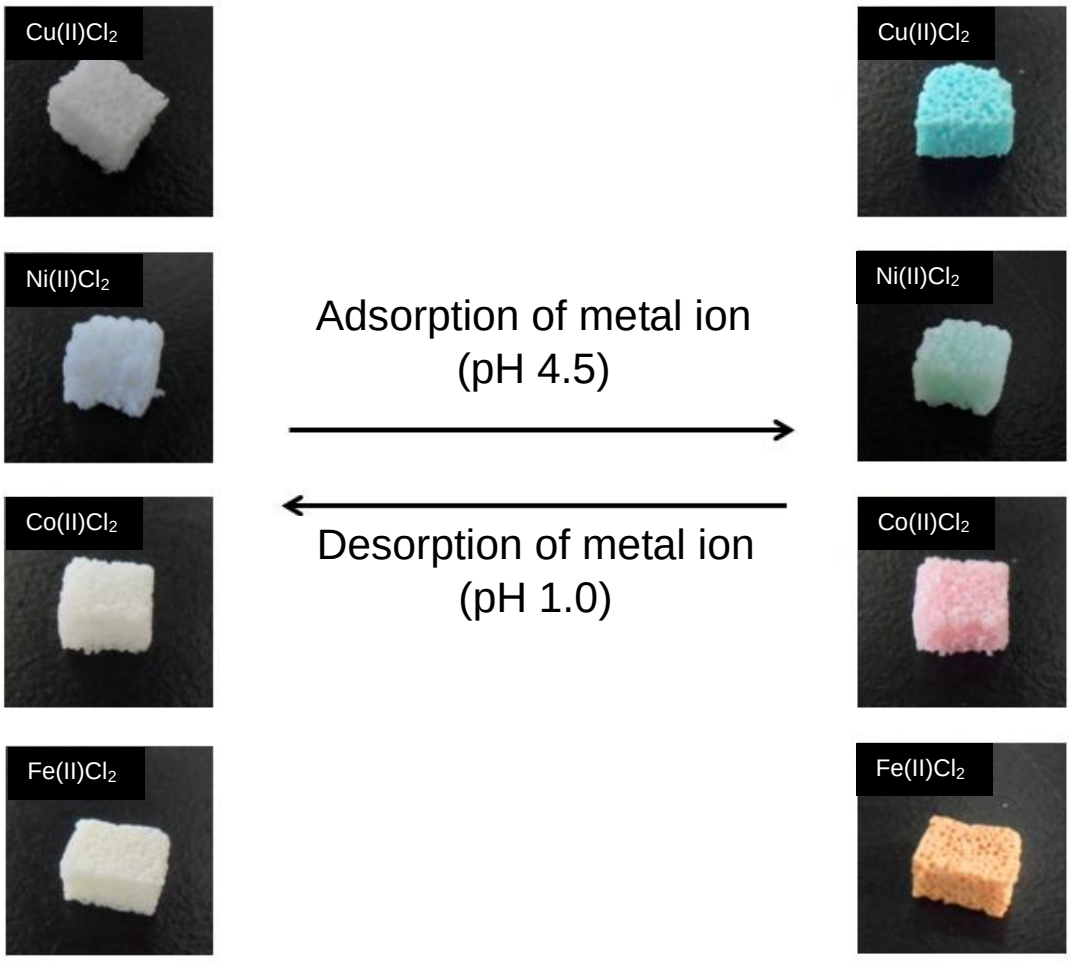

Figure 2-17. Repeated adsorption/desorption of various metal ions on the present PGA monolith.

2.4 Conclusion

A unique monolithic material based on PGA has been introduced. It was prepared by a simple and costless approach that combines the thermally induced phase separation technique with particulate salt templates. For use in water, the monolith was covalently stabilized by internal crosslinking. This also allowed the salt templates to be washed out of the monolith. Submillimeter-sized cavities were thus installed homogeneously in the monolithic matrix comprising a microporous network created by the phase separation. This solid material could readily absorb water and deform reversibly. More importantly, pH-responsibility of PGA was successfully integrated in the monolith. The monolith could expand-shrink and efficiently capture-release metal ions in response to pH changes. Such responsive behaviors were promoted by the internal cavities and found to be fully reversible and reproducible. These results qualify the present monolith as an attractive material that combines key advantages of PGA and the porous monolithic structure.

References

[1] M. Ashiuchi, T. Kamei, H. Misono, *J. Mol. Catal. B: Enzym*. **2003**, *23*, 101.

[2] M. Ashiuchi, C. Nawa, T. Kamei, J. J. Song, S. P. Hong, M. H. Sung, K. Soda, T. Yagi, H. Misono, *Eur. J. Biochem*. **2001**, *268*, 5321.

[3] T. Candela, A. Fouet, *Mol. Microbiol*. **2006**, *60*, 1091.

[4] S. K. Ahn, R. M. Kasi, S. C Kim, N. Sharma, Y. Zhou, *Soft Matter*. **2008**, *4*, 1151.

[5] B. Yao, C. Yang, K. Zhang, C. Ni, H. Song, Z. Ni, M. Chen, *Mater. Sci. Poland* **2009**, *27*, 319.

[6] Z. Yang, Y. Zhang, P. Markland, V. C. Yang, *J. Biomed. Mater. Res*. **2002**, *62*, 14.

[7] K. L. Deng, L. R. Dong, Q. Li, Y. B. Gou, P. F. Zhang, X. B. Ren, H. B. Zhong, *J. Appl. Polym. Sci*. **2011**, *120*, 3297.

[8] H. Poo, C. Park, M. S. Kwak, D. Y. Choi, S. P. Hong, I. H. Lee, Y. T. Lim, Y. K. Choi, S. R. Bae, H. Uyama, C. J. Kim, M. H. Sung, *Chem. Biodivers*. **2010**, *7*, 1555.

[9] S. R. Bae, C. Park, J. C. Choi, H. Poo, C. J. Kim, M. H. Sung, *J. Microbiol. Biotechnol*. **2010**, *20*, 803.

[10] J. M. Buescher, A. Margaritis, *Crit. Rev. In Biotechnol*. **2007**, *27*, 1.

[11] M. H. Sung, C. Park, C. J. Kim, H. Poo, K. Soda, M. *Ashiuchi, Chem. Rec*. **2005**, *5*, 352.

[12] I. L. Shih, Y. T. Van, *Bioresour. Technol*. **2001**, *79*, 207.

[13] M. Ashiuchi, H. Misono, Biopolymers, Vol. 7, Chapter 6, Fahnestock SR, Steinbuchel A. (eds.). Wiley-VCH, Weinheim **2002**, p. 123-174.

[14] P. van de Witte, P. J. Dijkstra, J. W. A. van den Berg, J. J. Feijen, *Membrane Sci*. **1996**, *117*, 1.

[15] Y. S. Nam, T. G. Park, *Biomaterials* **1999**, *20*, 1783.

[16] K. Okada, M. Nandi, J. Maruyama, T. Oka, T. Tsujimoto, K. Kondoh, H. Uyama, *Chem. Commun*. **2011**, *47*, 7422.

[17] M. R. Buchmeiser, *Polymer* **2007**, *48*, 2187.

[18] O. G. Potter, E. F. Hilder, *J. Sep. Sci*. **2008**, *31*, 1881.

[19] J. Courtois, E. Bystrom, K. Irgum, *Polymer* **2006**, *47*, 2603.

[20] F. Svec, *J. Chromatogr. A* **2010**, *1217*, 902.

[21] F. Svec, C. G. Huber, *Anal. Chem*. **2006**, *78*, 2100.

[22] S. Wei, Y. L. Zhang, H. Ding, J. Liu, J. Sun, Y. He, Z. Li, F. S. Xiao, *Colloids Surf. A* **2011**, *380*, 29.

[23] S. B. Park, T. Fujimoto, E. Mizohata, T. Inoue, M. H. Sung, H. Uyama, *J. Microbiol. Biotechnol*. **2013**, *23*, 942.

[24] Y. F. Yang, J. Zhao, Y. H. Zhao, L. Wen, X. Y. Yuan, Y. B. Fan, *J. Appl. Polym. Sci.* **2008**, *109*, 1232.

[25] C. J. Liao, C. F. Chen, J. H. Chen, S. F. Chiang, Y. J. Lin, K. Y. Chang, *J. Biomed. Mater. Res*. **2002**, *59*, 676.

[26] Q. Hou, D. W. Grijpma, J. Feijen, *Biomaterials* **2003**, *24*, 1937.

[27] L. Wu, D. Jing, J. Ding, *Biomaterials* **2006**, *27*, 185.

[28] R. G. Heijkants, R. V. van Calck, T. G. van Tienen, J. H. de Groot, A. J. Pennings, P. Buma, R. P. Veth, A. Schouten, *J. Biomed. Mater. Res. A* **2008**, *87*, 921.

[29] H. Kubota, Y. Nambu, T. Endo, *J. Polym. Sic. Part A Polym. Chem*. **1995**, *33*, 85.

[30] D. Gonzales, K. Fan, M. Sevoian, *J. Polym. Sci. Part A Polym. Chem.* **1996**, *34*, 2019.

[31] F. Y. Siao, J. F. Lu, J. S. Wang, B. S. Inbaraj, B. H. Chen, *J. Agric. Food Chem*. **2009**, *57*, 777.

[32] T. Tsujimoto, J. Kimura, Y. Takeuchi, H. Uyama, C. Park, M. H. Sung, *J. Microbiol. Biotechnol.* **2010**, *20*, 1436.

Chapter 3

Preparation of Poly(γ-glutamic acid)/Hydroxyapatite Monoliths *via* Biomineralization for Bone Tissue Engineering

3.1 Introduction

Poly(γ-glutamic acid) (PGA) is a hydrophilic, anionic and biocompatible polypeptide produced by microorganisms such as *Bacillus subtilis*.[1,2] On the basis of these characteristics, PGA-based materials such as hydrogels and nanofibers have been designed for a wide range of applications, especially in the biomedical field.[3-6] Of particular interest is PGA's hydroxyapatite (HAp) forming ability. HAp is one of the main inorganic components of the bone matrix, which confers mechanical strength to bone. Furthermore HAp promotes cellular attachment, proliferation and osteogenic differentiation of osteoblasts.[7] In natural bone, nucleation and crystal growth of HAp is induced by the glutamic acid–rich sequences present in type I collagen.[8] In a similar manner, the glutamic acid residues of PGA are known to induce the formation of HAp.[9]

Due to the structural similarity with the natural bone matrix, hybrid materials composed of polymers and HAp are considered to be potential candidate scaffolds for bone tissue engineering.[10-14] Taking advantage of the apatite forming ability of PGA, PGA/HAp hybrid materials have been prepared via biomineralization in simulated body fluid (SBF).[15,16] SBF is a solution with ion concentrations close to human blood

plasma, that has been widely used to deposit bone-like apatite on the surface of organic substrates.[12] It has been reported that PGA hydrogels, PGA-coated collagen sponges and silica–PGA hybrids were able to induce the nucleation of HAp in SBF.[15-17] In addition, several reports showed that the formation of HAp was further enhanced by incorporating Ca^{2+} ions in the scaffolds.[8,15] Although these PGA-based materials showed promise in bone regeneration, due to the hydrophilic nature of PGA, fabrication of well-defined structure often requires complicated procedures, which remains an issue in biological applications.

Apart from the chemical properties of the materials, there are several important morphological criteria in designing cell scaffolds. It is well documented that cell scaffolds with pores larger than several tens micrometer are required for three-dimensional cell proliferation. For example, pore size suitable for cell ingrowth is in the range of 100-400 μm for osteoblasts, 70-120 μm for chondrocytes, 38-150 μm for fibroblasts, and 63-150 μm for vascular smooth muscle cells.[11,18,19] Another requirement is efficient mass transfer which is essential to supply nutrition and oxygen to the cells. In addition, cell scaffolds should be able to incorporate bioactive molecules, such as growth factors, and release them in a controlled manner to stimulate cell proliferation and differentiation. For these reasons, it has been suggested that scaffolds with bimodal pore size distribution would be advantageous. Whereas large pores, generally >50 μm in diameter, offer space for cell ingrowth, smaller pores in the range of sub-hundred nanometer to several micrometer facilitate transport of nutrition and oxygen as well as supply high surface area for the incorporation of growth factors.[20,21]

The thermally induced phase separation (TIPS) technique is known as a simple method to prepare a well-defined monolith, a single-piece material having an interconnected porous network, from versatile polymers. Using this technique, our group have reported highly porous monoliths of poly(acrylonitrile), poly(bisphenol A

carbonate) and poly(vinyl alcohol).[22-24] PGA-based monolith prepared by the TIPS technique followed by chemical crosslinking showed reversible deformability and thermal stability.[25] Importantly, the monolith still had the unique properties of PGA such as hydrophilicity, metal-chelating ability and pH-responsiveness. By combining the TIPS technique with the well-known salt leaching technique able to fabricate a PGA monolith having homogeneously distributed sub-millimeter sized cavities within an interconnected porous network.[26] This unique morphology together with the chemical and physical properties of PGA prompted to investigate the potential use of this monolith as a cell scaffold in tissue engineering.

This chapter reports a hybrid monolith of PGA and HAp (PGA/HAp monolith) that may find application in bone tissue engineering. The PGA/HAp monolith was prepared via biomineralization of the PGA monolith in SBF. The effect of pretreatment with $CaCl_2$ aqueous solution on the HAp formation was evaluated. The behavior of murine osteoblastic cells (MC3T3-E1) on the monolith was also investigated. Furthermore, bone morphogenetic protein-2 (BMP-2) was adsorbed onto the monolith *via* electrostatic interaction and its biological effect on the osteogenic differentiation of MC3T3-E1 cells was assessed.

3.2 Experimental

Materials

PGA (acid form, M_w = 5×10^3 kDa) was provided by BioLeaders (Korea). Hexamethylene diisocyanate was purchased from Wako Pure Chemical Industries (Japan). Sodium chloride (+80 mesh particle size) was purchased from Sigma-Aldrich.

Recombinant human BMP-2 was purchased from R&D systems. Other reagents were commercially available and used without further purification. Water was freed from salt using a milliQ system and filtered (0.22 μm).

PGA monolith preparation

The PGA monolith was prepared as reported previously.[26] A typical procedure is as follows. PGA powder (450 mg) was dissolved in dimethyl sulfoxide/water/ethanol (9/1/20, 3 mL) at 80 ^{o}C. Sodium chloride particles (5.5 g) were then added to the solution and the mixture cooled at 25 ^{o}C for 12 h. The resultant sodium chloride particles incorporated PGA monolith was washed with acetone to remove the solvents and subsequently dried under vacuum. The as-prepared monolith (3.49 mmol monomer unit of PGA) was mixed with hexamethylene diisocyanate (1 mL, 5.89 mmol) in acetone (10 mL) and kept at 50 ^{o}C. After 6 h, water (300 μL) was added dropwise.[25,26] The monolith was washed with acetone and water to remove sodium chloride particles and unreacted crosslinker. Residual water was replaced with acetone and the monolith dried in *vacuo* to yield the crosslinked PGA monolith.

Biomineralization on the PGA monolith

SBF was prepared by dissolving NaCl (8.035 g), $NaHCO_3$ (0.355 g), KCl (0.225 g), $K_2HPO_4{\cdot}3H_2O$ (0.231 g), $MgCl_2{\cdot}6H_2O$ (0.311 g), $CaCl_2$ (0.292 g), Na_2SO_4 (0.072 g) into milliQ water (1 L). The pH was adjusted to 7.4 with tris-hydroxymethyl aminomethane (6.118 g) and HCl (1 M) aqueous solution at 37 ^{o}C.[12]

Hydroxyapatite formation on the PGA monolith was carried out in SBF at 37 ^{o}C as reported by Kokubo.[12] The PGA monolith was cut into cubic shape (8 × 8 × 8 mm) and immersed in $CaCl_2$ aqueous solutions (50 mL) at various concentrations (0.01, 0.1 and 1 M) at 37 ^{o}C for 24 h. The monoliths treated with and without $CaCl_2$ were

immersed in SBF (10 mL) at 37 ^{o}C for 1 and 7 d. SBF was replaced every day. Monoliths were washed with milliQ water and freeze-dried.

Characterization of the PGA/HAp monolith

Scanning electron microscopy (SEM) of the monoliths was done on a HITACHI S-3000N at an accelerated voltage of 15 kV. A thin gold film was sputtered on the samples before the images were collected. Energy dispersive X-ray (EDX) spectra were recorded on a Hitachi Miniscope TM3000 with a Swift3000 equipment. X-ray diffraction (XRD) patterns were recorded on a Rigaku Multiflex diffractometer at 40 kV and 30 mA in continuous scanning degrees of 2θ/min. Fourier transform infrared spectra (FT-IR) were measured on a Thermo Scientific Nicolet iS5 with an attenuated total reflection accessory (iD5 ATR accessory). Ca and P concentrations were measured by inductively coupled plasma atomic emission spectrometry (ICP-AES) using a Shimadzu ICP-7510 sequential plasma spectrometer.

Culture of MC3T3-E1 cells

MC3T3-E1 cells were obtained from the European Collection of Cell Cultures. Cells were cultured in α-minimum essential medium (α-MEM) supplemented with 10% fetal bovine serum (FBS; Gibco) and 1% penicillin/streptomycin in 75 cm^2 tissue culture flasks (Iwaki, Japan) at 37 ^{o}C under a humidified atmosphere with 5% CO_2. When cells reached 80-90% confluency, they were detached with 0.25% trypsin/EDTA and passaged at a ratio of 1:10.

Cell attachment on the monoliths

The PGA monolith and PGA/HAp monoliths were sterilized in 70% (v/v) ethanol/water and washed with sterile milliQ water to remove ethanol. A medical

biopsy punch (6 mm; Kai Industries) and rat brain slicer (RBS-1, 1mm; WPI) were used to cut the monoliths into small pieces (diameter 6 mm × thickness 1 mm).

Monolith pieces were placed in a 96-well culture plate and MC3T3-E1 cells in culture medium (200 μL) were seeded at a concentration of 1×10^4 cells per well and cultured for 24 h. Cells on the monoliths were stained with the LIVE/DEAD Viability/Cytotoxicity assay kit (molecular probes, UK) and observed with an Olympus FluoView FV1000-D confocal laser scanning fluorescence microscope.

Preparation of Rhodamine-labeled PGA monolith

Rhodamine B functionalized with ethylene diamine (Rhodamine-NH_2) was prepared as reported.[40] A PGA monolith piece (5 mg) was placed in MES buffer (2 mL, 100mM, pH 5) containing Rhodamine-NH_2 (0.4 mg). After adding EDC (74 mg) and sulfo-NHS (84 mg), the PGA monolith was incubated at 25 ^oC in the dark. After 20 h, the monolith piece was washed with phosphate buffer (pH 7.4) and water.

Cell proliferation assay

MC3T3-E1 cells were seeded on top of the monoliths (1×10^4 cells per well) in culture medium (200 μL). Cell viability was evaluated by the 3-(4, 5-dimethyl-2-thiazolyl)-2,5-diphenyl-2*H*-tetrazolium bromide (MTT) assay. After the formazan crystals were solubilized in SDS (0.1 g/mL) in HCl (0.01 M), the absorbance at 570 nm was measured on a Tecan M200 Pro series well plate reader using 96 well polystyrene plates.

BMP-2 loading

The PGA monolith (3.2 mg, diameter 6 mm × thickness 1 mm) and PGA/HAp monoliths (4.3 mg, diameter 6 mm × thickness 1 mm) were immersed in Dulbecco's

PBS (200 μL) containing BMP-2 (0.5 μg) and kept at 4 ^{o}C for 3 d. The concentration of BMP-2 in the supernatant was quantified by enzyme-linked immune sorbent assay (ELISA) kit (R&D Systems, USA).

Release of BMP-2 from the monolith in the presence of MC3T3-E1 cells

The PGA and PGA/HAp monoliths loaded with BMP-2 were placed in a 96-well culture plate. MC3T3-E1 cells (1×10^4 cells per well) in medium (200 μL) were seeded onto the monoliths and cultured for 12 d. The medium was replaced with fresh culture medium every third day. The concentration of BMP-2 in the culture medium was quantified by ELISA.

Alkaline phosphatase activity

MC3T3-E1 cells in medium (200 μL) were seeded onto the monoliths and cultured for 12 d replacing the culture medium every third day. As a control, the cells were cultured on a polystyrene plate for 12 d replacing the culture medium supplemented with/without BMP-2 (25 ng) every third day. Alkaline phosphatase (ALP) activity of MC3T3-E1 cells was measured using a LabAssay ALP kit (Wako, Japan) according to the manufacturer's instructions. The monolith pieces containing cells were washed with Dulbecco's PBS (without Ca^{2+} and Mg^{2+}) and the cells were lysed in 0.25% Triton X-100 solution (0.2 mL) by shaking for 20 min at RT followed by one freeze-thaw cycle. The solution was collected and centrifuged. The supernatant (20 μL) was mixed with 6.7 mM *p*-nitrophenyl phosphate (*p*NPP) (100 μL) in carbonate buffer (0.1 M, pH 9.8) containing $MgCl_2$ (2.0 mM) and incubated at 37 ^{o}C for 15 min on a bench shaker. The reaction was stopped by adding NaOH (0.2 mM, 80 μL). Absorbance at 405 nm was measured on a plate reader. Total protein content was determined by the

bicinchoninic acid (BCA) assay using QuantiPro BCA Assay kit (Sigma-Aldrich, USA).

3.3 Results and Discussion

HAp formation on the PGA monolith in SBF

The PGA monolith having an interconnected porous network (pore size: 200-800 nm) and cavities of 200-600 μm in dimension was prepared by combining the TIPS and salt leaching techniques.[26] This monolith was immersed in SBF to induce HAp formation. As shown in Figure 3-1A, we observed that small spherical particles in the range of 0.1-0.6 μm in diameter were deposited within the porous network of the monolith after 7 d. After 30 d of incubation in SBF, larger spherical particles in the range of 1.0-3.0 μm were homogeneously distributed over the network structure (Figure 3-2). It is interesting to note that the monolith seemed to accelerate the crystal formation. Sugita *et al*. reported that only amorphous calcium phosphate was deposited and no spherical structure was found on the PGA hydrogel after 7 d of incubation in SBF.[15] Since the nucleation of HAp progresses through formation of amorphous calcium phosphate,[27] the crystal forming process proceeded much faster on the monolith than hydrogel. Although the exact mechanism is not clear, it may be due to the high concentration of glutamic acid residues in the network structure where PGA molecules are bundled together.

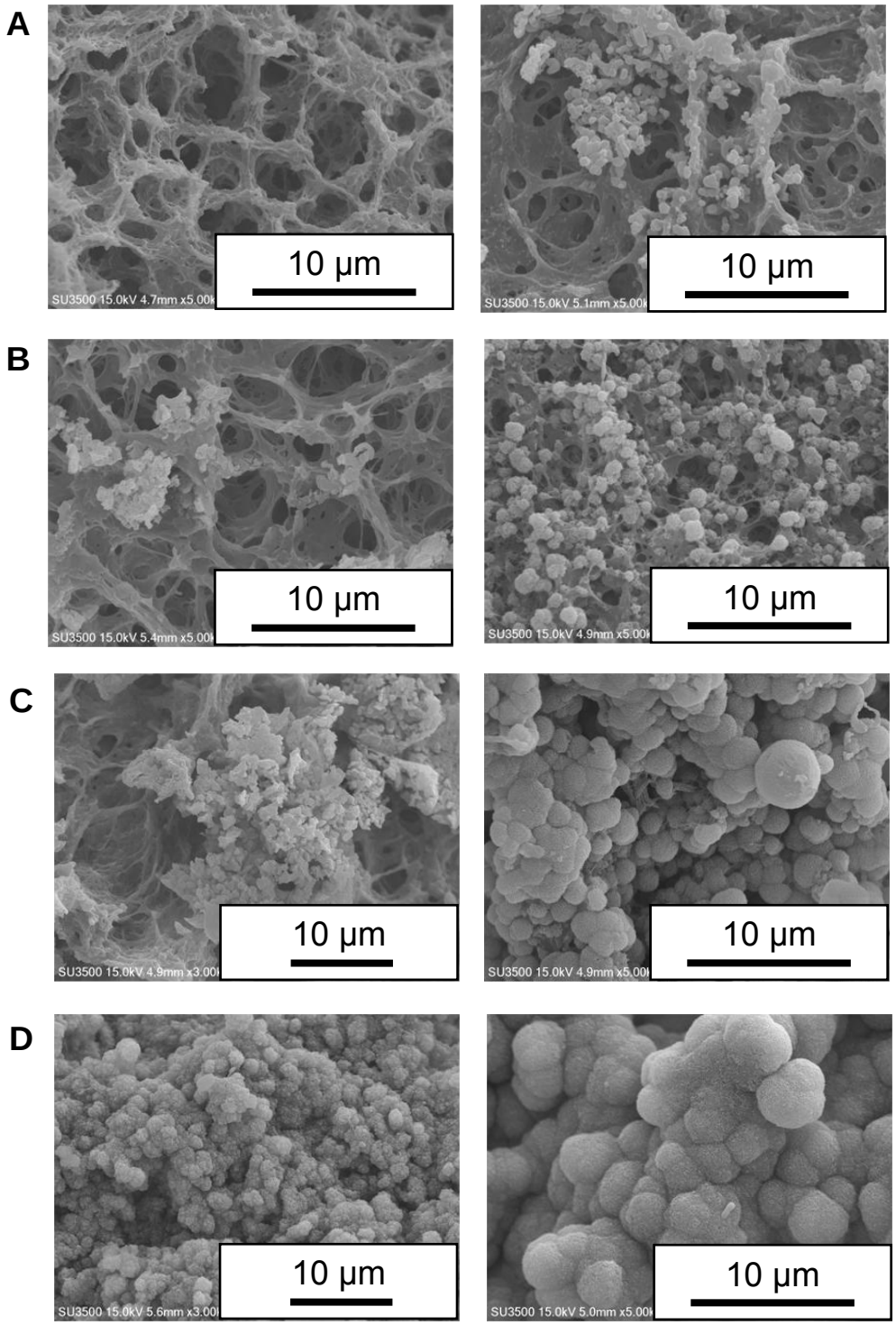

Figure 3-1. SEM images of the monoliths after soaking in SBF for 1 d (left) and 7 d (right). Monolith was pretreated with 0 (A), 0.01 (B), 0.1 (C) and 1 M (D) $CaCl_2$ (aq) solution.

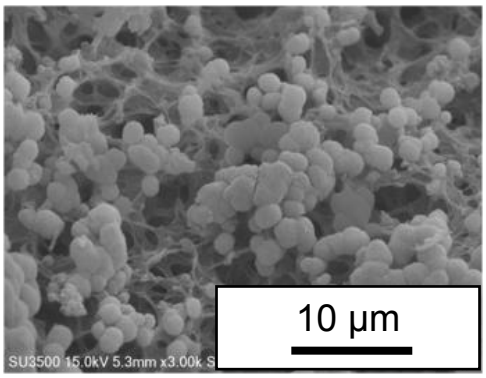

Figure 3-2. SEM image of the PGA monolith after soaking in SBF for 30 d.

To further accelerate apatite formation, the monoliths were immersed in aqueous $CaCl_2$ solutions at different concentrations before mineralization in SBF. It has been reported that the incorporation of $CaCl_2$ in the PGA matrix enhances the HAp formation by increasing the Ca^{2+} concentration in the close vicinity of the substrate surface.[8,15] As confirmed by EDX, Ca was homogeneously distributed in the monolith (Figure 3-3).

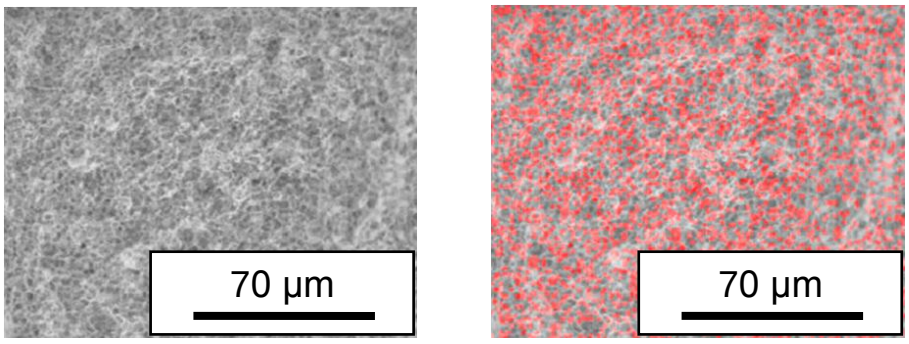

Figure 3-3. SEM/EDX images showing the distribution of Ca on the monolith treated with 1 M $CaCl_2$ aqueous solution. Left: SEM image of the monolith; right: overlay of SEM image with EDX showing Ca in red.

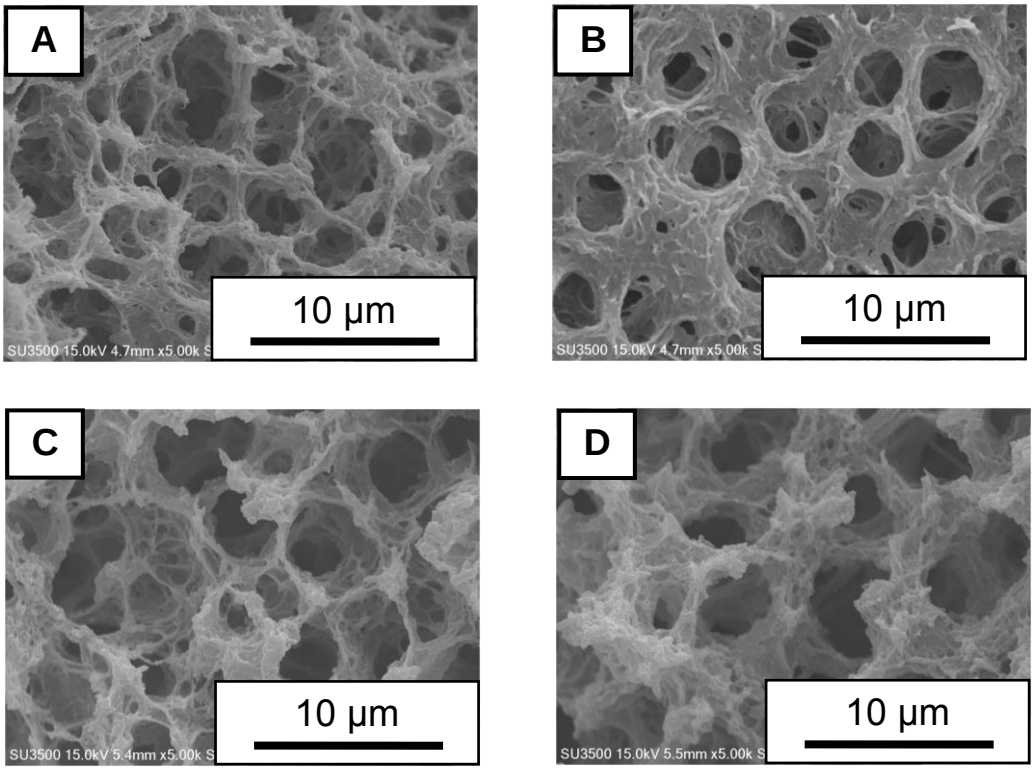

Figure 3-4. SEM images of the monoliths before (A) and after 0.01 (B), 0.1 (C), and 1 M (D) $CaCl_2$ treatment.

SEM images showed that the porous morphology of the monoliths was maintained after the $CaCl_2$ treatment (Figure 3-4). The $CaCl_2$ treated monoliths were immersed in SBF to induce HAp formation. Contrary to the untreated monolith, the $CaCl_2$ treated monoliths showed the formation of spherical crystals already after 1 d of incubation in SBF (Figure 3-1B,C,D). After 7 d, the apatite crystals had grown larger and were homogeneously distributed within the porous network of the monolith. It should be noted that the original porous network structure of the monolith was still visible after 7 d (Figure 3-5). Moreover, the concentration of the $CaCl_2$ solution showed a significant effect on the crystal growth. The size of the crystals increased as function of the $CaCl_2$ concentration; 0.2-1.0 µm for 0.01 M, 0.2-2.0 µm for 0.1 M and 0.8-5.0 µm for 1 M.

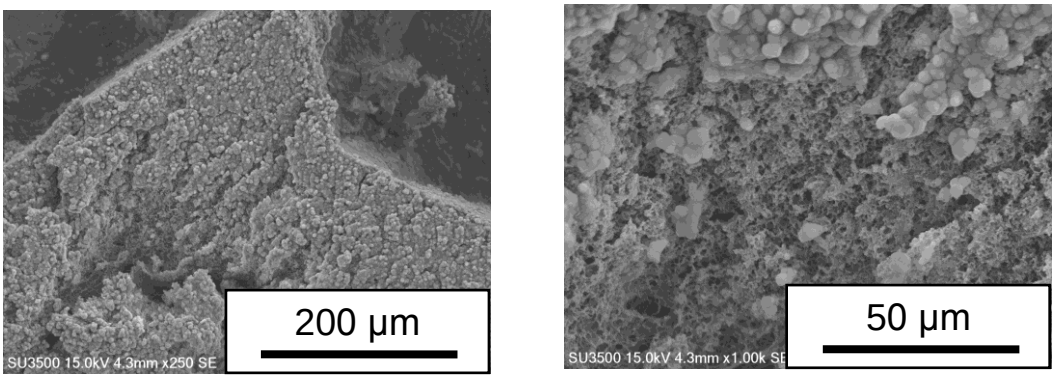

Figure 3-5. SEM images of 1 M $CaCl_2$ treatment PGA monolith after soaking in SBF for 7 d.

The mineralization process of the untreated and $CaCl_2$ treated monolith was compared by measuring the concentration of Ca^{2+} and PO_4^{3-} ions in the SBF solution. In this experiment, 1 M $CaCl_2$ was used to treat the monolith. Figure 3-6 shows the change of Ca and P concentration in the SBF as a function of time after the immersion of the monoliths. The Ca and P concentration in SBF gradually decreased in the presence of the untreated PGA monolith which is due to the consumption of Ca^{2+} and PO_4^{3-} ions during the HAp formation.[25,26] In the case of the monolith treated with 1 M $CaCl_2$, the P concentration in SBF also decreased as a function of immersion time and the decrease was 60% higher than that for the untreated monoliths. This result suggests that $CaCl_2$ treatment enhances HAp formation. On the other hand, the Ca concentration increased within 1 d and remained constant for 1 week. This initial increase can be attributed to the release of incorporated Ca^{2+} ions from the pores of the monolith. Interestingly, the decrease of Ca concentration due to the HAp formation was not observed after the initial burst release of $CaCl_2$. This contradicting data may be due to the fact that not all Ca^{2+} ions were released into the SBF during the initial release and that remaining Ca^{2+}

in the hydrated cross-linked monolith backbone were the calcium source for forming the HAp crystals.

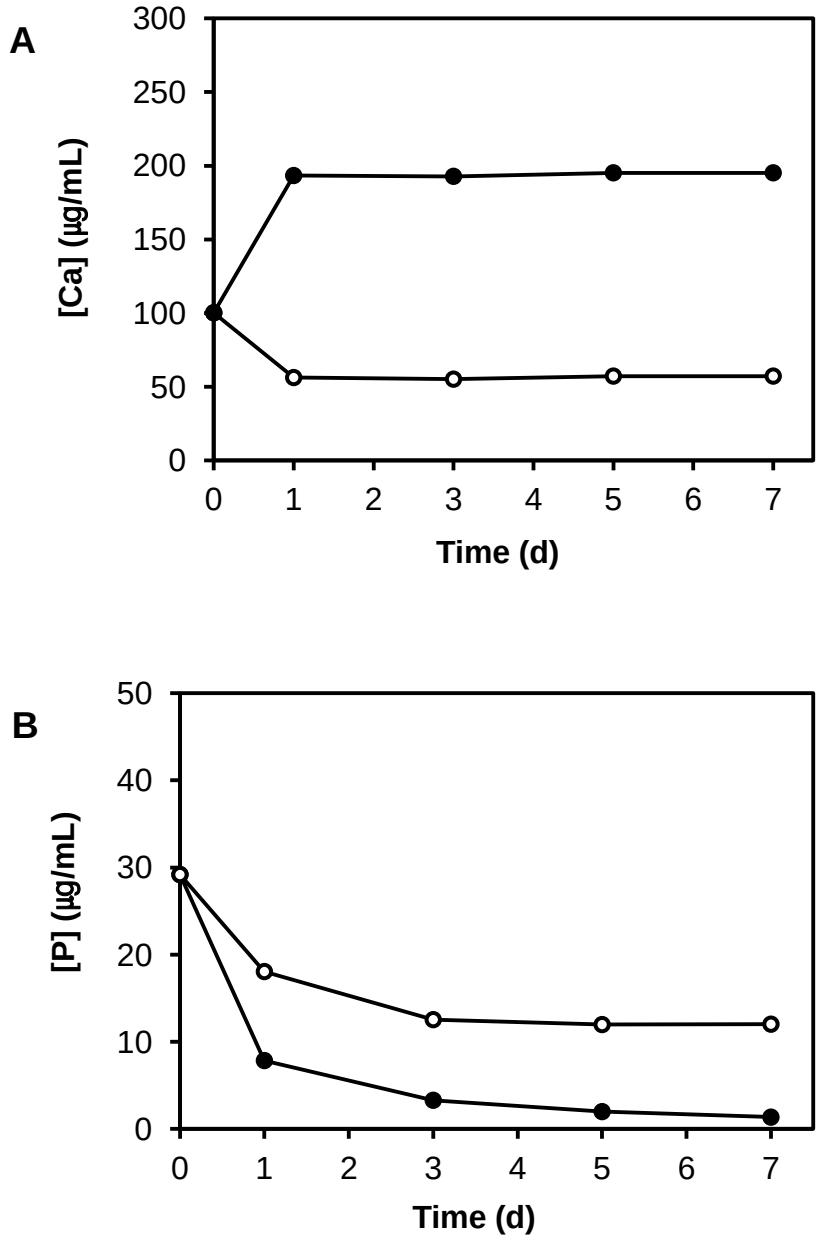

Figure 3-6. Ca (A) and P (B) concentrations in the supernatant as function of time after immersing the PGA monoliths in SBF (filled circle; 1M $CaCl_2$,treatment PGA monolith, empty circle; PGA monolith).

To further characterize the PGA/HAp monolith and confirm HAp formation we used EDX, FT-IR and XRD. EDX analysis showed the presence of both Ca and P on the 1 M $CaCl_2$ treated monolith after the immersion in SBF (Figure 3-7). FT-IR spectra of the PGA/HAp monolith showed peaks at around 560 and 600 cm^{-1} that can be assigned to Ca-P bending vibrations typical of calcium phosphate (Figure 3-8).[8,28,29] Furthermore XRD as shown in Figure 3-9 confirmed, the presence of HAp crystals on the monolith by showing two peaks at 32° and 46° (2θ) that can be assigned to the (211) and (222) planes of HAp.[8,30,31]

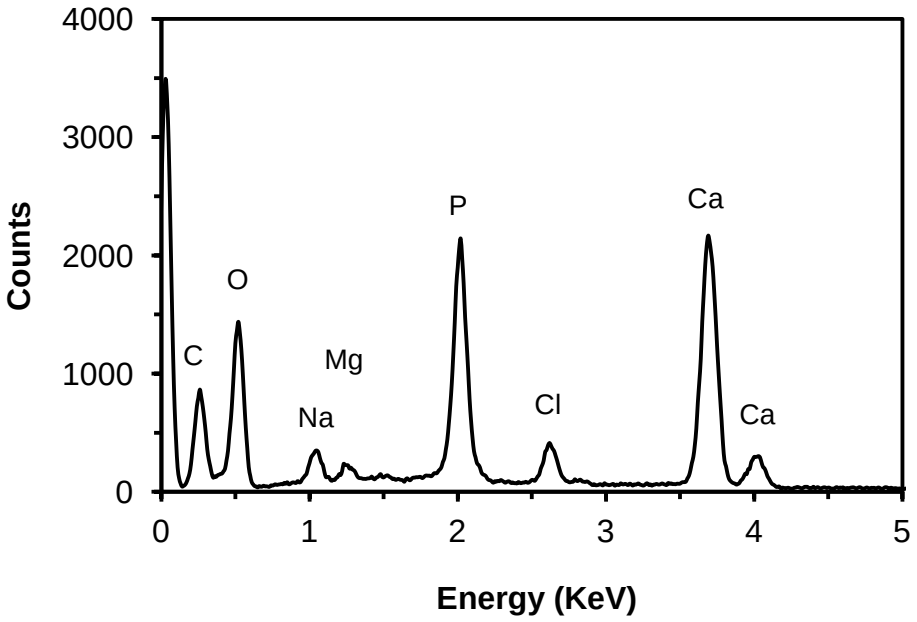

Figure 3-7. EDX spectrum of the PGA/HAp monolith.

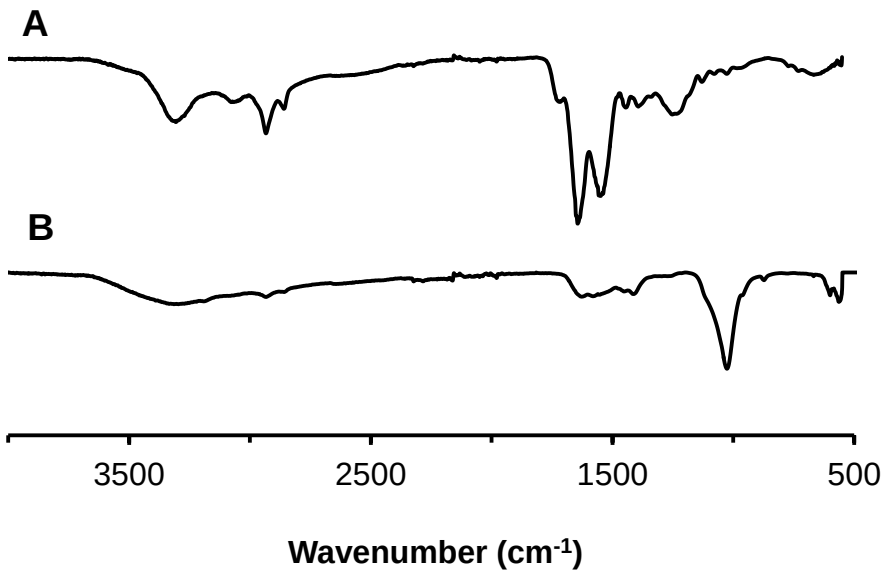

Figure 3-8. FT-IR spectra of PGA monolith (A) and PGA/HAp monolith (B).

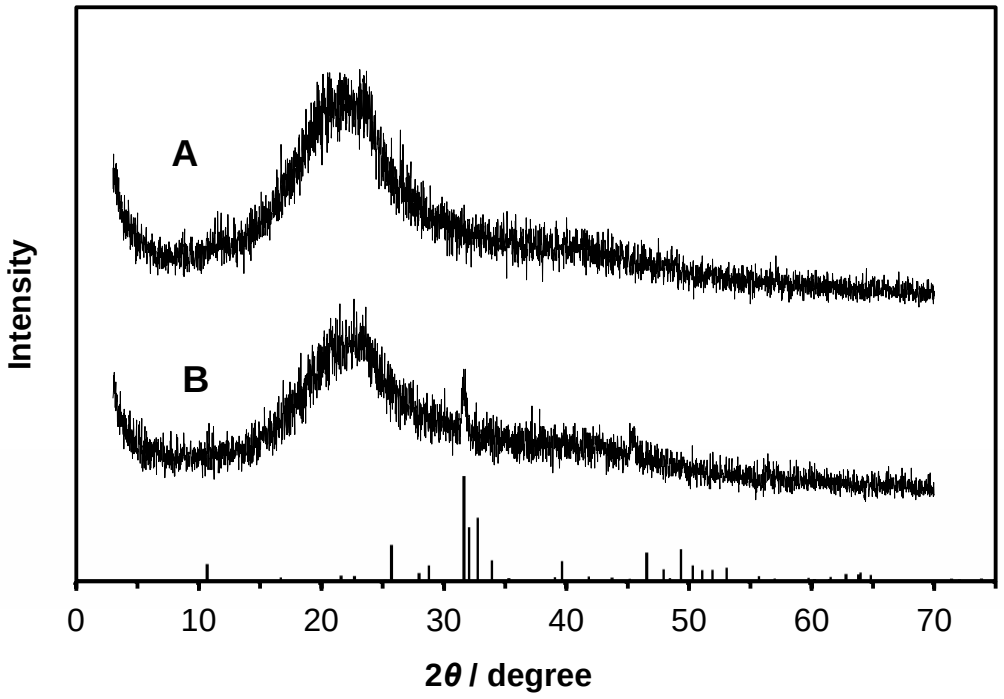

Figure 3-9. XRD patterns of the PGA monolith (A) and PGA/HAp monolith (B). Reference: JCPDS Card No. 74-0565.

Cell attachment and proliferation of MC3T3-E1 cells

MC3T3-E1 cells were cultured on the PGA and PGA/HAp monoliths and the potential of these monoliths as a cell scaffold in bone tissue engineering was evaluated. For this experiment, the PGA/HAp monolith was used that had been pretreated with 1 M $CaCl_2$ in SBF for 7 d. A polystyrene culture plate was used as a control. At first, whether the cells were able to attach on the PGA monolith tested using confocal laser scanning fluorescent microscopy (CLSFM). Cells were visualized with calcein AM and the monolith backbone had been labeled with Rhodamine B using the carboxylic acid groups of PGA. As can be seen in Figure 3-10, MC3T3-E1 cells attached and spread on the monolith surface.

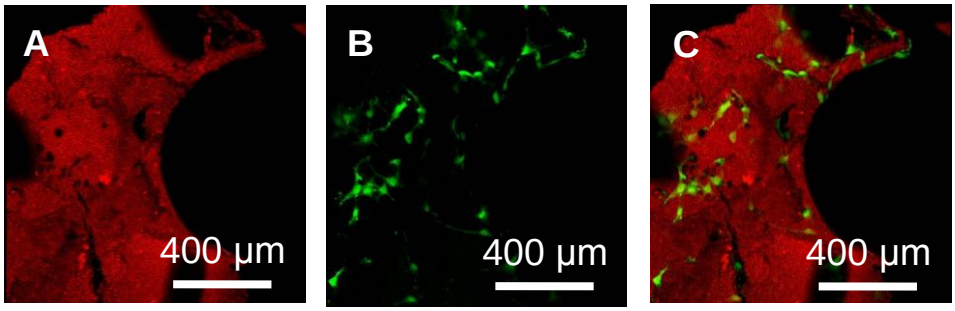

Figure 3-10. CLSFM images of Rhodamine-labeled PGA monolith (A), MC3T3-E1 cells on the PGA monolith (B), and the overlay of both (C). Green fluorescence: live cells; red fluorescence: PGA monolith.

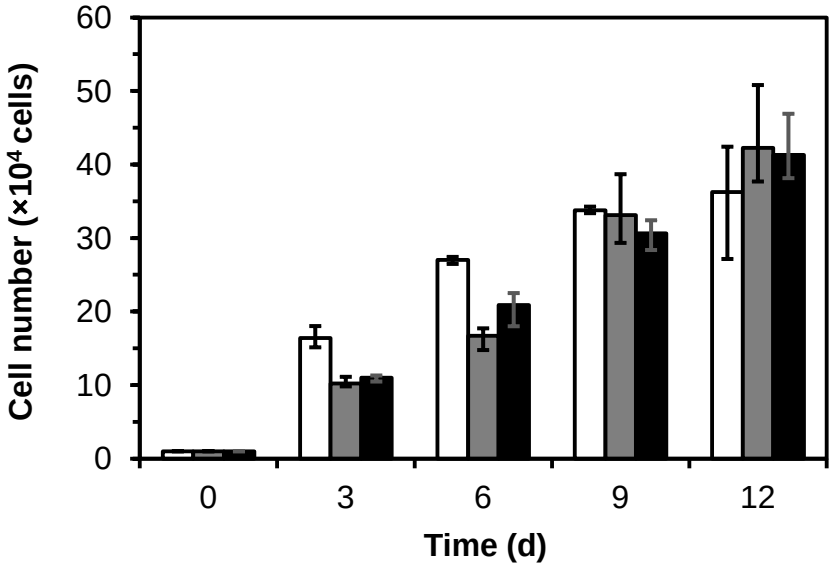

Figure 3-11. Viability of MC3T3-E1 cells on the PGA, PGA/HAp monoliths and a polystyrene plate (empty bar; polystyrene plate, gray bar; PGA monolith, filled bar; PGA/HAp monolith).

The viability of cells cultured on the PGA and PGA/HAp monoliths were evaluated by the MTT assay (Figure 3-11). The cells proliferated continuously for 12 d on the PGA and PGA/HAp monoliths while the cell number reached a plateau after 9 d for a polystyrene plate. No significant difference in cell number was observed between the PGA and PGA/HAp monoliths. This continuous growth on the monoliths can be attributed to the sub-millimeter cavities which allow cell infiltration. Figure 3-12 shows CLSFM images of MC3T3-E1 cells on the monoliths stained with the LIVE/DEAD cell viability assay kit after 1 and 7 d of culture. As can be seen, live cells are covering the monolith backbone. Importantly, there were very few dead cells indicating that the monoliths were not cytotoxic which is in line with the MTT data. In addition, the cells seemed to be spreading more on the PGA/HAp monolith than the PGA monolith, which may be attributed to HAp deposited on the monolith surface. It is known that HAp improves cellular adhesion.[32]

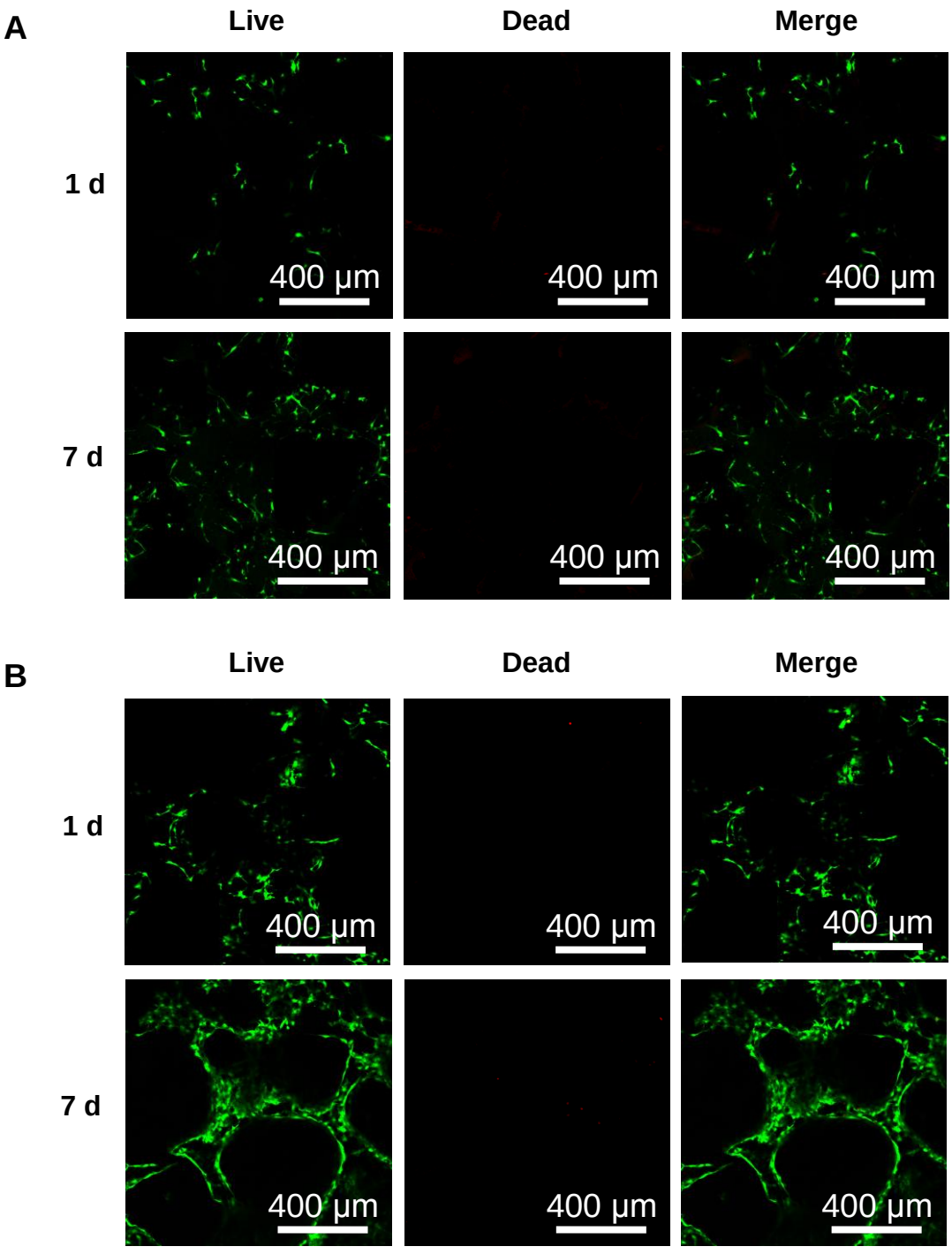

Figure 3-12. CLSFM images of MC3T3-E1 cells on the PGA monolith (A) and PGA/HAp monolith (B) after 1 d and 7 d. Green fluorescence: live cells; red fluorescence: dead cells.

Loading and sustained release of BMP-2

BMP-2 is one of the important growth factors involved in the development and regeneration of bone and cartilage.[33,34] This protein has an isoelectric point of 8.5 so that it is positively charged at physiological pH7.4. Since the PGA monolith possesses negative charged carboxylate groups (pK_a 4.8), it is expected that the monoliths can adsorb BMP-2 by electrostatic interaction.[35,36] Here, BMP-2 was physically entrapped to the PGA and PGA/HAp monoliths by simple electrostatic adsorption and evaluated their potential in controlled delivery of growth factors.

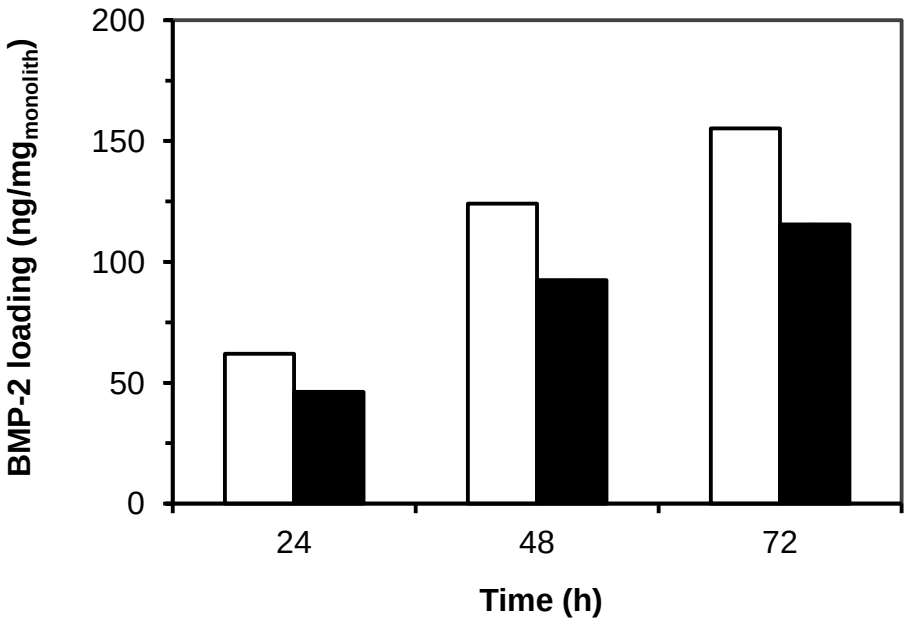

Figure 3-13. BMP-2 leading capacity of the monoliths. Sample size: diameter 6 mm × thickness 1 mm; sample weight: PGA monolith (3.2 mg) and PGA/Hap monolith (4.3 mg) (empty bar; PGA monolith, filled bar; PGA/HAp monolith).

The PGA monolith and PGA/HAp monoliths were immersed in PBS containing BMP-2 (500 ng) and incubated at 4 ^{o}C. As shown in Figure 3-13, the concentration of BMP-2 in the supernatant decreased over 72 h. After 72 h of incubation, the concentration of BMP-2 was below detection limit of ELISA meaning that the BMP-2 had been completely absorbed by the monoliths. No significant difference in the absorbing capacity was observed between the PGA and PGA/HAp monoliths.

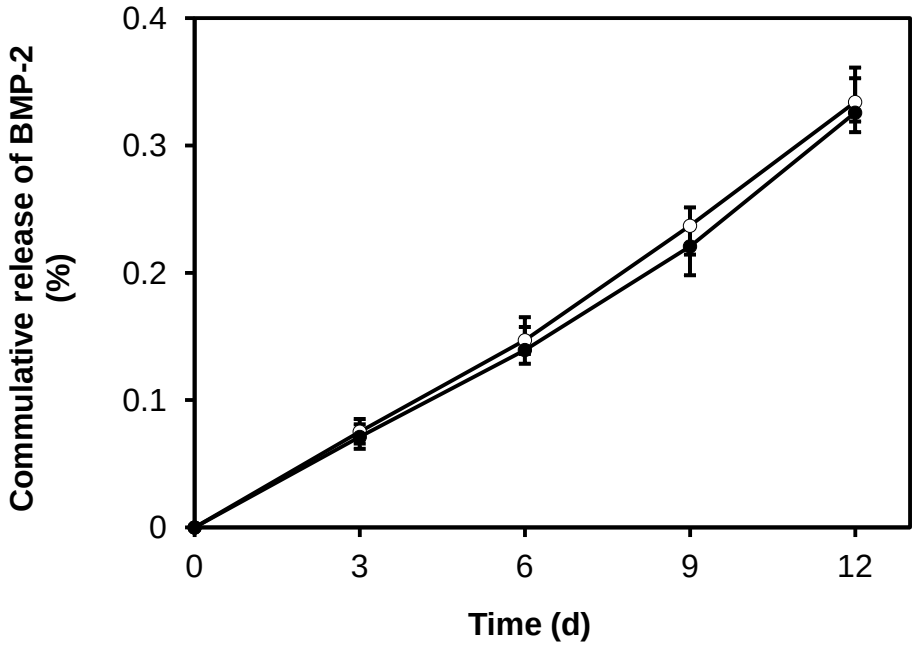

Figure 3-14. BMP-2 release from the PGA monolith and PGA/HAp monolith (empty circles; PGA monolith, filled circles; PGA/HAp monolith).

The sustained release of BMP-2 from the monolith was confirmed in the presence of MC3T3-E1 cells. The cells were seeded onto the monoliths loaded with BMP-2 (500 ng) and cultured for 12 d replacing the culture medium every third day. As

shown in Figure 3-14, both PGA and PGA/HAp monolith showed sustained release of BMP-2 without initial burst release. After 12 d of incubation, the amount of released BMP-2 was 0.33% (1.65 ng) for the PGA monolith and 0.32% (1.60 ng) for the PGA/HAp monolith, respectively. It has been reported that sustained release of BMP-2 promotes osteogenic differentiation and bone formation compared to fast release.[35,36] Thus, this slow release of BMP-2 may be useful in bone healing which generally requires a long-term treatment for several months.[37,38]

Osteogenic differentiation of MC3T3-E1 cells

MC3T3E-1 cells were cultured on the PGA and PGA/HAp monoliths loaded with BMP-2 (500 ng) for 12 d and the alkaline phosphatase (ALP) activity was evaluated, which is an early stage marker for osteogenic differentiation. As a control, cells were also cultured on a polystyrene plate for 12 d replacing the culture medium supplemented with BMP-2 (25 ng) every third day (total amount of BMP-2 added: 100 ng). As shown in Figure 3-15, in the absence of BMP-2, MC3T3-E1 cells showed a similar level of ALP activity for the PGA and PGA/HAp monoliths as well as the polystyrene plate. The addition of BMP-2 increased the ALP activity of the cells cultured on polystyrene. The PGA monolith loaded with BMP-2 showed comparable level of ALP activity to the polystyrene plate. Importantly, the cells showed 40% higher ALP activity when cultured on the PGA/HAp monolith compared to the PGA monolith and the polystyrene plate. Several reports have shown that the HAp surface enhanced the differentiation of preosteoblasts compared to plastic surfaces by promoting osteoblast adhesion, proliferation, differentiation and extracellular matrix synthesis.[11,39] Therefore, higher osteoblastic activity of MC3T3-E1 cells on the PGA/HAp monolith was due to the presence of HAp that facilitated osteogenic differentiation.

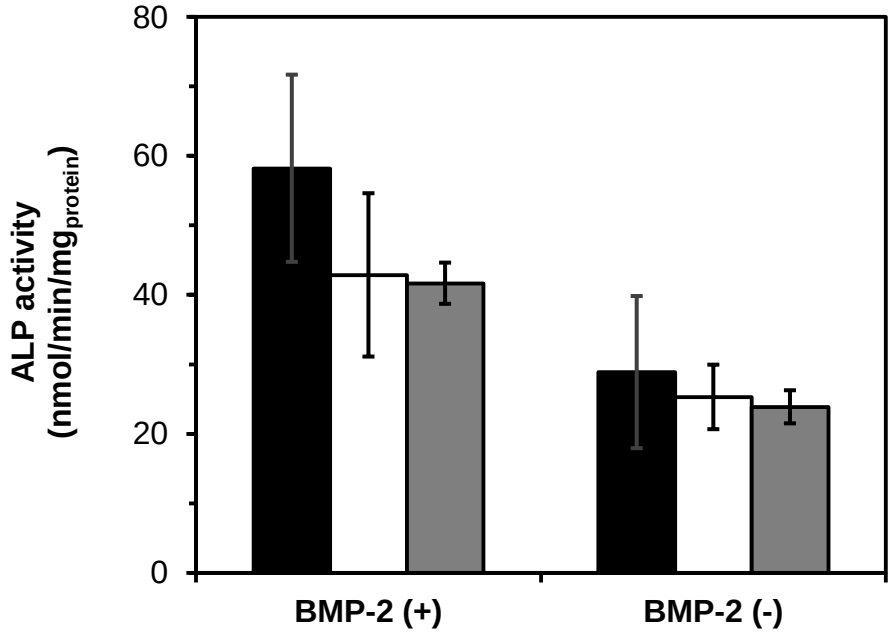

Figure 3-15. ALP activity of MC3T3-E1 cells on the PGA monolith, PGA/HAp monolith, and polystyrene plate in the presence and absence of BMP-2 after 12 d of culture (filled bar; PGA/HAp monolith empty bar; PGA monolith, gray bar; polystyrene plate).

3.4 Conclusion

The PGA/HAp monolith was prepared by biomineralization of a PGA monolith in SBF. The HAp nucleation and crystal growth on the $CaCl_2$ pretreated monolith was significantly faster than that of the untreated monolith. MC3T3-E1 cells efficiently attached and proliferated on both the PGA and PGA/HAp monolith without obvious cell

toxicity. These monoliths efficiently absorbed BMP-2 by electrostatic interaction, which was slowly released into the medium in the presence of cells. Moreover, BMP-2 remained bioactive and MC3T3-E1 cells cultured on the BMP-2 loaded PGA/HAp monolith showed increased ALP activity compared to the PGA monolith. Therefore, the unique morphology and bioactivity of the PGA/HAp monoliths would be advantageous in bone tissue engineering.

References

[1] T. Candela, A. Fouet, *Mol. Microbiol*. **2006**, *60*, 1091.

[2] M. Ashiuchi, C. Nawa, T. Kamei, J. J. Song, S. P. Hong, M. H. Sung, K. Soda, T. Yagi, H. Misono, *Eur. J. Biochem.* **2001**, *268*, 5321.

[3] M. H. Sung, C. Park, C. J. Kim, H. Poo, K. Soda. M. Ashiuchi, *Chem. Rec.* **2005**, *5*, 352.

[4] I. L. Shih, Y. T. Van, *Bioresour. Technol*. **2001**, *79*, 207.

[5] H. Poo, C. Park, M. S. Kwak, D. Y. Choi, S. P. Hong, I. H. Lee, Y. T. Lim, Y. K. Choi, S. R. Bae, H. Uyama, C. J. Kim, M. H. Sung, *Chem. Biodivers*. **2010**, *7*, 1555.

[6] J. M. Buescher, A. Margaritis, *Crit. Rev. Biotechnol*. **2007**, *27*, 1.

[7] I. Armentano, M. Dottori, E. Fortunati, S. Mattioli, J. M. Kenny, *Polym. Degrad. Stab*. **2010**, *95*, 2126.

[8] G. Poologasundarampillai, B. Yu, O. Tsigkou, E. Valliant, S. Yue, P. D. Lee, R. W. Hamilton, M. M. Stevens, T. Kasuga, J. R. Jones, *Soft Matter.* **2012**, *8*, 4822.

[9] G. K. Hunter, H. A. Goldberg, *Biochem. J.* **1994**, *302*, 175.

[10] T. G. Kim, H. S. Shin, D. W. Lim, *Adv. Funct. Mater.* **2012**, *22*, 2446.

[11] N. D. Luong, I. S. Moon, J. D. Nam, *Macromol. Mater. Eng.* **2009**, *294*, 699.

[12] T. Kokubo, H. Takadama, *Biomaterials* **2006**, *27*, 2907.

[13] R. Murugan, S. Ramakrishna, *Compos. Sci. Technol.* **2005**, *65*, 2385.

[14] H. Shin, S. Jo, A. G. Mikos, *Biomaterials* **2003**, *24*, 4353.

[15] A. Sugino, T. Miyazaki, C. Ohtsuki, *J. Mat. Sci., Mater. Med.* **2008**, *19*, 2269.

[16] G. Poologasundarampillai, C. Ionescu, O. Tsigkou, M. Murugesan, R. G. Hill, M. M. Stevens, J. V. Hanna, M. E. Smith, J. R. Jones, *J. Mater. Chem.* **2010**, *20*, 8952.

[17] T. Miyazaki, A. Kuramoto, A. Hirakawa, Y. Shirosaki, C. Ohtsuki, *Dent. Mater. J.* **2013**, *32*, 544.

[18] I. Sopyan, M. Mel, S. Ramesh, K. A. Khalid, *Sci. Technol. Adv. Mater.* **2007**, *8*, 116.

[19] Q. Zhang, H. Luo, Y. Zhang, Y. Zhou, Z. Ye, W. Tan, M. Lang, *Mater. Sci. Eng. C Mater. Biol. Appl.* **2013**, *33*, 2094.

[20] S. G. Lé vesque, R. M. Lim, M. S. Shoichet, *Biomaterials* **2005**, *26*, 7436.

[21] S. Sosnowski, P. Woźniak, M. Lewandowska-Szumieł, *Macromol. Biosci*. **2006**, *6*, 425.

[22] K. Okada, M. Nandi, J. Maruyama, T. Oka, T. Tsujimoto, K. Kondoh, H. Uyama, *Chem. Commun.* **2011**, *47*, 7422.

[23] Y. Xin, T. Fujimoto, H. Uyama, *Polymer* **2012**, *53*, 2847.

[24] X. Sun, T. Fujimoto, H. Uyama, *Polym. J.* **2013**, *45*, 1101.

[25] S. B. Park, T. Fujimoto, E. Mizohata, T. Inoue, M. H. Sung, H. Uyama, *J. Microbiol. Biotecnol*. **2013**, *23*, 942.

[26] S. B. Park, J. Sakamoto, M. H. Sung, H. Uyama, *Polymer* **2013**, *54*, 6114.

[27] H. Takadama, H. M. Kim, T. Kokubo, T. Nakamura, *J. Biomed. Mater. Res*. **2001**, *57*, 441.

[28] M. C. Chang, J. Tanaka, *Biomaterials* **2002**, *23*, 4811.

[29] B. O. Fowler, *Inorg. Chem*. **1974**, *13*, 194.

[30] T. Kokubo, H. Kushitani, S. Sakka, *J. Biomed. Mater. Res*. **1990**, *24*, 721.

[31] T. Furuzono, T. Taguchi, A. Kishida, M. Akashi, Y. Tamada, *J. Biomed. Mater. Res*. **2000**, *50*, 344.

[32] M. T. Bernards, C. Qin, S. Jiang, *Colloids Surf. B Biointerfaces* **2008**, *64*, 236.

[33] N. Y. Yu, A. Schindeler, D. G. Little, A. J. Ruys, *J. Biomed. Mater. Res. Part B Appl. Biomater.* **2010**, *93B*, 285.

[34] K. Whang, D. C. Tsai, E. K. Nam, M. Aitken, S. M. Sprague, P. K. Patel, K. E. Healy, *J. Biomed. Mater. Res.* **1998**, *42*, 491.

[35] V. Luginbuehl, L. Meinel, H. P. Merkle, B. Gander, *Eur. J. Pham. Biopharm.* **2004**, *58*, 197.

[36] M. L. Macdonald, R. E. Samuel, N. J. Shah, R. F. Padera, Y. M. Beben, P. T. Hammond, *Biomaterials* **2011**, *32*, 1446.

[37] C. Hayashi, U. Hasegawa, Y. Saita, H. Hemmi, T. Hayata, K. Nakashima, Y. Ezura, T. Amagasa, K. Akiyoshi, M. Noda, *J. Cell. Physiol*. **2009**, *220*, 1.

[38] S. J. Florczyk, M. Leung, S. Jana, Z. Li, N. Bhattarai, J. I. Huang, R. A. Hopper, M. Zhang, *J. Biomed. Mater. Res. Part A* **2012**, *100A*, 3408.

[39] K. Rezwan, Q. Z. Chen, J. J. Blaker, A. R. Boccaccini, *Biomaterials* **2006**, *27*, 3413.

[40] B.C. Roy, R. Peterson, S. Mallik, A. D. Campiglia, *J. Org. Chem*. **2000**, *65*, 3644.

Chapter 4

pH Controlled Degradation and Thermal Stability of a Porous Poly(γ-glutamic acid) Monolith Crosslinked with an Oxazoline-Functionalized Polymer

4.1 Introduction

Poly(γ-glutamic acid) (PGA) monolith holds great promise for a wide range of applications, especially in biomaterials and environmental fields due to its high surface area, high stability, pH-responsivity, chelating ability, and biocompatibility.[1-15] However, PGA monolith prepared by thermally induced phase separation (TIPS)[16,17] technique was soluble in water by itself, so it was subsequently crosslinked with hexamethylene diisocyanate (HDI) in previous study.[17] The resultant crosslinked monolith was found to be stable in aqueous media for repeated use as pH-responsive bulk material. Moreover, submillimeter-sized cavities could be introduced into the monolith, which opened up the possibility to cultivate cells inside the monolith.[18]

Chapter 4 describes further explorations to design the PGA monolith for cell scaffolding purposes. Specifically, a new PGA-based monolith is reported which is low-cytotoxic and readily degradable in water under controlled conditions. For its realization, the monolith was crosslinked with a low-toxic and hydrolytically removable polymer. Thereby, the crosslinker was gradually cleaved off from the monolith in a selected pH region, which triggered gradual dissolution of the monolith in water. The

monolith was also demonstrated to absorb calcium salts homogeneously over the surface, which we consider is a first step towards coating the monolith surface with a thin hydroxylapatite layer to promote cell adhesion and proliferation on it.[19-21]

4.2 Experimental

Materials

PGA (acid form, $M_w = 5\times10^3$ kDa) was provided by BioLeaders Corp. (Korea). A polymeric crosslinker with oxazoline side groups (EPOCROS WS-700; M_w = 40 kDa; aqueous solution with 25 wt% concentration) was a gift from Nippon Shokubai Corp. (Tokyo, Japan). Sodium chloride (+80 mesh particle size; Sigma-Aldrich) was used as particulate template. All reagents were of analytical grade and used as received without further purification.

Measurements

Scanning electron microscopic (SEM) images were recorded on a Hitachi SU-3500 instrument at 15 kV. A thin gold film was sputtered on the samples before the images were collected. Nitrogen adsorption/desorption isotherms were measured with a NOVA 4200e surface area & pore size analyzer (Quantachrome Instruments) at 25 ^oC. The Brunauer Emmett Teller (BET) method was utilized to determine specific surface areas. Before the measurements, all samples were degassed at 25 ^oC for 12 h under vacuum. Thermogravimetric analysis (TGA) was performed with an EXSTAR TG/DTA 7200 thermogravimetric analyzer from 40 to 500 ^oC at a heating rate of 10 ^oC/min, under a steady flow of nitrogen of 250 mL/min. Differential scanning calorimetry

(DSC) thermogram was taken using a Seiko DSC6220 instrument. The measurement was performed at the heating rate of 10 ^{o}C/min, under a steady flow of nitrogen of 250 mL/min. The energy dispersive X-ray spectrometric (EDX) measurement for elemental analysis of the monolith surface was conducted by a Hitachi Miniscope TM3000 with a Swift3000 equipment. UV-vis absorption measurements were performed with a Hitachi U-2810 UV-vis spectrometer at 610 nm to determine calcium concentrations.

Preparation of PGA monolith

A typical preparation procedure is as follows. A PGA powder (450 mg) was dissolved completely in a mixture of dimethyl sulfoxide (DMSO), water and ethanol (3 mL, DMSO/water/ ethanol = 9/1/20) by heating at 80 ^{o}C. Sodium chloride particles (5.5 g) were then added to the solution and the mixture was cooled at 25 ^{o}C. The resultant monolith was repeatedly washed with acetone to remove the solvents and subsequently dried under vacuum.[17,18] This as-prepared monolith (3.49 mmol monomer unit of PGA) was crosslinked in ethanol (10 mL) by slow addition of the aqueous solution of the polymeric crosslinker (3 mL, 13.5 mmol). The crosslinking reaction was carried out at 40 ^{o}C with stirring gently for 24 h. The obtained crosslinked monolith was repeatedly washed with 40% (v/v) acetone/water. Residual water was replaced with acetone and dried in *vacuo* to afford a salt-free crosslinked PGA monolith.

Hydrolytic degradation

The monolith (20 mg) was incubated at 37 ^{o}C for 7 d in 20 mL of 1 mM HCl solution, a phosphate buffered saline (PBS, 0.1 M, pH = 7.4) and 10 mM NaOH solution under sterile conditions. Each solution was replaced every 2 d with a fresh solution. The course of degradation was monitored by weight loss of each sample. Prior to each weight measurement, the monolith taken out from the solution was washed first

with 0.1 M HCl solution, then with acetone, and dried *in vacuo*. Remaining portion of the monolith was calculated by the following equation.

Remaining portion (%) = (Weight of dry monolith after degradation / Weight of dry monolith before degradation) × 100

Cytotoxicity test

The monolith was first immersed in 70% (v/v) ethanol/water for 24 h and then washed with sterile water to remove ethanol. The osteoblastic MC3TC-E1 cells in the density of 1×10^4 cells/well were seeded on top of the monoliths and cultured in a medium (α-minimum essential medium supplemented with 10% fetal bovine serum and 1% penicillin/streptomycin).[22,23] The cells on 1 mg of monolith were cultured at 37 ^oC under a humidified atmosphere with 5% CO_2 for 24 h. After 1 d and 5 d incubation periods, cytotoxicity was assessed by the 3-(4,5-dimethyl-2-thiazolyl)-2,5-diphenyl-2H-tetrazolium bromide (MTT) assay. The number of viable cells was measured by Synergy HT Multi-Detection Microplate Reader (Bio-TEK® Instruments, Inc., Winooski, VT) using 96 well polystyrene plates at 570 nm.

Calcium loading and release

The monolith (10 mg) was immersed in 20 mL of an aqueous solution of $CaCl_2$ (1 mg/mL) for 24 h at 4 ^oC. After drying the monolith at 40 ^oC, it was immersed in 20 mL of 1 mM HCl aq, PBS, or 10 mM NaOH aq at 37 ^oC for 1 h. The amount of the calcium salt released from the monolith into the solution was estimated by using Calcium-E test kit (Wako Pure Chemical. Industries, Ltd., Osaka, Japan).

4.3 Results and Discussion

Preparation of PGA monolith

According to a previous procedure,[17,18] a PGA monolith was prepared by the TIPS method from a PGA solution containing crystalline particles of sodium chloride (0.2-0.6 mm).[18] Since this as-prepared monolith was readily soluble in water by itself, it was internally crosslinked to resist water for subsequent use. A commercial low-toxic polymer carrying oxazoline groups (EPOCROS WS-700®) was chosen here as crosslinker (Figure 4-1). This polymeric crosslinker can react with the carboxylates of PGA by opening the oxazoline rings to form ester bonds.[24-26] As a consequence, the PGA chains were held together by the crosslinker that was hydrolytically cleavable.[27] The monolith was thus designed to be not merely biocompatible but readily degradable under controlled conditions in aqueous media, meeting requirements towards cell scaffolding applications.

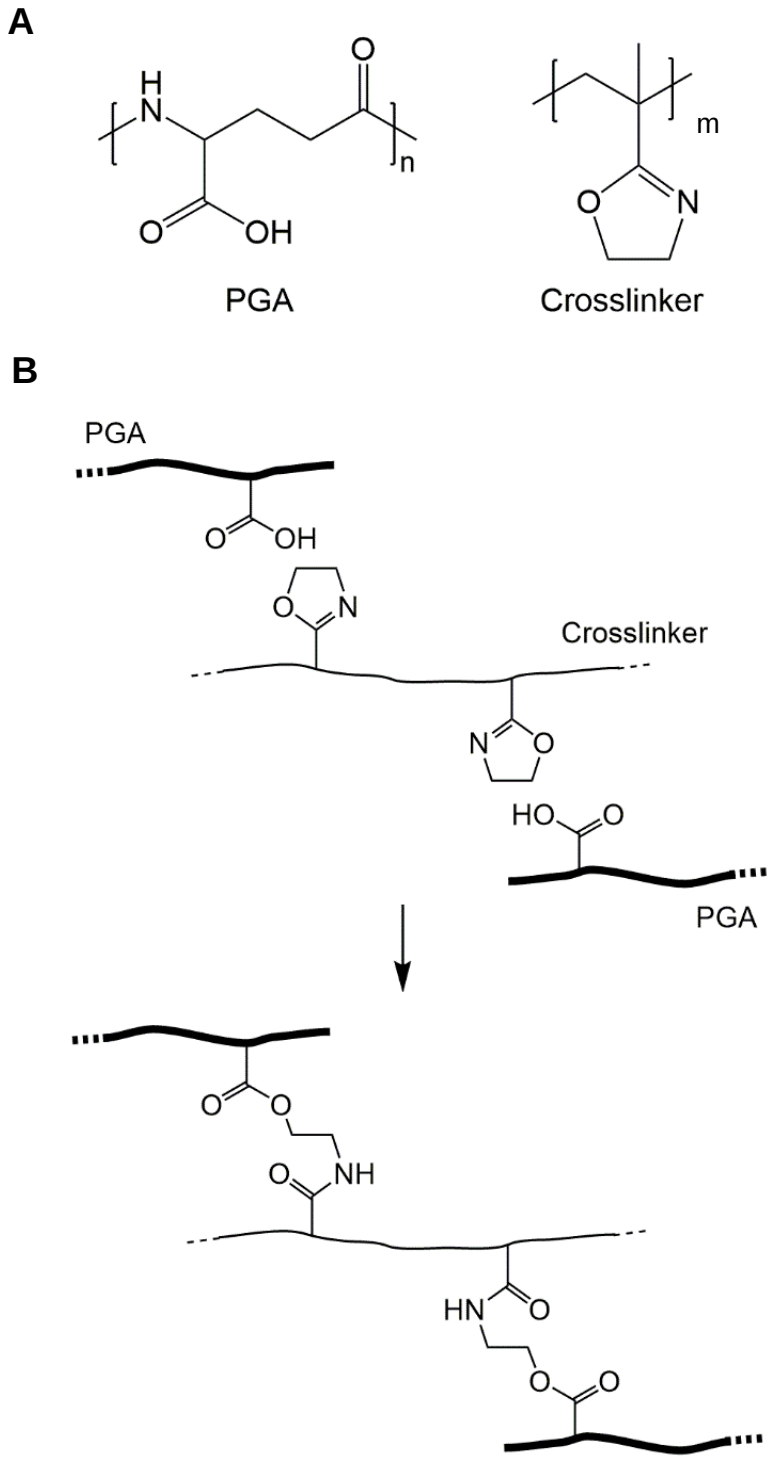

Figure 4-1. Chemical structures of PGA and the crosslinker (A) and a simplified depiction of the crosslinking scheme (B).

The crosslinked monolith was repeatedly washed with 40% (v/v) acetone/water to remove the crosslinker of excessive use and the salt templates incorporated in the monolith. The monolith did not lose the weight during the washing process. Cross-sectional analysis of the monolith by SEM revealed that the salt templates were selectively removed from the monolith, leaving the cavities whose shape and size were inherited from the templates (Figure 4-2). The SEM observation also confirmed that the monolith had interconnected porosity whereby water could permeate it to leach the templates away. The porosity was also suggested by a high specific surface area (118 ± 6 m^2/g) of the monolith estimated by the BET analysis assuming monolayer adsorption. These results proved that the monolith maintained the original porosity during the crosslinking process and gained resistance to water.

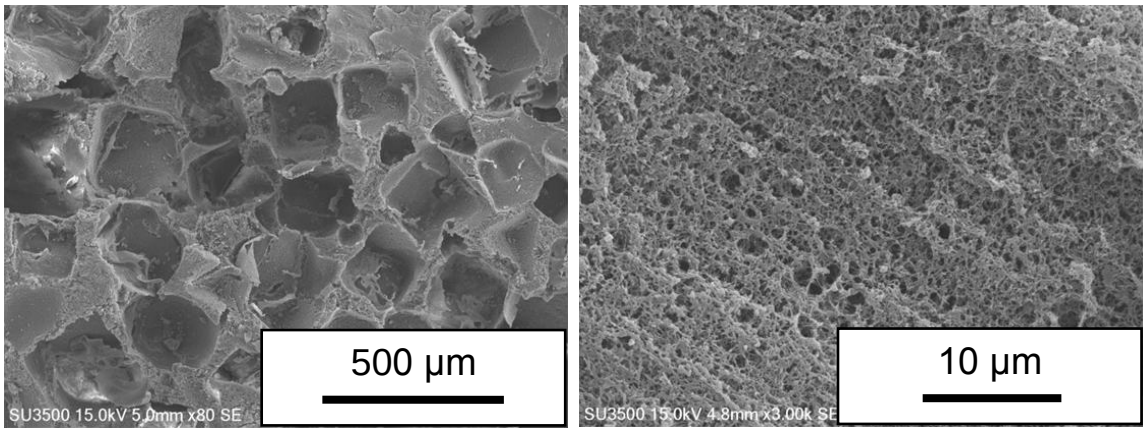

Figure 4-2. SEM cross-sectional images of the crosslinked monolith.

Stability and degradation

The monolith got swollen as soon as it was dipped in aqueous solutions whose pH values were higher than pK_a of PGA (2.27).[28] The swelling became more significant as the solution became more basic. The swelling could not be quantified because of concurrent occurrence of the monolith degradation; the monolith degraded into a homogeneous solution within 1 d in 10 mM NaOH aq, while the same monolith was stable over one week in 1 mM HCl aq (Figure 4-3). The monolith moderately degraded in a phosphate buffered saline (PBS, pH 7.4), indicating that the degradation rate could be controlled by selecting the pH of the solution. Note that a previous report by Sevoian and coworkers indicate that the ester bonds of the crosslinker are much more susceptible to hydrolysis than the amide bonds in the PGA chain.[27]

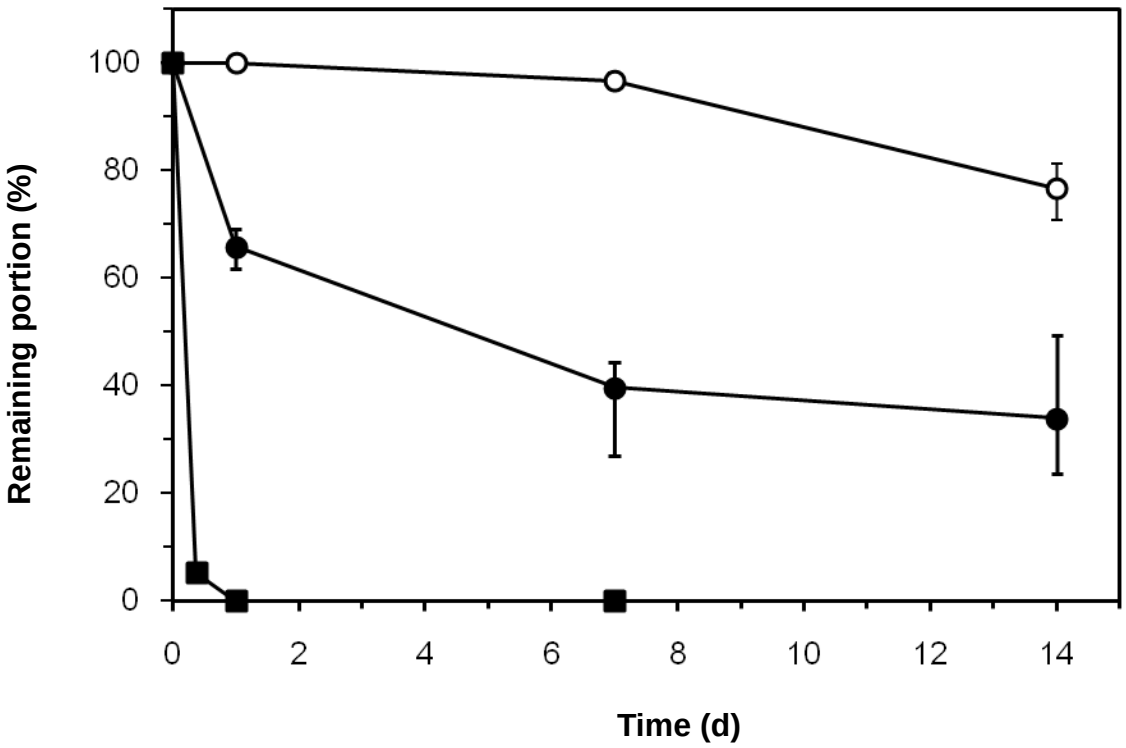

Figure 4-3. Time course of the weight loss of the monolith immersed in 10 mM NaOH aq (filled squares), PBS (filled circles) and 1 mM HCl aq (empty circles).

Figure 4-4 shows cross-sections of the monolith soaked in PBS for one week (A) and that for two weeks (B). In comparison with the original structure given in Figure 4-1, it was found that the degradation occurred co-instantaneously over the entire monolith keeping the macroscopic structural feature apparently little changed, while the small pores merged into larger pores as the degradation progressed.

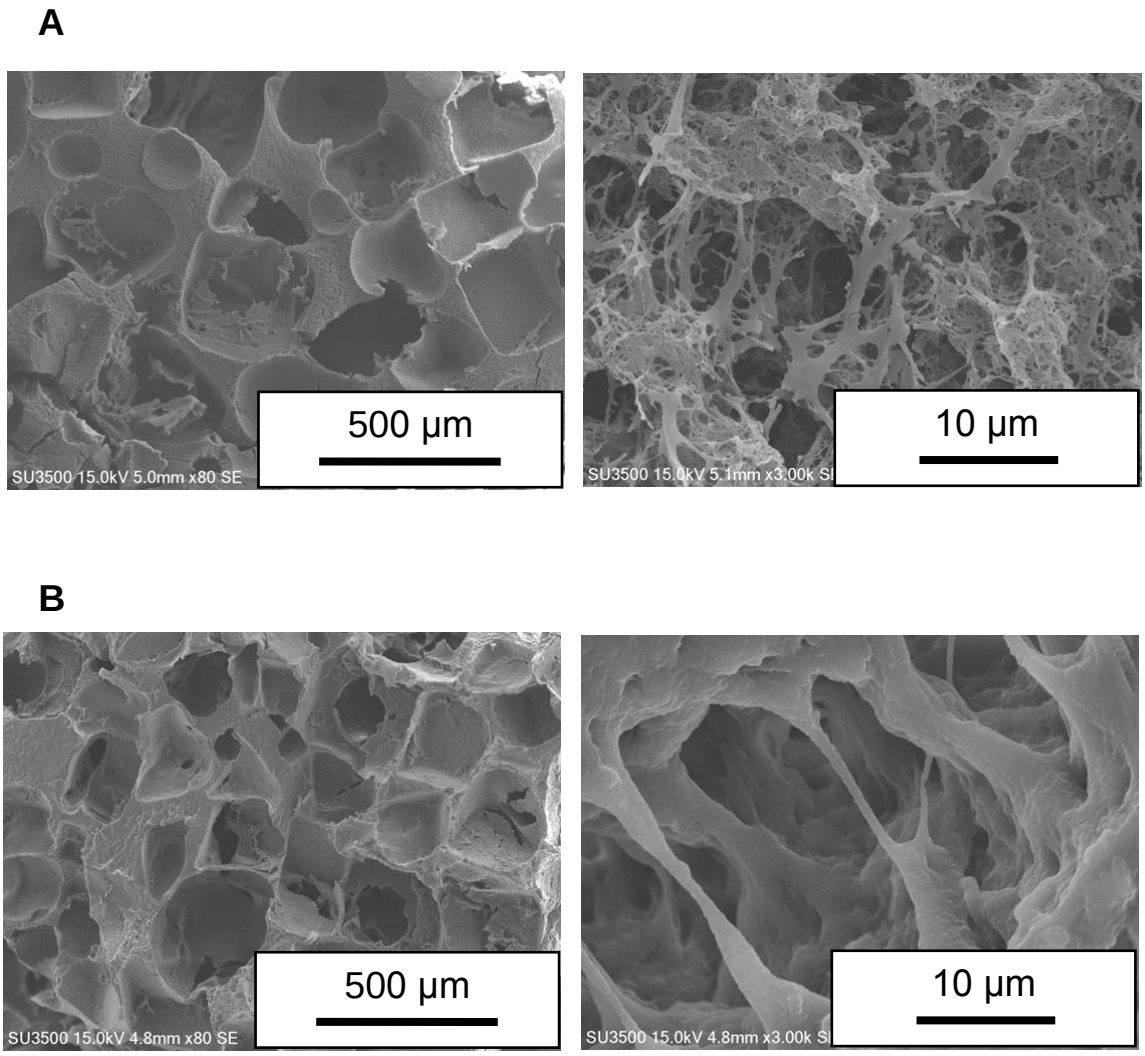

Figure 4-4. SEM cross-sectional images of the monolith immersed in PBS for 1 week (A) and for 2 weeks (B).

The monolith was also analyzed by TGA and DSC (Figure 4-5). The TGA results indicate that the monolith started to decompose at the temperatures higher than 200 ^{o}C, similar to a PGA powder as control. The weight loss before decomposition was attributed to desorption of adsorbates; the DSC results showed that an endothermic process over a wide range of temperature occurred only in the first heating of the monolith from 0 to 190 ^{o}C. The absence of any other endo-/exothermal processes indicated that neither reaction nor structural transition occurred in this temperature range. Cross-sectional analysis by SEM proved that the monolith structure remained little changed even after heated up to 190 ^{o}C, pointing to its high thermal stability (Figure 4-6). Note that such thermal stability may offer attractive options in application that include long-term storage of the monolith in a dry form and sterilization by heat prior to its use for cell scaffolding.[29]

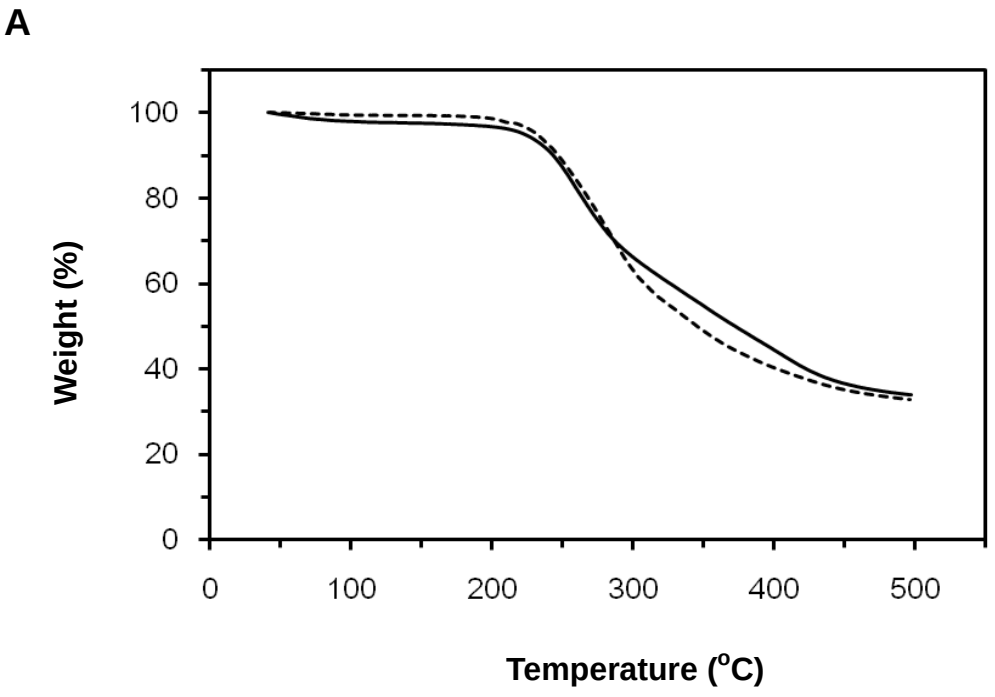

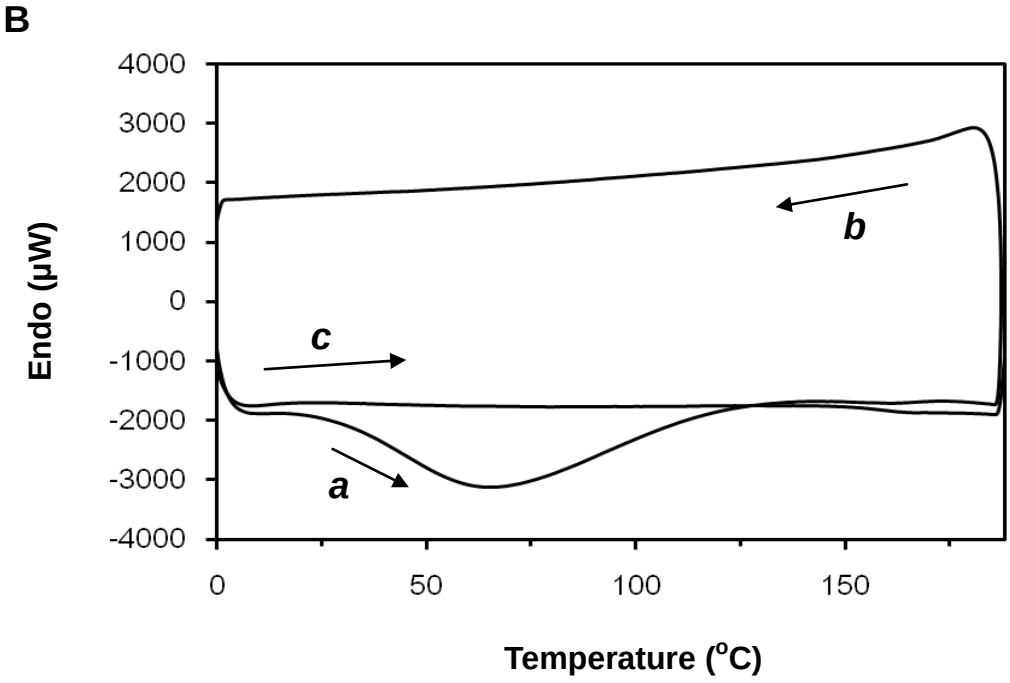

Figure 4-5. TGA (A) and DSC (B) results. The solid and broken curves represent the results obtained from the monolith and a PGA powder, respectively. The arrows in DSC thermograms show the directions of temperature change. The symbols *a*, *b* and *c* represent the first heating process from 0 to 190 ^{o}C, the subsequent cooling from 190 to 0 ^{o}C and the second heating from 0 to 190 ^{o}C, respectively.

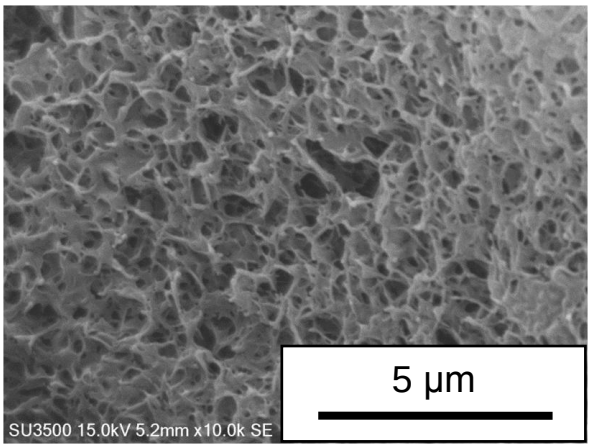

Figure 4-6. SEM cross-sectional image of the monolith after heated up to 190 ^{o}C.

Cytotoxicity test and calcium loading

The present monolith was composed of only PGA and the low-toxic crosslinker. Viability of MC3TC-E1 cells exposed to the monolith was assessed by the MTT assay.[30] The cytotoxicity of the monolith was confirmed to be as low as that of a polystyrene dish used as control (Figure 4-7).

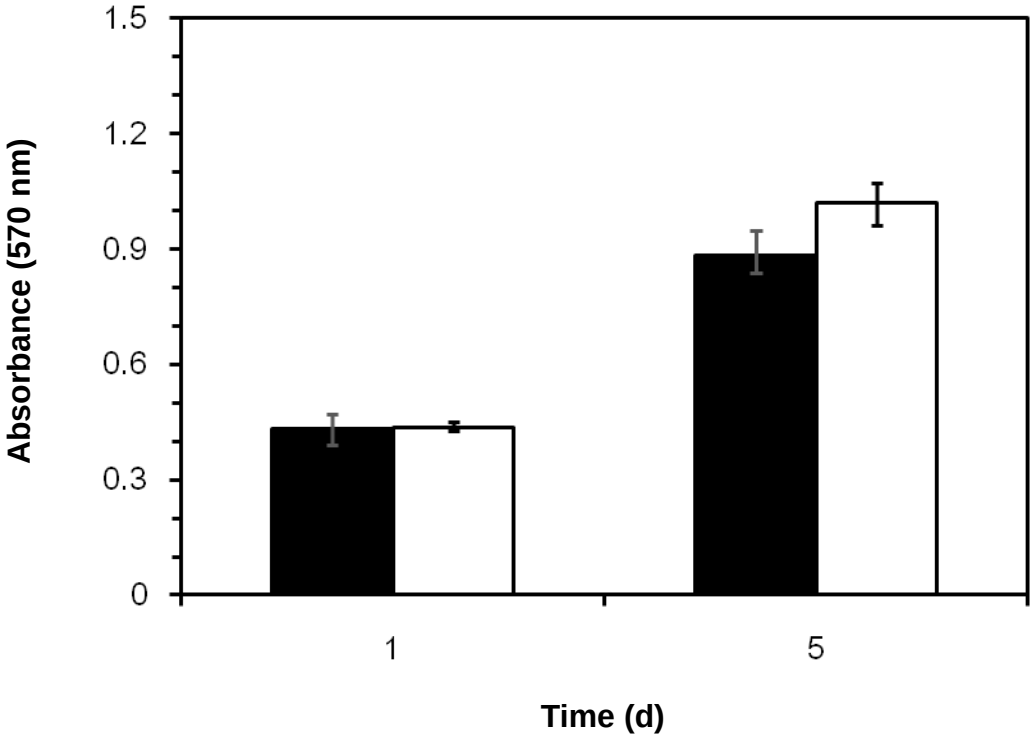

Figure 4-7. Viability of MC3TC-E1 cells exposed to the monolith (filled bars) or a polystyrene dish as control (empty bars) assessed by the MTT assay.

Towards applications of the present monolith for cell scaffolding, the highly hydrophilic nature of the monolith surface imparted by PGA may not always suit for cell adhesion and proliferation. This issue can be addressed by coating the monolith surface with a thin layer of a hydroxylapatite.[31,32] In this context, homogeneous

immobilization of a calcium salt on the surface of the present monolith was demonstrated. The monolith was soaked in an aqueous solution of $CaCl_2$ (1 mg/mL) at 4 ^oC for 12 h. Thereby, 1.9 mg of calcium was loaded on the monolith per unit mass. Cross-sectional analysis of the monolith using EDX proved that the calcium was homogeneously distributed over the monolith surface (Figure 4-8).

When the calcium-loaded monolith was subsequently soaked in PBS at 37 ^oC, 7% of the calcium salt was released in 1 h. For comparison, the same monolith soaked in 1 mM HCl aq released 18% of the calcium salt. This difference would be ascribed to the chelating activity of the carboxylate stronger than that of the carboxylic acid.[33] These results suggested that both loading amount and release rate of the calcium salt could be controlled by the solution pH, possibly affecting the expected growth of a hydroxylapatite layer on the monolith surface.

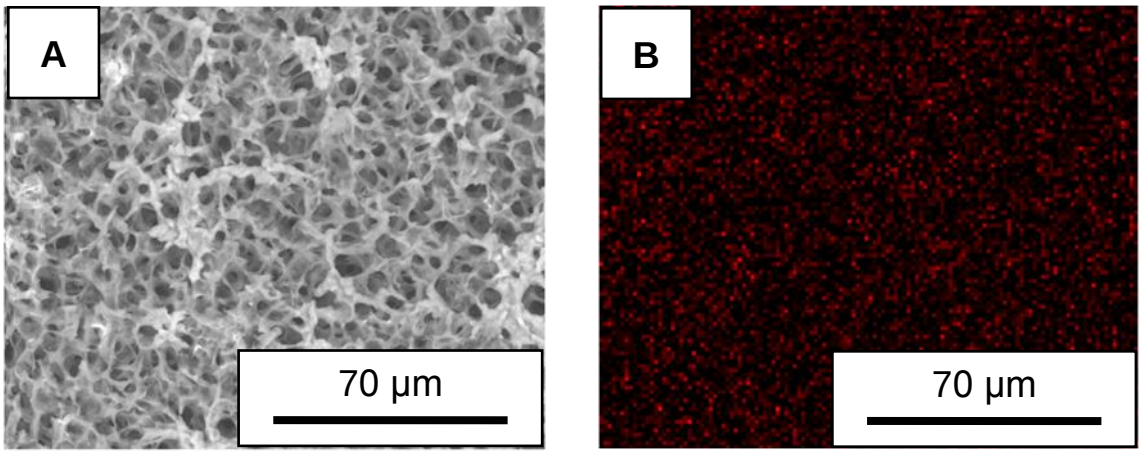

Figure 4-8. Cross-sectional analysis of the $Ca(II)Cl_2$ loaded monolith by SEM (A) and EDX (B). Red dots in the right picture represent where calcium locate in the monolith shown in the left picture.

4.4 Conclusion

A new monolithic porous material has been prepared from PGA, aiming at cell scaffolding applications. The monolith was crosslinked by a low-toxic polymer that is hydrolytically removable. The monolith was indeed demonstrated to be low-cytotoxic and degradable at the rate controlled by pH. Despite the degradability in aqueous media, the monolith was found thermally stable up to the decomposition temperature over 200 ^{o}C. It was also found that the monolith could absorb a calcium salt homogeneously over the surface and release it at a lower pH. Such control over adsorption/desorption of calcium salts may open the possibility to grow a hydroxylapatite layer on the monolith surface to promote cell adhesion and proliferation on it. These results indicate that the PGA monolith crosslinked with oxazoline-functionalized polymer has large potential as a cell scaffolding material.

References

[1] M. Ashiuchi, T. Kamei, H. Misono, *J. Mol. Catal. B: Enzym*. **2003**, *23*, 101.

[2] M. Ashiuchi, C. Nawa, T. Kamei, J. J. Song, S. P. Hong, M. H. Sung, K. Soda, T. Yagi, H. Misono, *Eur. J. Biochem*. **2001**, *268*, 5321.

[3] T. Candela, A. Fouet, *Mol. Microbiol*. **2006**, *60*, 1091.

[4] B. G. Park, H. S. Kang, W. Lee, J. S. Kim, T. I. Son, *J. Appl. Polym. Sci*. **2013**, *127*, 832.

[5] B. S. Inbaraj, B. H. Chen, *Int. J. Nanomedicine* **2012**, *7*, 4419.

[6] M. H. Sung, C. Park, C. J. Kim, H. Poo, K. Soda, M. Ashiuchi, *Chem. Rec*. **2005**, *5*, 352.

[7] H. Poo, C. Park, M. S. Kwak, D. Y. Choi, S. P. Hong, I. H. Lee, Y. T. Lim, Y. K. Choi, S. R. Bae, H. Uyama, C. J. Kim, M. H. Sung, *Chem. Biodivers*. **2010**, *7*, 1555.

[8] I. L. Shih, Y. T. Van, *Bioresour. Technol*. **2001**, *79*, 207.

[9] S. R. Bae, C. Park, J. C. Choi, H. Poo, C. J. Kim, M. H. Sun, *J. Microbiol. Biotechnol*. **2010**, *20*, 803.

[10] Z. Yang, Y. Zhang, P. Markland, V. C. Yang, *J. Biomed. Mater. Res*. **2002**, *62*, 14.

[11] M. R. Buchmeiser, *Polymer* **2007**, *48*, 2187.

[12] J. Courtois, E. Bystrom, K. Irgum, *Polymer* **2006**, *47*, 2603.

[13] O. G. Potter, E. F. Hilder, *J. Sep. Sci*. **2008**, *31*, 1881.

[14] F. Svec, *J. Chromatogr. A* **2010**, *1217*, 902.

[15] S. Wei, Y. L. Zhang, H. Ding, J. Liu, J. Sun, Y. He, Z. Li, F. S. Xiao, *Colloids Surf. A Physicochem. Eng. Asp*. **2011**, *380*, 29.

[16] K. Okada, M. Nandi, J. Maruyama, T. Oka, T. Tsujimoto, K. Kondoh, H. Uyama, *Chem. Commun.* **2011**, *47*, 7422.

[17] S. B. Park, T. Fujimoto, E. Mizohata, T. Inoue, M. H. Sung, H. Uyama, *J. Microbiol. Biotecnol*. **2013**, *23*, 942.

[18] S. B. Park, J. Sakamoto, M. H. Sung, H. Uyama, *Polymer* **2013**, *54*, 6114.

[19] M. Kawashita, M. Nakao, M. Minoda, H. M. Kim, T. Beppu, T. Miyamoto, T. Kokubo, T. Nakamura, *Biomaterials* **2003**, *24*, 2477.

[20] F. Zhao, W. L. Grayson, T. Ma, B. Bunnell, W. W. Lu, *Biomaterials* **2006**, *27*, 1859.

[21] E. H. Lee, Y. Kamigaito, T. Tsujimoto, S. Seki, H. Uyama, S. Tagawa, M. H. Sung, *Sen'i Gakkaishi* **2010**, *66*, 104.

[22] P. X. Ma, R. Zhang, G. Xiao, R. Franceschi, *J. Biomed. Mater. Res*. **2001**, *54*, 284.

[23] I. O. Smith, L. R. McCabe, M. J. Baumann, *Int. J. Nanomedicine* **2006**, *1*, 189.

[24] N. Adams, U. S. Schubert, *Adv. Drug Deliv. Rev*. **2007**, *59*, 1504.

[25] T. Tajima, S. Ueno, N. Yabu, S. Sukigara, F. Ko, *J. Appl. Polym. Sci*. **2011**, *122*, 150.

[26] R. Jeziorska, *Polym. Degrad. Stab*. **2005**, *90*, 224.

[27] D. Gonzales, K. Fan, M. Sevoian, *J. Polym. Sci. Part A: Polym. Chem*. **1996**, *34*, 2019.

[28] H. Kubota, Y. Nambu, T. Endo, *Nippon Kagaku Kaishi (Jpn)* **1993**, *1993*, 973.

[29] I. Armentano, M. Dottori, E. Fortunati, S. Mattioli, J. M. Kenny, *Polym. Degrad. Stab*. **2010**, *95*, 2126.

[30] L. Chen, J. M. Mccrate, J. C. M. Lee, H. Li, *Nanotechnology* **2011**, *22*, 105708.

[31] R. Zhang, P. X. Ma, *Macromol. Biosci*. **2004**, *4*, 100.

[32] N. Y. C. Yu, A. Schindeler, D. G. Little, A. J. Ruys, *J. Biomed. Mater. Res. B Appl. Biomater*. **2010**, *93*, 285.

[33] B. Manocha, A. Margaritis, *J. Nanomater*. **2010**, *2010*, 1.

Concluding Remarks

This thesis deals with the fabrication of PGA-based monoliths by thermally induced phase separation (TIPS) method. Through appropriate modification, these materials can be utilized in various fields. The results obtained through this study are summarized as follows.

In Chapter 1, new class of monolith based on PGA was successfully achieved by the TIPS technique. A combination of DMSO, water and ethanol enabled the production of the PGA monolith with uniform shape. The monolith had the relatively large surface area in the pore and skeleton sizes of sub-micron range. The PGA monolith was converted to the water-insoluble monolith by crosslinking with hexamethylene diisocyanate (HDI). The crosslinked monolith possessed high resistance toward water as well as organic solvents. The unique deformability of the wet crosslinked monolith was found. Furthermore, the crosslinked monolith effectively adsorbed $Cu(II)Cl_2$ from the aqueous solution and the copper(II)-immobilized crosslinked PGA monolith showed strong antibacterial activity against the *E. coli* cells.

In Chapter 2, a unique PGA monolith that included both large and small pores has been introduced. It was prepared by a simple and costless approach that combines the thermally induced phase separation technique with particulate salt templates. The monolith was covalently stabilized by internal crosslinking with HDI. This crosslinking also allowed the salt templates to be washed out of the monolith. Submillimeter-sized large cavities were thus installed homogeneously in the monolithic matrix comprising a microporous small porous network created by the phase separation. This monolith could readily absorb water and deform reversibly. More importantly, pH-responsibility of PGA was successfully integrated in the monolith. The monolith could expand/shrink

and efficiently capture/release metal ions in response to pH changes.

In Chapter 3, the PGA/hydroxyapatite monolith (PGA/HAp monolith) was prepared by biomineralization in simulated body fluid for bone tissue engineering. The HAp nucleation and growth on the $CaCl_2$ treated monolith was significantly faster than those on the $CaCl_2$ untreated monolith in SBF. MC3T3-E1 cells efficiently attached and grew on the both PGA monolith and PGA/HAp monolith. BMP-2 was effectively loaded onto the PGA monoliths and slowly released into the culture media. MC3T3-E1 cells cultured on the BMP-2 loaded PGA monoliths showed increased ALP activity.

In Chapter 4, pH-degradable PGA monolith was designed for cell scaffolding applications. The PGA monolith prepared by combination of TIPS and salt leaching method was crosslinked with a low-toxic oxazoline functionalized polymer. The monolith showed pH-controlled degradability in aqueous media and thermal stability up to the decomposition temperature over 200 ^{o}C. The monolith could absorb a calcium salt homogeneously over the surface and release it.

In conclusion, a series of polymer-based monoliths are prepared successfully by using PGA as the precursor and TIPS as the fabrication technique. The fabricated monolith has unique open-cellular three-dimensional continuous structure with large surface area. In addition, PGA monoliths showed variety properties such as pH-responsivity, metal ions chelating ability, anionic property, reversible deformability, low-cytotoxicity, degradability, and thermal stability. The results described in this thesis strongly support that the PGA monolith holds great promise for a wide range of applications, especially in environmental fields and biomaterials, *e.g.*, heavy metal chelating agent in wastewater treatment, rare metal recovering agent, scaffold for tissue engineering, drug deliverer, enzyme-immobilizing material etc.

List of Publications

1. Fabrication of Poly(γ-glutamic acid) Monolith by Thermally Induced Phase Separation and Its Application

   Sung-Bin Park, Takashi Fujimoto, Eiichi Mizohata, Tsuyoshi Inoue, Moon-Hee Sung, Hiroshi Uyama

   Journal of Microbiology and Biotechnology, **2013**, *23*, 942-952.

2. Macroscopic Cavities within a Microporous 3-D Network: a Poly(γ-glutamic acid) Monolith Prepared by Combination of Particulate Templates and a Phase Separation Technique

   Sung-Bin Park, Junji Sakamoto, Moon-Hee Sung, Hiroshi Uyama

   Polymer, **2013**, *54*, 6114-6118.

3. pH Controlled Degradation and Thermal Stability of a Porous Poly(γ-glutamic acid) Monolith Crosslinked with an Oxazoline-Functionalized Polymer

   Sung-Bin Park, Junji Sakamoto, Moon-Hee Sung, Hiroshi Uyama

   Polymer Degradation and Stability, **2014**, *99*, 99-104.

4. Preparation of Poly(γ-glutamic acid)/Hydroxyapatite Monoliths *via* Biomineralization for Bone Tissue Engineering

   Sung-Bin Park, Urara Hasegawa, André J. van der Vlies, Moon-Hee Sung, Hiroshi Uyama.

   Submitted

Acknowledgements

This study was performed at the Department of Applied Chemistry, Graduate School of Engineering, Osaka University, from 2011 to 2014.

First of all, I would like to express my deepest gratitude to my supervisor, Professor Dr. Hiroshi Uyama, for his scientific advice, many insightful discussions, and valuable suggestions. His kindhearted encouragement and continuous guidance always lead me to much success in my research. I really enjoyed my research with him and learned lot of good things from him.

I would like to express thanks to Professor Dr. Moon-Hee Sung of the Department of Bio and Fermentation Convergence Technology, Kookmin University, and CEO of BioLeaders Corp., Korea, for his helpful advice, assistance, and encouragement throughout my whole research. He is my role model for a scientist, mentor, and teacher.

I am profoundly grateful to Professor Dr. Toshikazu Hirao and Professor Dr. Takashi Hayashi for their valuable comments and suggestions on preparation of this thesis.

I would like to express grateful appreciation to Assistant Professor Dr. Urara Hasegawa and Assistant Professor Dr. Takashi Tsujimoto for their helpful suggestions and supports.

I wish to express my sincere thanks to Dr. Junji Sakamoto, Dr. André J. van der Vlies and, Dr. Jun-ichi Azuma for their expert advices and valuable help.

I deeply thank Professor Dr. Tsuyoshi Inoue, and Assistant Professor Dr. Eiichi Mizohata, for their kind help with the microorganism experiment.

I would like to thank Professor Dr. Susumu Kuwabata and Assistant Professor Dr. Taro Uematsu for their kind help with the ICP-AES measurement.

I also appreciate the support from Professor Dr. Nobuhito Imanaka and Associate Professor Dr. Shinji Tamura for the XRD measurement.

I would like to express sincere appreciation to Dr. Mahasweta Nandi, Dr. DiDi Derks, Dr. Yasushi Takeuchi, Dr. Eun-Hye Lee, Dr. Yuanrong Xin, Mr. Takashi Fujimoto, Mr. Keisuke Okada, Ms. Xiaoxia Sun, Mr. Nao Hosoda, and all the members in Uyama laboratory. I can finish my research and enjoy my life in Japan with their kind help, advice, and encouragement.

I deeply appreciate the help from Ms. Yoko Uenishi, Ms. Tomoko Shimizu for their kind help, support, and encouragement all through my life in Japan.

I would like to thank Ms. Mie Iwamoto of BioLeaders Corp., Japan, for her kind help and assistance.

I would like to thank all my dear friends, for their kind help, valuable advice and encouragement.

Thanks to Japanese Government (Monbukagakusho: MEXT) Scholarship for founding my academic training studies and my stay in Japan.

Finally, I would like to express particular appreciation and thanks to my family, Joo-Sik Park, Sang-Min Ryu, Soo-Bin Park, Jung-Bin Park and Jun-Chang Park, for their continuous support, understanding, and encouragement throughout my whole research.

This doctoral thesis would not have been possible without the help and support of the kind people around me. Thanks.

2014

Sung-Bin Park